Université de Sherbrooke

Damage to simple DNA components induced by secondary electrons

Yi Zheng

Département de médecine nucléaire et de radiobiologie

Thesis presented to the Faculty of Medicine
To obtain a diploma of Philosophy Doctorate (Ph.D.)

Sherbrooke, Québec, Canada
May 2005

ENTRE LA PAGE 36 ET 44, IL Y A UNE SÉRIE DE 23 PAGES AVEC UNE PAGINATION DIFFÉRENTE. IDEM POUR 5 PAGES ENTRE 44 ET 47.

Your file Votre référence
ISBN: 0-494-14879-9
Our file Notre référence
ISBN: 0-494-14879-9

Abstract

A major objective of our research group is to understand the mechanism of DNA damage induced by secondary electrons and its relationship to radiosensitization. My project focuses on simple systems, in which small DNA components, nucleosides (dThd), nucleotides (dTp), oligonucleotides (GCAT and CGTA) and modified oligonucleotides, are exposed to low energy electrons, and the subsequent reactions are studied by chemical analysis of the products.

A new low-energy electron irradiation system was constructed in which a relatively large area of target compounds can be irradiated. Thus, this system provides sufficient amount of damage products for further chemical analysis by HPLC, GC/MS and LC/MS. Our systematic studies revealed two main types of LEE-induced fragmentation reactions in DNA: 1) cleavage of the N-glycosidic and 2) cleavage of the phosphodiester bond. The results show that phosphodiester bond cleavage by 4-15 eV electrons involves cleavage of the C-O bond rather than the P-O bond. Below 14 eV, the yield of LEE-induced damage products in DNA is dominated by the formation of transient anions located around 6 and 10 eV. Beyond 14 eV, direct LEE impact is believed to contribute substantially to damage. Our studies suggest that electron transfer occurs from the base moiety to the sugar-phosphate backbone in DNA, but the inverse does not occur, in agreement with theoretical studies. The present study provides a chemical basis for the formation of strand breaks by the reaction of LEE with DNA. The capture of non-thermalized electrons with 4-10 eV of energy by DNA bases may be an important factor in DNA damage in living cells.

Résumé

L'un des objectifs majeurs de notre groupe de recherche est la compréhension des mécanismes de dommages à l'ADN induits par les électrons secondaires et de leur lien avec la radiosensibilisation. Mon projet porte sur des systèmes simples où de petits composants de l'ADN, soit des nucléosides (dThd), des nucléotides (dTp), des oligonucléotides (GCAT et CGTA) et des oligonucléotides modifiés, sont exposés à des électrons de faible énergie. Les réactions induites sont par la suite étudiées par analyse chimique des produits.

Un nouveau système d'irradiation par des électrons de faible énergie a été construit à l'intérieur duquel une zone relativement grande de produits-cibles peut être irradiée. De cette façon, cela permet de créer suffisamment de produits de dommage pour poursuivre l'analyse par HPLC, GC/MS et LC/MS. Les études systématiques ont révélé deux types principaux de réactions de fragmentation de l'ADN induits par les LEE : 1) le clivage du lien N-glycosidique et 2) du lien phosphodiester. Cela montre que le bris du lien phosphodiester par les électrons de 4-15 eV implique le bris du lien C-O plutôt que celui du lien P-O. En dessous de 14 eV, le rendement des produits créés par les LEE dans l'ADN est dominé par la formation d'anions transitoires localisés entre 6 et 10 eV. Au-delà de 14 eV, nous croyons qu'un impact direct des LEE contribue aux dommages de façon substantielle. Nos études ont démontré que les LEE transfèrent de la base au squelette de l'ADN, tel que suggéré par des études théoriques. La réaction inverse ne se produit pas. Un tel mécanisme de dommage suggère que la capture d'électrons non thermalisés de 4-15 eV par les bases de l'ADN pourrait être un agent important du dommage à l'ADN cellulaire. Cette étude fournit une base chimique pour la formation des bris à la suite de la réaction des LEE avec l'ADN.

To my parents and Sirui

CONTENTS

List of tables and illustrations

List of abbreviations

Ade	Adenine
BrU	Bromouracil
BrUdR	Deoxybromouridine
Cyt	Cytosine
dCyd	2'-deoxycytidine
dR	2-Deoxyribose
DD	Dipolar dissociation
DEA	Dissociative electron attachment
DFT	Density functional theory
DNA	Deoxyribonucleic acid
DSB	Double strand break(s)
dThd	Thymidine
dTp	Thymidine monophosphate
EEL	Electron energy loss
ESD	Electron stimulated desorption
ESI	Electrospray ionization
eV	Electron volts
FWHM	Full width at half maximum
Gua	Guanine
GC/MS	Gas chromatography/ mass spectrometry
HREEL	High resolution electron energy loss

HPLC	High-performance liquid chromatography
keV	Kilo electron volts
LC	Liquid chromatography
LEE	Low energy electron(s) (0-30 eV)
LEEEF	Low energy electron enhancement factor
LUMO	Lowest unfilled molecular orbital
MFP	Mean free path(s)
ML	Monolayer(s)
MS	Mass Spectrometry
Oligos	Oligonucleotides
RNA	Ribonucleic acid
SAM	Self assembled monolayer(s)
SE	Secondary electron(s)
SSB	Single strand break(s)
Thy	Thymine
THF	Tetrahydrofuran
Ura	Uracil
UHV	Ultra high vacuum
UV	Ultraviolet
XPS	X-ray photoelectron spectroscopy

Chapter I - Introduction

I.1 Ionizing radiation and radiobiology

In 1895 the German physicist Wilhelm Conrad Roentgen discovered "a new kind of ray", which he called X ray ----the X representing the unknown. This unknown ray started the new century of radiation research, which has become a diverse field that covers many areas of knowledge. Ionizing radiation is a type of radiation that produces a separation of charge in matter by transfer of sufficient energy to overcome the electron-binding energy in atoms or molecules. It has been found that ionizing radiation induces a variety of destructive, mutagenic, and potentially carcinogenic modifications, principally in DNA (von Sonntag, 1987). Thus the investigation of ionizing radiation in living organisms is the basis of radiobiology.

Radiation therapy is a clinical treatment modality where ionizing radiation is used to treat patients with malignant neoplasms. The goal is to deliver a measured dose of radiation to a defined volume with minimal damage to surrounding normal tissue, resulting in eradication of the tumor. The application of radiotherapy relies essentially on the understanding of how cells respond to stress produced by ionizing radiation.

I.1.1 Direct and indirect effect of radiation

When any form of radiation ---- X or γ rays, charged or uncharged particles is absorbed in biologic material, one possibility is that it will interact directly with the critical targets in cells. The target atoms itself may be ionized or excited; thus initiating a chain of events that leads to a biologic change. This is called direct effect of radiation.

Alternatively, the indirect effect involves the interaction of cellular water rather than with macromolecules within the cell. The indirect action initiated with the hydrolysis of

water which produces $HO^{\bullet}$, e_{aq}, $H^{\bullet}$, H_2, etc. These radicals may diffuse a short distance and further react with critical targets, such as DNA. It is known that 80% of a cell is composed of water, which absorbs about 66% of the energy. Indirect action is estimated to compose nearly 50% of the ionizing radiation. The indirect effect of ionizing radiation on DNA is briefly described in section I.4. In this thesis all the results are obtained in the condensed phase, therefore, major efforts are focused on the direct effect of radiation.

I.1.2 Process time scale of ionizing radiation

The time scale of events triggered by ionizing radiation is illustrated in the fig. 1. There are vast differences in the time scale involved in these various events. First the physical process e.g. the initial ionization, takes place in 10^{-15}s. Second the primary radicals are produced by physico-chemical processes having a lifetime of about 10^{-10} to 10^{-9} s. The reaction of those radicals with target molecules leads to chemical changes from bond breakage. Finally, expression of the biological effect may take longer time depending on the consequences involved. For example, if radiation damage is oncogenic, its expression as a cancer may be delayed several years. However, all those biological effects depend on the chemical modifications that have already occurred. Therefore, the chemical analysis of ionizing radiation damages plays an important role in understanding radiobiological pathways.

physical	**physical-chemical**		**chemical**	**biological**
non-thermal electrons (e^-)	ion radical	free radical		
10^{-16}s ----------10^{-12}s	-----10^{-10}s	------10^{-9}s	--------10^{-6}s ----------	10^{0}s ------10^{6}s

Figure 1. The characteristic events observed after the process of ionizing radiation.

I. 2 Events induced by interaction of fast charged particles

Taking a simple example of the initial interaction of a fast charged particle with a molecular solid composed of organic molecules R-H, the pre-chemical stage of radiation damage is shown in fig. 2 (Sanche, 2002). As the fast charged particle passes near the molecule R-H, the molecule is perturbed by the rapid change of electric field induced by the moving charge. Because this perturbation leaves the energy and momentum of the fast particle practically unchanged, the energy transfer can be described as an absorption of electromagnetic radiation by the molecules of the medium. The most probable energy loss of fast primary charged particles is 22 eV. This absorption can lead to the formation of electronically excited species [R-H]*, and ionization (Fig. 2). Most of the energy of high-energy particles is deposited within irradiated systems by the emission of such succession of low-energy quanta (22 eV).

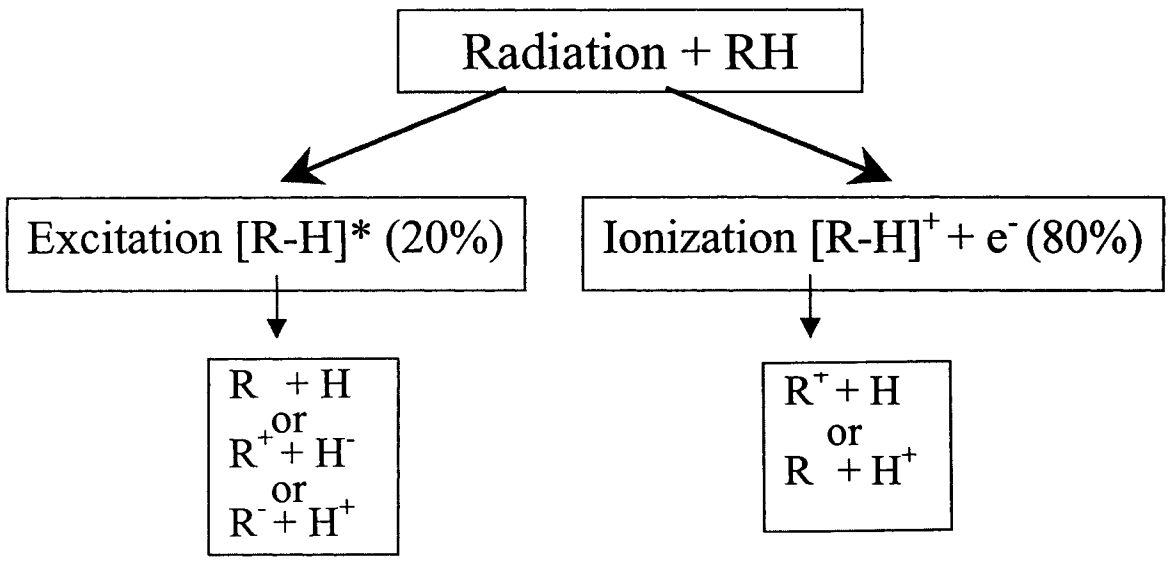

Figure 2. Initial events induced by a fast charged particle that penetrates an organic or biomolecular solid composed of molecules RH (H = hydrogen, R = rest of molecule). The percentage of the average energy deposited is indicated.

One can estimate that *ca.* 20% of the energy deposited by fast charge particles in organic matter leads to [R-H]* production, whereas the rest leads to ionization. The ionization energy is shared as the kinetic energy of secondary electrons and the potential energy of the cation, with the largest portion of the energy going to the secondary electrons. The sequence of events of ionization and electronic excitation may lead to hydrogen-atom abstraction, as an example of possible fragmentation produced by ionizing radiation (Fig. 2).

Many species are produced along the ionization track, which consist of excited atoms and molecules, radicals, ions, and secondary electrons. Among these species, secondary electrons are generated abundantly (*4×10^4 per MeV of deposited energy*) by the absorption of energy from primary high energy photons such as X, γ rays, and fast charge particles (Cobut et al., 1998). Secondary electrons have low energies with a distribution that lies essentially below 70 eV and a most probable energy below 10 eV. An example of SE distribution and emission coefficient induced by X-ray irradiation is shown in figure 3 (Cai et al., 2005). The spectrum was recorded with a current of 0.14 ± 0.02 nA of SE emitted from a 1.4 x 1.4 cm^2 tantalum substrate. The energy-integrated electron yield was 0.039 ± 0.003 electrons per photon. It indicates that most of SE are LEE with kinetic energy below 10 eV.

Within the thermalization distances of the order of 1-10nm, the highly excited atomic, molecular and radical species, ions and low-energy electrons (LEE) can induce non-thermal reactions. A majority of these reactive species, which can initiate chemical reactions, are created by the secondary LEE. Thus, in order to understand the ionizing radiation process in living cell, the mechanism of action of LEE must be understood.

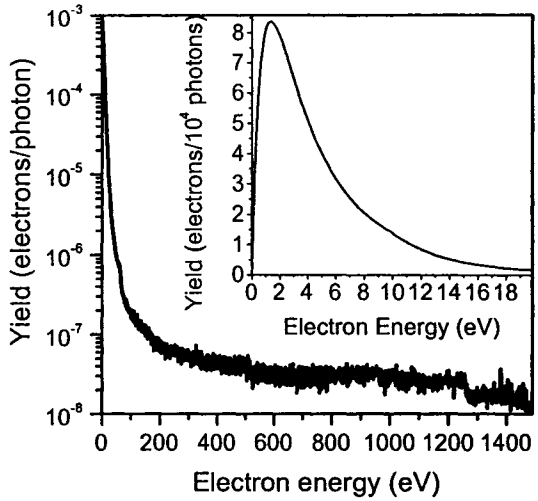

Figure 3. Energy distribution of Al Kα X-ray induced secondary electron emission from tantalum.

I. 3 Electron-molecule interactions in condensed phase

Electrons are small negatively charged particles that can be accelerated to high energy and to a speed close to that of light by means of an electrical device, such as a betatron. In order to interpret the processes induced by electrons, especially LEE on biomolecular films, it is necessary to discuss the basic interaction between an electron and a molecule.

In general, the interaction of an electron with an atom or a molecule can be described in terms of forces derived from the potential that acts between them. Electron-molecule collisions can be divided into two main types: direct and resonant interactions.

I. 3.1 Nonresonant scattering

Direct scattering has short interaction times characterized by the usual duration of the electron transit through the dimensions of a molecule. Because the potential interaction

is always present, direct scattering occurs at all energies above the energy threshold for observed phenomenon. It produces a smooth, usually rising signal that does not exhibit any particular features.

Depending on the amount of energy transferred from the electron to the target, scattering can be elastic or inelastic. In elastic collisions, according to momentum conservation, the energy transfer, i.e. $\Delta E/E$, to the atom or molecule is on the order of m/M (m and M are the mass of the electron and target, respectively) of the electron's initial energy. Because of the very small electron mass (m) compared to even the lightest atom H (1: 1836), the loss of electron energy through momentum transfer to the target is negligible.

In contrast, inelastic collisions may create electronically excited states and subsequent reactions which are described as following:

$$e^- + M \rightarrow M^* + e^-$$

$$M^* \rightarrow R + X \text{ (dissociative excitation)}$$

$$M^* \rightarrow R^+ + X^- \text{ (ion pair dissociation)}$$

$$M^* \rightarrow M^+ + e^- \text{ (autoionization)}$$

$$M^* \rightarrow M^{2+} + 2e^- \text{ (multiple ionizations)}$$

I. 3.2 Resonant scattering

Electron resonances are well described in many reviews (Palmer & Rous, 1992; Sanche, 1991; Sanche, 1995; Sanche, 2000). Resonant electron scattering occurs when the incoming electron is bound into discrete energy level of the target for a much longer time than the usual scattering time in the neighborhood of a target. From a molecular orbital perspective, the resonant state may be considered as a transient negative ion (TNI) formed by an electron which temporarily occupies a previously unfilled orbital of the molecule.

Thus, resonance scattering occurs at specific energies that correspond to the formation of transient anions. At the resonance energy, product yield is usually enhanced, whereas a strong peak is observed in the yield function.

I.3.2.1 Major types of resonances

There are two major types of resonances: shape and core-excited resonance. If the additional electron occupies a previously unfilled orbital of the target in its ground state, the transitory state is referred to as a single-particle or "shape" resonance. Shape resonance applies specifically when temporary trapping of the electron is due to the shape of the electron-molecule potential. When the transitory anion if formed by two electrons occupying previously unfilled orbitals, the resonance is referred as a two-particle, one-hole or core-excited state. The first step in the latter resonance includes one core electron to be excited from the ground state, leaving a hole and an electron in the LUMO. Then a second electron is captured by the positive electron affinity of the electronically excited state or exciton, forming a core-excited anion (Sanche, 1991).

I.3.2.2 Lifetime of the resonance Δt

When the electron is temporarily captured by the target, it has an increased interaction time. This causes additional distortion of the target whose magnitude depends on the lifetime of the resonance, Δt. Long-lived resonances with lifetimes larger than 10^{-14} s cause a significant displacement of the nuclei of a molecule when the additional electron occupies a strongly bonding or antibonding orbital. When the electron leaves the molecule, nuclear motion is initiated toward the initial internuclear distance, causing excitation of many vibrational overtones of the molecule, due to the strong overlap between the nuclear wave function of the resonant state and that of many vibrational states of the ground state of

the molecule. On the other hand, when the Δt is much smaller than a typical vibrational period ($\Delta t << 10^{-14}$ s), the nuclei are not significantly displaced. Thus, for short resonance times only the lower vibrational levels become excited with considerable amplitude.

According to the uncertainty principle (i.e., $\Gamma \bullet \Delta t \approx h/2\pi$), the transient state has a width in energy Γ which serves to characterize and identify the process in the energy dependence of the scattering cross-sections or excitation functions. Resonance lifetime Δt could be reflected by the energy width. Long-lived resonances ($\Delta t \geq 10^{-14}$ s) in atoms produce sharp peaks in elastic and electronic excitation and ionization cross-sections. In molecules such resonances may lead to more decay channels due to the additional degrees of freedom introduced by nuclear motion. When the resonance are short-lived ($\Delta t << 10^{-14}$ s), they produce broad peaks in their decay channels.

I.3.3 LEE interaction with a molecule AB

The possible decay channels of a diatomic molecule AB induced by LEE are illustrated in figure 4 (Bass & Sanche, 2004). The direct electron interaction may produce an excited neutral state of the molecule AB* *via* pathway a. The departing electron may leave the molecule in a rotationally, vibrationally, or electronically excited state (pathway a). Then, AB* may dissipate its excess energy *via* photon emission and/or energy transfer to the surrounding medium (a1). If the resulting electronically excited neutral state is dissociative, ground state or excited fragments can be produced (a2). Above a certain energy threshold (~14-16 eV), dipolar dissociation (DD) becomes possible to yield an anion and a cation (a3).

In the case of resonant scattering, the incident electron temporarily attaches to the molecule *via* pathway b. The resulting transient anion may autoionize *via* b3. The other

important process is called **dissociative electron attachment (DEA)**, i.e., the anion may dissociate into a stable anion and a neutral fragment in an excited or the ground state (b1). DEA occurs when the resonance meets several conditions: a) the lifetime of the resonance is, at least, of the order of a vibrational period; b) the AB^- state is dissociative in the Franck-Condon (FC) region, c) at least one of the possible fragment has a positive electron affinity. If during its lifetime, the transient anion transfers energy (ΔE) to another system (e.g., by collisional interaction with another molecule, or phonon creation in a surrounding medium), it may stabilize as long as the parent molecule has a positive electron affinity (process b2). Finally, the incoming electron can directly ionize the molecule *via* path c. If the resulting cation is dissociative, it may fragment as shown in c1.

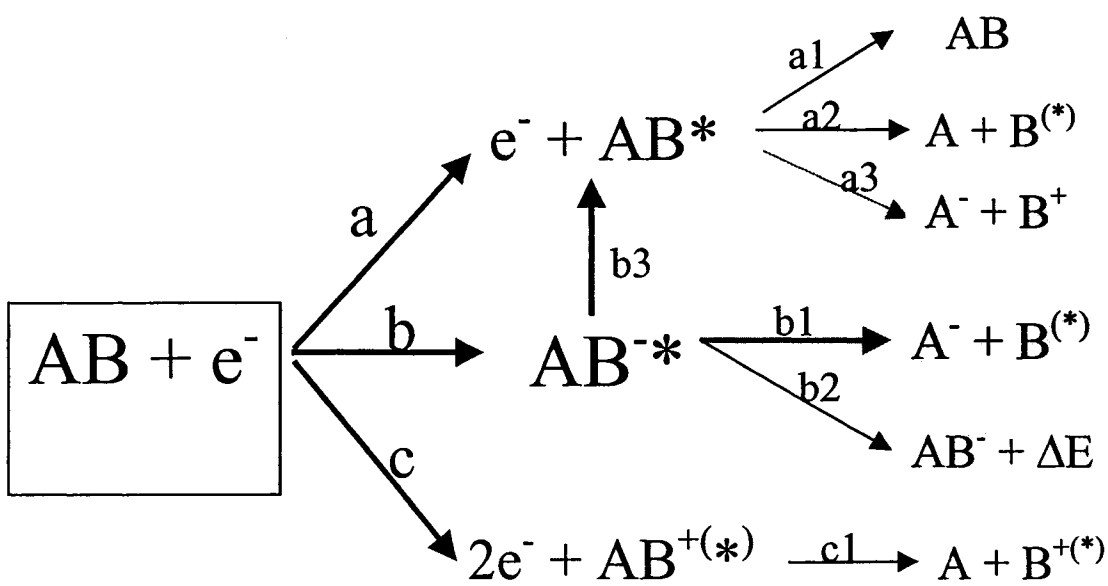

Figure 4. Energy transfer and unimolecular fragmentation pathways that follow LEE interaction with a molecule AB.

I. 4 DNA damage induced by ionizing radiation

I.4.1 Structure of DNA

Deoxyribonucleic acid (DNA) DNA is a polymer (Adams et al., 1981). The monomer units of DNA are nucleotides, which consists of a 5-carbon sugar (deoxyribose), a nitrogen containing base attached to the sugar, and a phosphate group. There are four different types of nitrogenous bases in DNA: adenine (A), guanine (G), cytosine (C) and thymine (T). A DNA molecule consists of two polynucleotide antiparallel stands having the form of a right-handed helix. The two strands achieve contact through hydrogen bonds between A-T and G-C and also by base to base π stacking between adjacent bases on the same strand (Scheme 1).

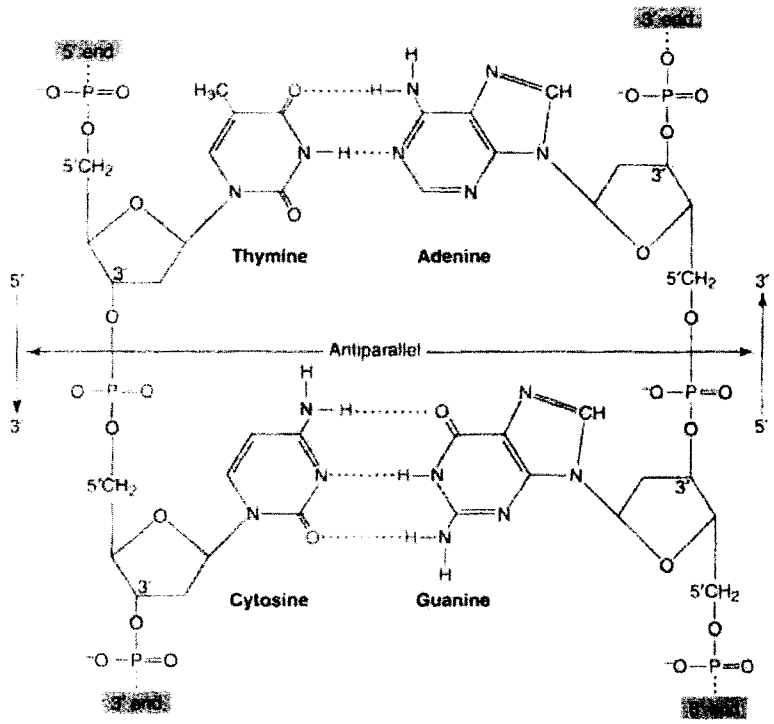

Scheme 1. Schematic drawing of DNA strands

With such unique chemical structure, DNA achieves a supreme coding effectiveness and serves as the carrier of genetic information in both prokaryotes and eukaryotes. An undifferentiated mammalian fetal cell contains only a few picograms (10^{-12}g) of DNA, which determine the synthesis of as many as 30,000 distinct proteins (Devlin, 1997). In summary, DNA is the macromolecule that ultimately controls cellular functions, primarily through protein synthesis. Also, DNA plays an exclusive role in heredity, by transfer of biological information from one generation to the next (McGowan, 2003).

The double helix exists in various geometries depending on the base composition and physical conditions, i.e., A, B and Z form. B-DNA is the most common form in cells. It should be noted that H_2O molecules, which easily fit in the grooves of the helix, are an integral part of the DNA structure. Even under dry conditions, DNA may still contain on average 2.5 water molecules per base pair (Swarts et al., 1992). In the dried state, B-DNA may convert to A configuration. Therefore, even in the condensed phase the radiation-induced hydrolysis of water should also be considered. In dilute solution, DNA damage induced by ionizing radiation is mainly caused by the reactive species formed from water, including hydroxyl radicals, solvated electrons and H atoms.

I.4.2 Hydroxyl radicals

The action of hydroxyl radicals on DNA constituents in aqueous solution (indirect effect of ionizing radiation), which is also called "oxidative damage to DNA", has been extensively studied (von Sonntag, 1987; Cadet, 1997; Dizdaroglu et al., 2002; Wagner et al., 1999). The relevant information on the transient $^{\bullet}OH$ radical adducts to pyrimidine and purine nucleic acid components has been obtained from electron spin resonance

investigations (Davies et al.1995). Most of the $^{\bullet}$OH-mediated resulting products have been characterised and reviewed (Cadet, 1997; Cadet 2003).

OH radical can abstract hydrogen atoms within the sugar moiety with a preference at C4' position. In this respect, each sugar in DNA attacked by an OH radical forms a strand break in alkali, with a G value (the number of specified chemical events produced in an irradiated substance per 100 eV of energy absorbed from *ionizing radiation*) of at least 0.6 ($1G \simeq 10^{-7}$ mol/J). It is estimated that about 2.7 OH radicals are formed per 100 eV of radiation energy absorbed. There is no evidence for reactions of $^{\bullet}$OH with phosphate groups. Therefore, at least 0.6 (>20%) $^{\bullet}$OH react with sugars and less than 2.1 (< 80%) with bases (Hutchinson, 1985). However, the actual distribution favours the sugar because OH radicals are more accessible to the sugar moiety.

I.4.3 Solvated electrons e^-_{aq}

Solvated electrons are one of the species formed by ionization process of ionizing radiation after the electron becomes solvated in liquid water (Eq. 1). In N_2 saturated water the G value of e^-_{aq} is about 2.65, whereas in N_2O it could be scanvagered and converted into OH radicals (von Sonntag, 1987).

$$e^- + n\,H_2O \rightarrow e^-_{aq} \qquad (1)$$

Solvated electrons form electron adducts in the reaction with pyrimidines and purine bases and lead to further products by protonation. From the studies of model system poly(U) it was found that e^-_{aq} hardly makes any strand break or base release compared to OH and H radicals (von Sonntag, 1987).

I.4.4 Base ionization

From the process of base ionization, the primary species are radical cations and radical anions, which can be observed by ESR. The radical anions have been observed with the nucleotides at liquid He temperature (Box et al. 1975). However, in DNA, due to the difference in electron affinity of bases only the cytosine and thymine anions, guanine and adenine cations were detected (Sevilla et al., 1991). It was also found that menadione-mediated photosensitization to UVA radiation leads to photo-ionization of pyrimidine bases, whereas photoexcited riboflavin is only able to ionize purine bases (Cadet 2003).

I.4.5 Typical methods of detection (PAGE, HPLC, MS)

Owing to its negative charge, DNA migrates on polyacrylamide gels upon electrophoresis (PAGE). This method can clearly distinguish between two pieces of DNA that differ in length by one or more nucleotide unit. The resulting electropherograms are analyzed by autoradiography using labeled DNA and improved by computer-assisted spectrophotometry. For example, supercoiled, circular and linear forms of plasmid DNA induced by LEE were separated by this method (Boudaiffa et al., 2000).

Chemical analysis of products includes first the separation by high-performance liquid chromatography (HPLC), and then characterization using suitable spectroscopic measurements, e.g. mass spectroscopy (MS). Recently HPLC coupled to the electrospray ionization tandem mass spectrometry (HPLC/ESI-MS/MS) represents one of the most powerful analytical tools, providing high sensitivity and specificity to the measurement. It has been used to search for the unidentified radiation-induced DNA lesions (Regulus et al. 2004).

I. 5 DNA damage induced by LEE

According to the fundamental interactions that lead to subsequent events in a target, the biological effects of radiation are not produced by the mere impact of primary quanta, but mostly by the secondary species that are generated along the radiation track. Because LEE are the most abundant of the secondary species produced by the primary interactions, it is crucial to determine their action within cells, particularly in DNA, where LEE lead to mutagenic and potentially lethal DNA damages (Boudaiffa et al., 2000). Since the pioneer study of Sanche's group, much works focuses on the LEE induced processes in DNA and its constituents.

I.5.1 Reaction of LEE with DNA components

I.5.1.1 DNA bases and uracil

Systematic gas-phase investigations of stable anion production by LEE impact on uracil (U) (Denifl et al, 2004a; Feil et al., 2004; Hanel et al., 2003) and other DNA bases (Denifl et al, 2004b; Sukhoviya et al., 2001; Abouaf et al., 2003; Denifl et al., 2003; Gohlke et al., 2003; Abdoul-Carime et al, 2004; Ptasińska et al., 2005) provided considerable insight into the mechanisms of damage to DNA induced by SE of low energies. Electron attachment to these biomolecules leads to dissociation into various fragments without a measurable amount of stable parent anions. The fragment anions with highest abundance from uracil, adenine and the pyrimidines were $(U\text{-}H)^-$, $(A\text{-}H)^-$, $(C\text{-}H)^-$ and $(T\text{-}H)^-$, respectively. In addition, five other fragment anions were formed by DEA to cytosine and eight additional product anions were detected in the case of thymine. Yield functions were measured for all fragment anions in the electron energy range from about 0 to 14 eV.

Twelve fragments were produced by DEA to uracil but with lower cross sections than for $(U\text{-}H)^-$. Energy thresholds for dissociation into cation fragments by LEE impact on U were also determined (Huels et al., 1995).

Subsequent gas-phase studies showed that the high hydrogen loss induced by LEE impact on the DNA bases was site-specific (Abdoul-Carime et al., 2004). In principle, dehydrogenation of nucleobases can arise from either C-H or N-H bond cleavage. To clarify this point, these authors carried out experiments on partly deuterated thymine at non-exchangeable carbon positions, T_D. Below 3 eV, both the energy dependence and the absolute intensity of the yield function of $(T_D\text{-}H)^-$ (129 amu) were virtually identical to those obtained from thymine $(T\text{-}H)^-$ (125 amu). By switching the mass spectrometer to mass 128 amu [corresponding to $T_D\text{-}D)^-$], the ion signal completely disappeared. This observation provided direct evidence that DEA generates the N-dehydrogenated anion $(T_D\text{-}H)_N^-$ as confirmed by DFT calculations. The structures in the $(T_D\text{-}H)_N^-$ ion yield curve suggested that different electronic states of the precursor ion are involved. Any of these states, however, decay by hydrogen cleavage from the N sites, but not from the carbon positions (Abdoul-Carime et al, 2004; Ptasińska et al., 2005).

The four DNA bases were also investigated in thin multilayer films, but fewer anions of different masses were measured than in the gas phase. *The difference is principally due to the inability of the heavier anions to overcome the polarization potential that they induce in the film causing them to remain trapped in the target* (Huels et al., 1995). In fact, only the light anions H^-, O^-, OH^-, CN^-, OCN^-, and CH_2^- were found to desorb by the impact of 5-35 eV electrons on the physisorbed bases *via* either single or complex multi-bond dissociation (Huels et al., 1995; Abdoul-Carime et al., 2001). The H^-

yield functions exhibited resonance structures at around 9 and 20 eV, typical of DEA to the molecules. A monotonic increase in the anion yield functions was interpreted to arise from non-resonant stable-anion production *via* dipolar dissociation (DD). The resonance features were attributed to electron capture by the positive electron affinity of excited states that involves the excitation of the lone-pair $n \rightarrow \pi^*$, $\pi \rightarrow \pi^*$, and/or $\sigma \rightarrow \sigma^*$ (i.e., formation of a two-electron one-hole transitory anion).

I.5.1.2 Deoxyribose and phosphate backbone

The backbone of DNA consists of a long chain of repeated deoxyribose-phosphate units. Investigation of LEE-interaction with this unit and its two basic constituents are of special interest in relation to DNA damage. In DNA, a SSB occurs when one of the two backbones is broken. If breaks occur on two chains within a short distance (~ 10 base pairs or 30 Å), then the damage is referred to as a DSB. The latter damage is difficult to repair by the cell and without reparation the cell can mutate or die. To understand how such breaks can occur *via* LEE impact, specific sub-units of the backbone were investigated in both the gas and condensed phases (Ptasińska et al., 2004; Antic et al., 1999; Antic et al., 2000; Huels et al., 2004; Lepage et al., 1998; Breton et al., 2004; Pan & Sanche, 2005).

The formation of anions and cations by LEE on the gaseous 2-deoxy-D-ribose ($C_5H_{10}O_4$) (Ptasińska et al., 2004) as well as solid films of the sugar-like analogs, THF (**I**), 3-hydroxytetrahydrofuran (**II**), and α-tetrahydrofuryl alcohol (**III**) (Antic et al., 1999; Antic et al., 2000) were investigated by mass spectrometry (Scheme 2). In these experiments, the yield functions for H^- ion desorbed by the impact of 1-20 eV electrons on 10-ML films were characterized by an onset at 6.0, 5.8, and 6.0 eV, and a maximum centered at 10.4, 10.2, and 10.0 eV for **I**, **II**, and **III**, respectively. No other anions were observed to desorb.

All features below 15 eV in H^- ESD yield functions were characteristic of DEA to **I, II,** and **III**. A steep rise in the H^- signal with an energetic threshold near 15 eV was characteristic of nonresonant DD. Owing to the strong similarity of the H^- desorption profiles for **I, II,** and **III**, the authors concluded that the majority of the anion yield for all three systems arises from at least one transient anion associated with electron attachment to the furan ring and located near 10 eV (Antic et al., 1999; Antic et al., 2000). Considering the large Rydberg character of the excited states in **I** near the energy range of the observed resonance, they further suggested that this resonant state is of the core-excited type,

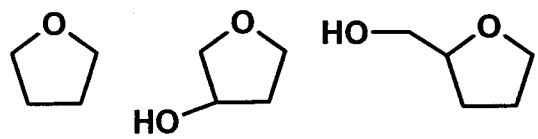

I **II** **III**

possibly with dissociative valence σ* configurational mixing.

Scheme 2. Structure of deoxyribose analogues: tetrahydrofuran **(I)**, 3-hydroxytetrahydrofuran **(II)**, and R-tetrahydrofurfuryl alcohol **(III)**.

The only structural difference between compound **III** and 2-deoxyribose (dR) is the addition of two OH radicals at the 1 and the 3 positions. However, in the case of gaseous deoxyribose, anions of much larger masses were observed to be formed by LEE impact compared to similar experiments with condensed molecule **III**. As explained previously, this difference arises from the polarization field present at the surface of dielectrics. Heavy anions such as $(D\text{-}H)^-$, $C_5H_7O_3^-$ and $C_5H_6O_2^-$ in the gas-phase experiments were observed (Ptasińska et al., 2004). The highest measured cross section (1.2×10^{-15} cm^2) for the formation of stable anions from gaseous dR was observed for the fragment anion $C_5H_6O_2^-$.

The mechanism leading to this anion could be interpreted as *s*-wave electron attachment followed by the removal of two water molecules. For $C_5H_6O_2^-$ only this resonance near 0 eV was observed. The other two fragments, $C_5H_7O_3^-$ and $(D–H)^-$ reveal, besides a strong resonance at 0 eV, a second resonance at 1.2 and 1.5 eV, respectively, which is about 30 times lower in intensity. In contrast to the results of DNA bases, dehydrogenation is not the predominant reaction channel for deoxyribose, but the relative amount of fragment ions compared to that of the parent cation is about an order of magnitude larger than in the case of nucleobases. This result indicates the weakness of sugar moieties in the backbone to attack by LEE.

In a molecule as complex as DNA, the products of fragmentation are expected not only to involve single-step processes such as DEA, but also the reaction of the primary radicals and ions with other surrounding constituents within the molecule. The possibility of reactive scattering within the backbone of DNA has been demonstrated in experiments with condensed films containing O_2 and THF (Huels et al., 2004). Their 0-20 eV electron impact measurements show that all of the OH^- and some of the H^- desorption yields are the result of reactive scattering of the 1-5 eV O^- fragments produced initially by DEA to O_2. These O^- reactions involve hydrogen abstraction and atom exchange with THF, and result in the formation of THF-yl radicals such as alkoxyl radicals, as well as THF oxidation products, such as lactones. O^- was found to scatter over nanometer distances, comparable to DNA dimensions, and its reaction involves formation of a transient $(OC_4H_8O)^{*-}$ collision complex.

HREEL spectra of resonance-enhanced vibrational excitations of gaseous and solid THF were recorded (Lepage et al., 1998; Breton et al., 2004). The production of aldehydes

fragments, which remained trapped within the bulk of the THF film, were detected in situ via the $^{3,1}(n \quad \pi^*)$ and $^{3}(\pi \quad \pi^*)$ electronic transitions and vibrational excitation modes. The synthesis of aldehyde were discussed in terms of the formation of transient anion states, which may lead to the fragmentation of the molecule. The strong rise in the energy dependence data observed from about 6 eV was correlated to the electronic excitation threshold of THF which was suggested, in the solid phase, to involve electron transition to an unoccupied molecular orbital of σ^*_{CO} character. Core-excited resonances, previously identified from vibrational excitation functions in multilayer films of THF around 9 and 10 eV (Lepage et al., 1998), were also suggested to contribute to the strong rise from 6 to 10 eV via the formation of neutral dissociative states. The small feature found around 3 eV was proposed to result from a σ^* shape resonance also previously measured in the anion yields of multilayer films of THF (Antic et al., 1999), and involving the temporary trapping of an electron in either one of the two lowest unoccupied molecular orbitals (LUMO), both possessing a σ^*_{CO} character. The features seen in the energy dependence above 11 eV were explained by considering more specific core-excited resonances involving a hole in the *7b* or *6b*, *7a* or *5b*, and *4b* orbitals, and two electrons in the σ^*_{CO} orbitals. The DEA process, mentioned previously (Antic et al., 1999; Antic et al., 2000), known to lead to fragmentation of THF via the formation of a core-excited resonance around 10 eV, was also proposed as a possible cause of damage. Non-resonant fragmentation of THF via the formation of several cations was finally suggested to increasingly contribute to the cross section from about 11 eV.

So far, the phosphate unit of DNA has only been investigated in the condensed phase (Pan and Sanche, 2005). They reported ESD of OH^- anions from a solid film of Na

$PO_2(OH)_2$. Their OH^- yield function exhibits a single broad peak with a maximum around 8 eV indicating the existence of an intermediate anion state leading to OH^- production, possibly via temporary electron localization in antibonding σ* orbitals of the molecule. In trimethylphosphate (Folkard et al., 1993), a surrogate for the DNA phosphate group, and in recent DFT studies of electron attachment to a sugar-phosphate-sugar unit of DNA (Li et al., 2003), electron localization into the lowest antibonding σ* orbitals was found to lead to DEA. These results suggest the existence of a resonance at the phosphate unit resulting from a core-excited state formed by a positive ion core binding two electrons in σ* orbitals.

I.5.1.3 Short single-strand DNA and oligonucleotides

Short DNA strands may easily be prepared as SAM chemisorbed on gold. Such samples have the advantage of being more uniform in coverage, better oriented and more pure than those made from bacterial DNA. Using such short single and double strands of DNA having well defined base sequences, further insight into the mechanisms of LEE-induced DNA damage was obtained (Dugal et al., 1999; Dugal et al., 2000; Abdoul-Carime et al., 2000; Abdoul-Carime & Sanche, 2001; Abdoul-Carime & Sanche, 2002; Abdoul-Carime et al., 2001). Much of the ESD data from short single strand DNA (i.e., oligonucleotides) have been performed by measuring the yields of *neutral* fragments induced by 1-30 eV electrons impinging on SAM oligonucleotides that consisted of 6 to 12 base units (Dugal et al., 1999; Dugal et al., 2000 and Abdoul-Carime et al.2000; Abdoul-Carime & Sanche, 2001; Abdoul-Carime & Sanche, 2002). Their results were obtained from mass spectrometric measurements of the residual atmosphere near the target during its bombardment in UHV by a 10^{-8} A electron beam. They showed that LEE-impact dissociation of DNA bases led to the desorption of $CN^•$, $OCN^•$, and/or H_2NCN neutral

species, as the most intense observable yields. No sugar moiety phosphorus-containing fragments or entire bases were detected. Comparison with anion yield functions, two possible pathways were suggested for the formation of CN and OCN by electron impact (Scheme 3): a DEA route (Eq. 1-3) and attack by OH radical on adjacent bases (Abdoul-Carime et al., 2001). From various results, it was also indicated that the sequence context played an important role in LEE-induced damage to the bases within oligonucleotides

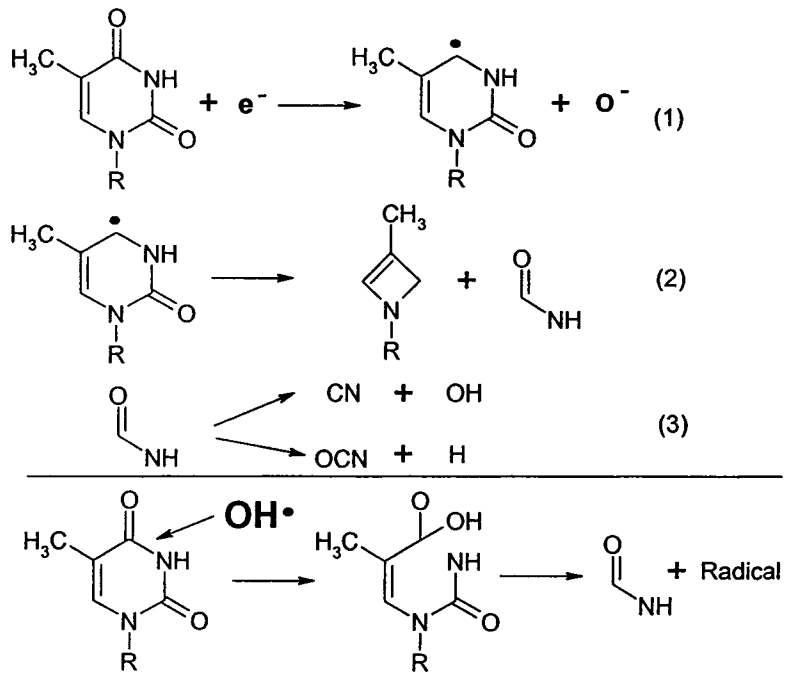

(Abdoul-Carime & Sanche, 2002).

Scheme 3. Hypothetical reaction pathways for thymine ring cleavage, leading to the formation/desorption of CN and OCN neutral fragments via: (a) DEA, (b) secondary reactions induced by an OH radical created via DEA to an adjacent base.

Electron conduction (Nogues et al., 2004) and temporary trapping (Ray et al., 2005) of LEE by DNA were investigated. In the experiments, photoelectrons are ejected by an excimer laser operating at 193 nm (6.4 eV) from a gold substrate on which the molecules are chemisorbed (Ray et al., 2005; Naaman et al., 1998). The LEE (< 2 eV) transmitted

through SAM of short DNA oligomers ML into vacuum are energy analyzed by time of flight. Electrons that are not transmitted are captured by DNA and transferred back to the grounded metal substrate. Because of the short lifetime of the captured electrons and the low-laser intensity and repetition rate, the ML is not charged by electrons between laser pulses. Thus, the instantaneous transmitted current reflects the capturing efficiency of the layer during the duration of the laser pulse (20 μsec). With such transmission experiments, the dependence of the capture probability on the base sequence and the state of the temporarily captured electrons was determined (Ray et al., 2005). It was found that the capture probability scales with the number of guanine bases in the single-strand oligomers and depends on their clustering level.

In the two-photon electron ejection from DNA SAM experiment, electrons are excited in the metal substrate with photon energy below the work function of the substrate (Ray et al., 2005). Some of these electrons are transferred to the LUMO of the adsorbed layer. A second photon is used to eject these electrons from the LUMO to the vacuum, where their kinetic energy is measured. The kinetic energy of ejected electrons is related to their binding energy. It was concluded that, (1) once captured, the electron is not localized on one of the bases, but instead lies either on the sugar phosphate backbone or between the molecules in the ML, in a nonlocalized state; (2) the state of the captured electrons is insensitive to the sequence of the oligomer and (3) double-strand DNA does not capture electrons as efficiently as single-strand DNA, but, once captured, the electrons are more strongly bound in the double than in the single strand configuration.

I.5.1.4 Plasmid DNA

Plasmid DNA was first bombarded with electrons of energies lower than 100 eV with threshold energies for SSB and DSB at 25 and 50 eV, respectively (Folkard et al., 1993). Later, dry samples of plasmid DNA films were bombarded with 5 eV to 1.5 keV electrons in a supercoiled configuration (Boudaiffa et al., 2000a, 2000b, 2000c; Huels et al., 2003). Their samples were analyzed by electrophoresis to measure the percentage of circular and linear forms of DNA produced corresponding to SSB and DSB, respectively. By measuring the relative quantities of these forms in their 5-ML sample as a function of exposure to electrons, these authors measured the total effective cross-section ($\sim 4 \times 10^{-15}$ cm^2) and effective range (~ 13 nm) for the destruction of supercoiled DNA, at 10, 30, and 50 eV (Boudaiffa et al., 2002).

Figure 5 shows the measured yields for the induction of SSB, DSB, and multiple DSB in plasmid DNA induced by 5-100 eV electrons. The apparent SSB yield threshold near 4-5 eV is due to the cut-off of the electron beam at low energies, whereas the DSB yield begins near 6 eV. Both yield functions possess a strongly structured signature below 15 eV and have a peak around 10 eV, a pronounced minimum near 14-15 eV, a rapid increase between 15 and 30 eV, and above 30 eV roughly constant yields up to 100 eV. In stark contrast, the multiple DSB yield has an apparent threshold near 18-20 eV and a very weak peak at 25 eV, above which it increases monotonically by about 1 order of magnitude up to 100 eV. Both peaks in the SSB and DSB yields around 10 eV incident electron energy are similar in magnitude to the respective yields above 30 eV. The relatively high yield below 15 eV may be due to electron diffraction within DNA, which amplifies the captured cross section at specific DNA sites (Pendry, 1974).

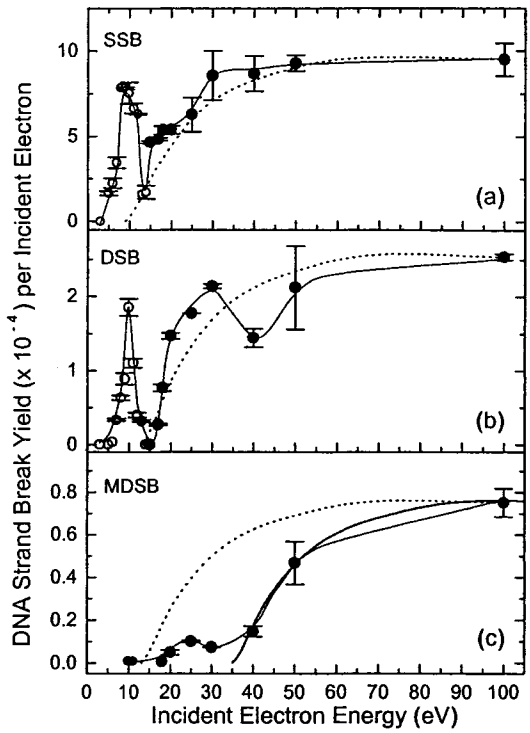

Figure 5. Open and solid symbols are the measured quantum yields (events per incident electron) for the induction of SSB (a), DSB (b), and multiple DSB (c) in DNA films by 4-100 eV electron impact. At each electron energy, the error bars correspond to the standard deviation of the average reported value, while the experimental uncertainty is about ±10% (Reprinted from Huels et al., 2003).

The incident-electron energy dependence of the damage to elementary constituents of DNA, probed in the form of desorbed anions and neutral species, exhibits strong variations due to electron resonances. From comparison of the maxima in the anion and neutral production yield functions of these DNA constituents to the DNA results, it becomes quite obvious that the strong energy dependence of the DNA strand breaks below 15 eV in Fig. 5 can be attributed to the initial formation of transient anions, decaying into the DEA and/or dissociative electronic excitation channels. However, because the basic DNA components (i.e., the sugar, phosphate and base units and structural H_2O) can all be

fragmented *via* DEA between 5 and 13 eV, it is not possible *a priori* to unambiguously attribute SSBs and DSBs to the initial dissociation of a specific component.

A more deterministic interpretation of DNA damage below 15 eV came from the experiments that ESD of anions from plasmid and 40 base-pair synthetic DNA was directly measured within the 3-20 eV range (Pan et al., 2003). Resonant structures were observed with maxima at 9.4 ± 0.3, 9.2 ± 0.3, and 9.2 ± 0.3 eV, respectively, in the yield functions of H^-, O^-, and OH^-. The yield function for H^- desorption, from linear and plasmid double strand DNA exhibit a similar behavior as the yield functions for O^- and OH^- desorption. The prominent 9-eV feature observed in all anion yield functions is a typical signature of the DEA process. The maxima in the H^-, O^- and OH^- yield function from DNA can be correlated with the maximum spreading from 8 eV to 10 eV in the SSB yield and the one occurring at 10 eV in the DSB yield induced by LEE impact on films of supercoiled DNA (Fig. 5) (Boudaiffa et al., 2000a; Huels et al., 2003). Comparing the H^- yield functions for desorption from films of thymine (the results obtained for the three other bases are similar to that shown for thymine) (Abdoul-Carime et al., 2001), amorphous ice (Pan et al., 2005), and α-tetrahydrofuryl alcohol (Antic et al., 1999), it was found that the H^- peak energy from amorphous water is definitively too low to be associated with DEA to the structural water of DNA, unless the strong hydrogen bonding in DNA shifts considerably the H_2O^- resonance energy. In contrast, it indicates that the bases are an important source of desorbed H^- desorption with an intensity about 3 times the one arising from the sugar ring. A similar conclusion can be reached from comparison with gas-phase H^-/D^- abstraction from the carbon position in thymine (Ptasińska et al., 2005). Thus, comparison of line shapes and magnitude of the yield functions in both phases suggests that *LEE-induced* H^-

desorption from DNA below 15 eV occurs mainly via DEA to the bases with a substantial contribution from the deoxyribose ring. Similar comparisons with anion yield functions from basic constituents with those of O^- and OH^- from DNA films (Martin et al., 2004) indicate that O^- production arises from temporary electron localization on the phosphate group. The OH^- desorption yield function resembled that of the O^- yield, but has a considerably lower intensity. This result suggests a two step process: formation of O^- via DEA to the phosphate group followed by reactive scattering of the O^- ion with the nearby deoxyribose unit (i.e. reactive scattering as described in section I.5.1.2).

In these ESD experiments, the counter-ion on the phosphate group was Na^+ due to the method of preparation. Later, SAM of linear single and double strand DNA chemisorbed on a gold substrate with different orientations with respect to the substrate was studied (Pan & Sanche, 2005), but this time in their samples, the Na^+ counter ion was replaced by H^+. In this case, electron impact on DNA below 19 eV with OH in the phosphate unit produced OH^- essentially via DEA to the phosphate group in the backbone. Between 2 and 5 eV, this process occurred exclusively via direct DEA. Above 5 eV, direct DEA to the phosphate unit was still the dominant mechanism, but they could not completely rule out a possible contribution to the OH^- yield, arising from reactive scattering of O^-. Their results showed that the phosphate-counterion part of DNA plays a significant role in LEE induced DNA damage.

It was only after the development of more sensitive techniques to detect SSB and DSB in DNA that the electron energy range below 4 eV was investigated (Martin et al., 2004). Two peaks, with maxima of $(1.0 \pm 0.1) \times 10^{-2}$ and $(7.5 \pm 1.5) \times 10^{-3}$ SSB per incident electron, respectively, are observed in the yield function of SSB at electron

energies of 0.8 eV and 2.2 eV. The peaked structure provides unequivocal evidence for the role of low lying temporary anion states in the bond breaking process. The curve could be reproduced in magnitude and line shape by a model that simulates the electron capture cross section as it might appear in DNA owing to the π^* anion states of the bases (Aflatooni et al., 1998). The lowest peak in the modeled capture cross section, which occurs at 0.39 eV in the gas phase, was shifted by 0.41 eV to match that in the SSB yield and its magnitude normalized. Usually, in moving from the gas phase to the condensed phase, polarization effects shift the π^* resonances observed in the gas-phase to lower energies. However, in DNA the electric dipole fields created by the negatively charged phosphate groups and positive counter ions play a major role. The 0.4 eV positive shift could be explained by the phosphate charge which is closer to the bases, thus produces a net destabilization that slightly exceeds that of the polarization induced by the transient anion (Martin et al., 2004).

This interpretation of electron capture by the bases below 5 eV is corroborated by direct comparison with the DEA results (Denifl et al., 2004a, 2004b). The narrow peak near 1 eV has been interpreted as due to a dipole-bound anion (Scheer et al., 2004), which may not exist in DNA due to a cut-off of the long-range potential. There are two other features exhibiting a good energy correspondence with the maxima of 0.8 eV and 2.2 eV in DNA. Thus, both comparisons offer support for the charge transfer mechanism, an anionic potential surface exists that connects the initial π^* anion state of the base to a σ^* anion state of the phosphate group (Barrios et al., 2002). The σ^* state leads to rupture of the C-O bond connecting the phosphate group to the sugar. Transport of an electron from the base to the C-O σ^* antibonding orbitals of the sugar-phosphate takes place through three saturated

bonds. This is not surprising since there is ample precedence for such transfers leading to bond breaking in gas-phase DEA studies (Barrios et al., 2002; Cai et al., 2005). Furthermore, electron transfer from the bases is consistent with electron localization on the sugar-phosphate backbone leading to DNA damage (Boudaiffa et al., 2000a).

It is difficult to compare directly the yields obtained by LEE impact under UHV conditions, with those obtained from experiments in which DNA or other biomolecules are irradiated by high energy particles, mainly because of different experimental conditions, including the composition and conformation of the DNA. In addition, the dosimetry for LEE beam experiments is not available due to problems related to the energy imparted both to the DNA film and the metal substrate (Boudaiffa et al., 2000a, 2000b). By using an X-ray SE emission source, DNA damage induced by high energy photons ($Al_{k\alpha}$X-rays of 1.5 keV) and LEEs (average energy of 5.8 eV) under identical experimental conditions were directly compared (Cai et al., 2005). The exposure curves for the formation of SSB, DSB, and interduplex cross-links were obtained for both ML and thick films of DNA, respectively. The lower limits of G values for SSB and DSB induced by SE were derived to be 86 ± 2 and 8 ± 2 nmol J^{-1}, respectively; the average G values were about 2.9 and 3.0 times larger than those obtained with 1.5 keV photons.

Taking only the dose imparted by the slow SEs emitted from the tantalum substrate, a LEE enhancement factor (LEEEF) is defined as the ratio of yield of products in ML DNA induced by the LEE (slow SE, $E \leq 10$ eV) emitted from the metal substrate vs. that induced by the photons in a particular experiment. The LEEEF for 1.5 keV photons was derived to be at least 0.2 for both SSB and DSB, by taking average G values for SE (Henke et al., 1981). The extrapolated LEEEF for X-rays from 1.5 keV to 150 keV (i.e. to energies of

medical diagnostic X-rays) indicates that *SE electrons with the distribution and emission coefficient of Fig. 3 are 20-30 times more efficient to damage DNA than the X-ray photons of 40-130 keV that create them.* It can be seen that when electrons with the distribution of Fig. 3 strike a single DNA molecule, *they have on average a probability about 10^5 larger to damage DNA than 40-130 keV photons.* Hence, this first comparison study of DNA damage induced by X-rays and SE under identical experimental conditions shows LEE (E < 10 eV) to be much more efficient in causing SSB and DSB than X-rays.

I.5.2 Measurement of LEE interactions with DNA

I.5.2.1 Measurement of ions and neutral species by mass spectrometry

Some of the damage induced by LEE impact on biomolecules can be assessed by monitoring the *ions and neutral species* that desorb in vacuum during bombardment. Such measurements can be performed by placing the effusive beam or sample film near a mass spectrometer (Hervé du Penhoat et al., 2001). Generally, a LEE beam, emanating from an electron monochromator or a focusing electron gun, impinges onto the target. The full-width at half-maximum (FWHM) of the electron energy distribution varies from 0.03 to about 0.5 eV, depending on the type of electron source, for typical beam currents of 2-400 nA. In the gas phase experiments, the electron energy scale and the cross section for ion production are usually calibrated by measuring the anion signal from a gas which exhibits a resonance at a well defined energy, and whose DEA cross section is accurately known. Although this method provides an accurate energy calibration, it may overestimate the magnitude of the cross sections for non volatile biomolecules, since the latter may condense on chamber walls and thus reduce their background pressure relative to the calibrating gas.

Neutral species that desorb from the films and reach the ionizer of the mass spectrometer, can also be ionized and focused onto the quadrupole rods (Hervé du Penhoat et al., 2001). Charged particles are kept from reaching the ionizer by placing suitable potentials on grids or lenses located between the target and the ionizer. To increase the detection efficiency of desorbing neutral species, the latter can be ionized close to the target surface by a laser (Kimmel & Orlando, 1995). With a standard electron ionization source, the background signal can be discriminated by beam modulation lock-in techniques (Rakhovskaia et al., 1995).

Ions that emerge from an effusive beam or a film can be focused by ion lenses located in front of the mass spectrometer. In certain systems, the ion energies can be determined by a retarding potential or a deflector. Relative ion yields can be obtained from three different operating modes (Sanche, 1995): (1) the ion-yield mode, in which ions of a selected mass are detected as a function of incident electron energy, (2) the ion-energy mode, in which the ion current at a selected mass is measured for a fixed electron energy as a function of the retarding potential, and (3) the standard mass mode, in which the intensity of mass peaks is measured for a fixed electron energy.

I.5.2.2 Measurement by high resolution electron energy loss spectroscopy

High resolution electron energy loss (HREEL) spectroscopy, has recently been applied to probe *vibrational and electronic excitations* in biomolecules. With this technique (Sanche & Michaud, 1984; Ibach & Mills, 1982), electrons leaving a monochromator are focused on a gas jet or a metal substrate on which molecules are condensed. Electrons re-emitted from the target within a narrow cone at another angle are energy analyzed by a second electron deflector (i.e. the analyzer). Depending on the

apparatus, it may be possible to vary the angle of incidence or the analyzing angle or both. HREEL spectra are recorded by sweeping the energy of either the monochromator or the analyzer. The energy dependence of the magnitude of a given energy loss event (i.e. the excitation function) is obtained by sweeping the energy of both the monochromator and the analyzer with a potential difference between them corresponding to the probed energy loss. HREEL spectra are usually recorded at overall resolutions ranging from 6 to 80 meV FWHM with corresponding incident currents in the $10^{-10} - 10^{-8}$ A range.

HREEL spectroscopy has also been applied to the measurement of total absolute cross sections for fragment production by LEE impact on biomolecular films (Breton et al., 2004). In this case, the fragments, which remain trapped within the bulk of the film, are detected and quantified *in situ* by recording their electronic and/or vibrational HREEL spectra (Sanche & Michaud, 1984, Lepage et al., 1998).

I.5.2.3 Measurement of fragmentation products by X-ray photoelectron spectroscopy (XPS)

As with HREEL spectroscopy, XPS can also be utilized to probe the products formed by LEE impact on thin biomolecular films. In this case, changes in the binding energy of electrons in atomic shells serve to identify fragmentation products remaining in the film. The apparatus is similar to the one used to analyzed neutral and ion species (Hervé du Penhoat et al., 2001), but the mass spectrometer is replaced by an electron analyzer to measure the energy of photoelectrons; a source is added to irradiate the film with X-rays. Two different types of electron sources can be used to fragment the biomolecules: an electron gun or the photoelectrons emitted by the metal or semi-conductor substrate. As an example of a photoelectron electron source, Figure 3 shows the energy

spectrum of $Al_{k\alpha}$ X-ray induced SE emission from tantalum; it has a peak at 1.4 eV and an average energy of 5.8 eV (Cai et al., 2005). When the biomolecular film is sufficiently thin (< 5 nm), the number of X-ray photons absorbed by the biomolecules are negligible and the induced damage may be considered to result from electrons with the energies of the distribution shown in Fig. 3.

The cross sections for electron-induced reactions are determined by assuming that the analytical XPS elemental signals from the original compound and radiation products are described by exponential functions (Klyachko et al., 1999):

$$I_c = I_o \bullet \exp(-\sigma N t);\ I_r = I_o \bullet [1 - \exp(-\sigma N t)] \qquad (2)$$

where I_c and I_r represent the measured signals (XPS intensities) from a particular element in the original compound and the same element in the radiation products, respectively; σ is the cross section for the corresponding process, N is the flux density of incident X rays or electrons; t is the time of irradiation, and I_o is the maximum signal from the same element in the original compound as well as in the radiation products (i.e. measured at t = 0 and t T, respectively). Generally, measurements fit the above equations to within less than 10-15 % standard deviation (Klyachko et al., 1999). The validity of the above equations requires that the zone of analysis coincide with that of damage. This condition can be met for the experiments with SE from X-rays, but not with certainty for those with the electron-beam irradiation. Thus the absolute values for the cross sections of electron beam-induced damage may be lower than their true values. In principle, photons of energy lower than that of X-rays (UV and visible photons) could also be used to probe LEE induced processes within condensed biomolecules. So far, only electron trapping and transmission through short DNA oligomers have been measured with such techniques (Ray et al., 2005).

I.6 Description of the research project

The existing LEE techniques are only capable of analysing degradation products trapped in or desorbed from a condensed film, i.e. positive ion, negative ion, and neutral species can be measured. However, most of the non-volatile radiation products, which remain on the surface, have not been identified. There is a missing link of initial fast radiation process to the final damage to elucidate the chemistry involved in the electron-initiated reactions. Therefore, it is necessary by coupling chemical analysis with LEE irradiation to obtain the information of the structure of final products. The objective of this research project is to study chemical modifications of DNA induced by LEE, starting with basic DNA components.

A novel sample spin coating and LEE irradiator system has been set up that can prepare a uniform film of biomolecules and bombard the inside surface of a cylinder target. With this configuration, we are able to irradiate a surface a hundred times larger than with a conventional electron gun, and therefore, provide a sufficient amount of damaged sample for chemical analysis outside vacuum. After recovered from the substrate, the sample is first separated by HPLC, then collected and further analyzed by GC-MS or ESI/MS/MS. The detailed description can be found in chapter II.

By using this new apparatus, films of biological molecules can be investigated. The initial study is a relatively simple DNA nucleoside, thymidine and constitutes the second article (chapter III). The results show that LEE irradiation induces glycosidic bond cleavage in thymidine and gives thymine as a major product, via a non-ionizing resonant process. In

contrast, this reaction is very inefficient upon DNA ionization and does not occur by the reaction of solvated electrons with DNA. It points to a new mechanism of DNA damage involving LEEs that is different than the well-studied pathways of DNA damage, involving base ionization, OH radical and solvated electrons.

Furthermore, LEE irradiation of more complex DNA components: nucleotide and oligonucleotides are studied. First thymidine monophosphate (Tp) was exposed to LEE (15 eV) that leads to two major products: thymine and thymidine. This indicates two major pathways induced by LEE-induced damage of dTp: one involving cleavage of the glycosidic bond separating the base and sugar phosphate moieties, which leads to the release of non-modified thymine; and the other implicating cleavage of the phosphodiester bond, which leads to the release of non-modified thymidine.

Two oligonucleotide tetramers (CGTA and GCAT) were irradiated with mono-energetic LEE, which is included in the third and fourth article (chapter IV and V). The products of irradiation were examined by HPLC and identified as 16 non-modified nucleobase, nucleoside and nucleotide fragments resulting from the cleavage of phosphodiester and *N*-glycosidic bonds of each tetramer. This is consistent with results of the nucleotide. In addition, the distribution of non-modified products suggests a mechanism of damage involving initial electron attachment to nucleobase moieties, followed by electron transfer to the sugar-phosphate backbone, and subsequent dissociation of the phosphodiester bond. These results demonstrate that the phosphodiester bond breaks by a distinct pathway in which the negative charge localizes on the phosphodiester bond giving rise to non-modified fragments with an intact terminal phosphate group.

It is difficult to distinguish between initial attachment of LEE to phosphate groups and initial attachment to bases followed by transfer to phosphate groups. To solve this problem, the cleavage of modified oligonucleotide with an abasic site, where electrons can only go to the phosphodiester backbone, is studied and compared with non-modified oligos. In detail, four modified tetramers: XCAT, GXAT, GCXT and GCAX were examined, where X denotes a stable abasic site. These analyses show that the yield of strand breaks induced by LEE was much higher for GCAT compared to abasic tetramers. Interestingly, LEE induced cleavage reactions were greatly impeded next to the abasic site. A likely interpretation is that DNA bases initially capture LEE, and then, the electrons are transferred to the sugar-phosphate group, which induces sugar-phosphate C-O bond rupture.

In conclusion, our studies support electron transfer of LEE from the base moiety to the sugar-phosphate backbone in DNA as suggested by theoretical studies. Such a mechanism of damage suggests that the capture of non-thermalized electrons with 4-15 eV of energy by DNA bases may be an important factor in DNA damage in living cells. The present research provides a chemical basis for the formation of strand breaks and base release by the reaction of LEE with DNA.

Chapter II – First article

Irradiator to Study damage induced to large nonvolatile molecules by Low-energy Electrons

Yi Zheng, Pierre Cloutier, J. Richard Wagner, Léon Sanche

Review of Scientific Instruments, **2004**, *75*, 4534.

Irradiator to Study Damage Induced to large Non-Volatile Molecules by Low-energy Electrons

Yi Zheng,[a] Pierre Cloutier, J. Richard Wagner, and Léon Sanche

Group in the Radiation Sciences, Faculty of Medicine, University of Sherbrooke, Sherbrooke, Québec, Canada J1H 5N4

Abstract

We report on the design and performance of an irradiator to study the fragmentation of large non-volatile molecules induced by low-energy electron impact under ultra-high vacuum. The apparatus consists essentially a new type of electron gun which can bombard molecules spin-coated on the inside surface of a cylinder. With this configuration, it is possible to irradiate a relatively large area (26 cm^2) of a solid molecular film and thus, produce a sufficient amount of degraded material for subsequent analysis, outside vacuum, of the compounds remaining on the inner surface of the cylinder. The electron energy is tunable from 3 to 130 ± 0.5 eV and the current density adjustable up to 2.6 ± 0.5 × 10^{12} electron s^{-1} cm^{-2}, respectively. Choosing thymidine as a model system for DNA damage, we show that non-volatile fragments produced by 5-100 eV electron irradiation can be characterized by High-pressure liquid chromatography/Ultraviolet detector (HPLC/UV) and Gas chromatography/Mass spectroscopy (GC/MS).

a) Author to whom correspondence should be addressed; electronic mail: Yi.zheng@usherbrooke.ca

INTRODUCTION

Molecular decomposition and reactions induced under ultrahigh vacuum (UHV) conditions, by low energy electrons (LEEs) impinging on molecules deposited on various metallic surfaces have recently received considerable attention. This research has been in large part motivated by the important role of LEEs in radiobiology,[1,2,3] dielectric aging[4,5] and surface chemistry.[6,7] Detection of the various fragments generated by low-energy (0-100 eV) electron impact often provides information to determine the many dissociation pathways and the major products formed. In this regard, several methods, having their own specificities and limitations, have been proposed and used in the past. If sufficient kinetic energy is imparted to charged fragments, they may be ejected from the surface and detected on the basis of their negative or positive charge, energy, and mass.[8,9,10] Conversely, if they are trapped in the solid, an energy dependent charging rate can be measured.[11] Desorbed neutral fragments[12,13] are most efficiently detected when they are electronically excited (e.g., metastable).[4] For those remaining trapped in the solid or at its surface, one often relies on vibrational[14,15] spectroscopy of the fragments as well as UV and x-ray photoemission spectroscopy.[16] The common goals shared among these various methods are the identification of the products along with the electron energy dependence of their yields. With some methods the first goal is often not tackled satisfactorily. For example in the case of temperature programmed desorption,[17] which essentially relies on heating and sublimation techniques for the detection of neutral products, subsequent recombination and composition may be induced by heating and thus possibly complicate identification of the initial fragments.

In the case of complex non-volatile molecules (e.g., large biomolecules), deposited as single and multilayer films, the analysis of the neutral products remaining on the metal surface may be much more difficult. The molecule may have too many degrees of freedom and energy levels to allow unambiguous identification of new surface species by vibrational and UV and X-ray photoemission spectroscopies, respectively. If analysis *in vacuo* is not possible, in principle, one could recuperate and analyze the products remaining on the surface by chemical methods such as electrophoresis, chromatography and GC/MS outside the vacuum chamber. However, for such analysis much larger quantities of fragments must be produced than in the desorption and micro-analysis experiments, particularly if the yields are small (e.g. <1%). More products can be made by increasing the thickness of the deposited film, the electron current and the bombarded surface area of the target. However, for most organic and biomolecules which are insulators, the film must be kept sufficiently thin (10-100 Å) to avoid significant surface charging by the impinging electron beam. In the desorption experiments, the electron beam is usually well focused on a small spot on the target film and the neutral and ionic species desorbed from that location are analysed by a mass spectrometer. It is possible to detect and analyze desorbing ions and volatile neutral products with incident currents in the range 1-100 nanoampere, down to about 1-3 eV, without significant beam divergence due to space charge, film charging and loss of beam resolution. This is no longer possible with higher current and/or thicker films. Furthermore, if the electron dose is too large, secondary reactions occur and do not allow unambiguous identification of the primary dissociation products.

A simple solution to these problems is to design an electron gun capable of bombarding a large sample area, so as to lower the density of trapped electrons, the current density, and the effects of space charge in the beam, while increasing the total current at the target and the amount of fragmented material. Another possibility is to produce only a very small amount of degraded material, with a standard electron gun,[18] but find a technique to amplify considerably specific damages to the molecules. For example, in experiments with supercoiled plasmid DNA, irradiated by an electron gun focused on a 7 mm^2 area in the energy range 3-1500 eV, the samples are recuperated from UHV and the strand breaks are analyzed by electrophoresis out of vacuum.[19,20,21] *Ex-vacuo* detection of single and double strand breaks in DNA is possible due to the large amplification factor that results from the change in the topological form of the plasmid (e.g., from the supercoiled to the circular and linear configuration, respectively), when one or two strands are broken. However, such a huge amplification factor does not exist for most non-volatile molecules and biomolecules; in any case, the method is limited to a specific type of damage. Thus, the analysis of most of the non-desorbing fragments produced by LEE impact on any film consisting of large non-volatile molecules requires the development of a more general technique.

We describe in this article a novel LEE irradiator capable of processing large quantities of non-volatile organic and biomolecules, spread out on a large surface area. A method for preparing films of such molecules over a large area is also described and the performance of the irradiator reported. Since we are principally interested in applying this method to LEE damage induced to biomolecules, we have chosen a basic DNA constituent, thymidine, as model compound.

The application of our technique to LEE-induced fragmentation of biomolecules is of particular importance to investigate the mechanisms of radiobiological damage, more specifically to study the modification of genetic material.[3,22,23,24] Modification of cellular biomolecules and DNA is the result of energy transfer via a variety of excitation and ionization processes triggered by the motion of fast particles along their tracks,[3,25] leading to the production of copious amounts of ionic species, reactive free radicals and secondary LEEs (<30 eV).[22,23,26] It is relatively well understood how ions and radicals participate in the production of biologically significant lesions.[1,2] However, much less is known about the action of secondary electrons having energies lower than 100 eV, which acquire over 40% of the energy transferred by the fast primary particles.[26] Since the interactions of LEEs with vital cellular components, such as DNA, occur at very early times (< 10^{-13} s) after their creation, their specific action cannot be time-resolved with present techniques of pulse radiolysis.[27] However, such interactions can be studied in experiments where the primary radiation is a source of LEEs.[28,29,30,31,32,33,34,35,36,37,38] Recently, it has been possible to perform electron stimulated desorption experiments on solid films of biomolecules, which are condensed onto a metal substrate in a UHV system or transported into UHV from a controlled atmosphere. In this manner, some of the immediate small fragments produced by high-energy radiation at short times were detected in biomolecules such as H_2O,[28] 2-deoxyribose analogues,[29] DNA and RNA bases,[30,31,32] amino acids,[33] oligonucleotides[34,35,36] and DNA.[37,38] The present method provides the possibility to analyze the non-desorbing products induced by LEE impact from such biomolecules.

I. DESIGN AND PROCEDURE

A. Spin coating

The biomolecules under investigation are spin coated onto the inner surface of tantalum cylinders. A schematic diagram of the spin coating apparatus is shown in Figure 1. The apparatus is housed in a stainless steel vacuum chamber (I) equipped with a plexiglass cover. In this chamber, a long sleeve (J) holds the seven cylinders (K), which can be filled with a solution containing the sample molecules. The cylinders can rotate on ball-bearing shafts (L1 and L2) which are magnetically coupled (M) to an external electric motor (N).

Seven tantalum cylinders (K) are packed into the sleeve (J) with Teflon spacers (O) that isolate each cylinder with a rim on each side. Each spacer has three apertures for injection of a solution of the sample molecules independently onto the inner surface of each cylinder. The entire assembly is inserted into the sleeve (J) along which were drilled symmetric holes for the injection of the solution and to provide adequate pumping speed to rapidly eliminate the solvent. Prior to filling with the solution, the sleeve is mounted onto the shaft axis of the spin coating system (L1 and L2), the horizontal position of which is adjusted with a spirit-level via a set of screws. Afterwards, the chamber is closed and the tube rotated to an angular velocity up to around 1500 rpm. At this speed, the centripetal acceleration reaches 32 g and the liquid is uniformly distributed over the inner surface of each cylinder. Pumping is then initiated causing the pressure to rapidly drop from atmosphere to 2-5 Torr. During this time the liquid cools down and freezes onto the metal-substrate. Sublimation is assumed to be completed when the pressure drops below the 2-5 Torr range, and then rapidly reaches 100 mTorr. This step

usually takes between 15 and 30 minutes depending on the solvent. At this time, rotation is stopped and the vacuum chamber (I, in Figure. 1) is transported into the glove box (G) shown in Figure. 2 and opened under a dry N_2 atmosphere to transfer the coated cylinders into the irradiator chamber without exposure to the contaminants in the ambient atmosphere.

Biomolecules can be dissolved in water or some other appropriate solvent at a concentration C. Each tantalum cylinder (inner radius = 13 mm and height = 32 mm) can receive about 0.7ml of solution. Assuming that the molecules are uniformly distributed on the inside surface of the cylinder, the thickness D of molecular films deposited on the metal substrate is determined from the following equation, viz.

$$D = \frac{C \cdot V \cdot M}{\rho \cdot S} \qquad (1)$$

where V is the volume of solution, M the molecule weight, ρ the density of molecules and S the surface area of the inside wall of the cylinder.

B. Low energy electron irradiator

Figure 2 presents a schematic diagram of the principal components of the LEE irradiator and the UHV chamber. The assembly consists essentially of a new type of electron gun (A) mounted on a linear drive (B), and a rotatable circular platform (C) supporting a cylindrical multiple-electrode electron current detector (D) with holes to secured the seven tantalum cylinders (E). Rotation of the cylinders secured to the platform C allows each sample to be bombarded by the electron gun E at a specific energy and current for a given time. The UHV chamber can be opened by a quick access

port (F) from the inside of a glove box (G), kept under a dry N_2 atmosphere. Oil-free turbomolecular drag and diaphragm pumps allow the chamber to be pumped rapidly from atmospheric pressure to the 10^{-9} Torr range without significant hydrocarbon contamination.

The gun A can irradiate the inner surface (26 cm^2) of a tantalum cylinder with 3-130 eV electrons having an absolute energy spread of 0.5 eV full width at half maximum. Figure 3 shows the principle of operation of this new type of electron gun. Electrons are emitted from a tantalum disk cathode and pass through the apertures at the center of four molybdenum discs which are electrically isolated by sapphire balls (Figure 3b). These disks serve as a defocusing electron lens to expel electrons away from the gun axis and thereby, produce a divergent electron beam. Subsequently, electrons with kinetic energy around 2 eV, enter an electric field free region. In this region, a small coil (average r = 6 mm) of 20 turns produces a non-uniform magnetic field, **B**, of 5-50 gauss at the coil centre, which modifies the trajectories of the electrons; first by collimating them on the axis and then, in the diminishing **B** field region, by releasing them toward a molybdenum cylindrical mesh grid (transmission = 86%), integrated into the gun assembly. As shown in Figure. 2, by placing the gun A on top of a cylinder secured to the rotating platform, the cylindrical grid can be inserted inside E by adjusting the linear feedthrough B. Applying an appropriate potential energy difference between the cylinder walls and the filament of electron gun allows one to control the electron impact energy.

Figure 3a shows the gradient of the magnetic field **B** in the irradiator. Between the last electrode of the lens system and the coil, the electrons are progressively confined on the axis and gyrate under the action of the combined electric and magnetic fields. In the

grid region, where there is a considerable reduction of **B**, the velocity vector of the electrons perpendicular to the axis previously confined by **B** is released, and the beam starts to disperse in a direction perpendicular to the axis. After they have reached the grid, electrons are accelerated to the desired energy by the electric field between the grid and the metal substrate. In order to optimise the physical parameters of the electron gun to obtain the most uniform distribution of the electrons on the sample, we have simulated many electron trajectories for different parameters [i.e. the distance between the electron source and the coil (3 cm), the dimension of the grid (2.1 cm diameter x 5.5 cm length), the position of the cylindrical substrate, etc.]. The appendix shows the solution of the equation of motion ($\mathbf{F} = e\mathbf{v} \times \mathbf{B}$) with the "refixed function" of the Mathcad Software. Note that the coil has been discretised into 30 portions and the magnetic field calculated at all points of the trajectory. An example of an electron trajectory is illustrated in Figure 3b.

Once the geometrical parameters have been determined, four others can still be varied to obtain a uniform electron current density at the sample surface: 1. the different voltages applied on the first four disks of the lens creating the divergent electron beam; 2. the kinetic energy of the electrons in the magnetic field region; 3. The intensity of the magnetic field (5-50 gauss measured at the coil center); 4. the axial position of the electron gun with respect to the sample substrate. Before irradiation, the grid is inserted into the detector, shown in Figure 3c, which is composed of twelve cylindrical electron collectors. Its inner dimensions are the same as those of the cylinders. The currents arriving at each of the twelve collectors are amplified and graphically displayed simultaneously on a computer screen. By tuning the four parameters of the electron gun,

the currents on the twelve detectors are adjusted to be the same within 10% of the average current. For example, to achieve a uniform current density at an electron energy at 15 eV, the potential of the filament is set at minus 15 V with respect to the ground potential (0 V) of the cylinders. The four disks of the lens and magnetic coil-grid region are set at 6.3, 34, 22.2, 33.8 and 2.8 V with respect to the potential of filament, respectively. The magnetic field in the center of the coil is set at 17 gauss. This procedure ensures a uniform incident current over the entire sample surface of the cylinder during bombardment. The electron current density can be adjusted up to $2.6 \pm 0.5 \times 10^{12}$ electron s^{-1} cm^{-2}.

After irradiation, the tantalum cylinders are mounted with Teflon caps for recovery, and each of them filled with 12ml of the same solvent as used for spin coating and placed in an ultrasonic bath to completely dissolve the irradiated sample. Finally, the resulting solution is analyzed by HPLC/UV and GC/MS.

II. Performance

A. Sample distribution on the cylinder surface

The spatial distribution of the molecules spin-coated onto tantalum cylinders was monitored by autoradiography. The autoradiograms of the inner surface of the cylinders were recorded after deposition of a methanoic solution of thymidine containing P^{32} labeled adenosine 5'-triphosphate (ATP). The photographic film, which reflected the amount of P32 ATP on the surface, was scanned with the software UNSCANIT GEL (Silk Scientific Corp.) along the dimension of the length of the cylinder. The film was divided into 13 sections, B to N, which represented bands parallel to the length of the

cylinder. For each band, each pixel was digitized corresponding to its gray scale defining the white as equal to zero, giving a continuous line along the length axis. In this manner, we were able to construct a 3-dimensional image of the cylinder surface shown in Figure 4. The coordinate intensity represented the relative number of surface molecules that were deposited on the inside surface of the tantalum cylinder, as a function of length along the axis and angular position (bands B to N). The distribution was reasonably uniform with an average intensity of 620 in the middle of the surface, except for an increase near the edges of the cylinder.

B. Results of the HPLC analysis

In this section, we performed a series of experiments to validate the new LEE irradiator using thymidine (amu=242) as a biomolecular target. A thymidine film cannot easily be prepared by evaporation on a metal substrate in vacuum, because it readily decomposes above 150 °C below its melting point of 185 °C.[39]

Thymidine (Sigma Chemical) was dissolved in methanol (HPLC grade) at a concentration 54 μM and 0.7 ml of this solution was spin-coated onto the cylinder wall to produce a film with an average of 5 monolayers. After electron bombardment, each tantalum cylinder was filled with 12 ml methanol and placed in an ultrasonic bath for 10 minutes. Afterwards, the irradiated solution was concentrated to 60 μl and subjected to an HPLC analysis. The LEE induced products were then separated using an ODS-AQ column (150×6mm) with 10% methanol solution at a flow rate of 1 ml/min, and the products were monitored using a photodiode array detector (Waters Model 996).

The background level of damage was determined by the analysis of samples that were spin coated on tantalum, introduced into the vacuum chamber, and subsequently recuperated from the substrate without irradiation. Figure 5 displays the HPLC analysis of different samples. From comparison with control samples, the most important changes in the profile of products were observed for thymine (8.3 min) and thymidine (15.9 min). Although some thymine was produced in unirradiated sample, i.e., due to its interaction with tantalum, Figure 5 clearly showed that a large amount of thymine was induced by LEE irradiation. It was also obvious from Figure 5 that electrons with different incident energies lead to different quantities of damaged thymidine. In recent work using this apparatus,[40] the HPLC peak at 8.3 min was identified as thymine by GC/MS. In conclusion, irradiation of large biomolecules by this type of LEE gun can produce sufficient amounts of fragments for recuperation and analysis by HPLC/UV and GC/MS.

C. Reproducibility of product analysis

In order to verify the reproducibility of our measurements, at different stages of the experiment, we measured the magnitude of the thymidine peak in HPLC chromatograms to determine the percentage of recovery under different conditions. Table 1 shows the results obtained from seven samples. For the first batch (A), the seven samples were recuperated after spin-coating and analyzed by HPLC. The measured areas under the peaks are compared with those of two other batches: one was transferred to the irradiation chamber but not irradiated (B) while the other was irradiated (C). We conclude that neither spin-coating nor UHV affects the decomposition of thymidine, whereas electron bombardment leads to a significant decrease in the amount of thymidine remaining on the surface. The total standard deviation of these measurements was 8%,

6% and 8%, respectively, indicating that these analyses can be performed with good reproducibility, from an average of different measurements.

D. The yield of thymine vs electron energy

The formation of thymine as a function of exposure time to the LEE beam was measured at different electron energies. With a constant electron beam flux of 10.6 μA = 6.6 x 10^{13} electrons/sec, the amount of thymine produced was determined by HPLC/UV analysis for 6 different irradiation times (1-8 min). At exposure times >3 min, the yield of thymine reached a plateau, whereas for shorter times, the yields of thymine were linear with exposure. Under these conditions, the formation of thymine should result from a single electron collision. The quantum yields of thymine were determined from the initial slopes of the exposure-response curves recorded at different electron energies. The yield function of thymine thus obtained is displayed in Figure. 6. It reveals the presence of a broad peak in the 10-20 eV region, a dip around 20-30 eV and a maximum at 100 eV. In large molecules, this behavior is characteristic of molecular dissociation via a combination of resonance and direct scattering.[41] Direct electronic excitation leads to the formation of neutral products or to the creation of a cation and an anion. The yields of these products, formed via direct scattering, usually exhibit an increase as the function of electron energy and reach a maximum above 50 eV. In large molecules, resonance scattering (i.e. dissociative electron attachment or resonance decay into a dissociative state) usually produces a maximum around 10 to 15 eV. Combining these two processes may produce a minimum around 20-30 eV as seen in Figure 6. An example of a similar observation may be found in the electron stimulated anion desorption yield from DNA bases[42] and DNA stand breaks[43]. Thus, the maximum around 10-20 eV in the yield

function can be attributed to electron attachment to thymidine leading to the formation of transient anions.[41] These latter can decay by electron emission or can dissociate into a stable anion and a neutral fragment. Electron emission could also leave the target in a dissociative electronic state that could produce two radical fragments or a pair of ions. Both of these pathways could lead to the formation of thymine by cleavage of at the N1-glycosidic bond, as previously suggested.[40] Thus, the present results indicate that our apparatus can provides quantitative data allowing one to define the energy of electron resonances as well as their role in the fragmentation of biomolecules by LEEs.

ACKNOWLEDGMENTS

The authors would like to thank Drs Darel Hunting and Xifeng Li for helpful comments and suggestions. Also the professional assistance of Dr. Andrew Bass in electron trajectory calculations is gratefully acknowledged. Financial support for this work was provided by the Canadian Institutes of Health Research.

Appendices:

Calculation of an electron trajectory

Coil definition:

Coil current	Coil radius	Number of turns	Number of current elements
$I := 2.4$	$R := .006$	$S := 20$	$N := 30$

Constants:

$$\mu_0 := 4\cdot\pi\cdot 10^{-7} \qquad \kappa := \frac{\mu_0 \cdot I \cdot S \cdot R}{2 \cdot N} \qquad \chi := \frac{1.602 10^{-19}}{9.109 10^{-31}} \quad \text{(e/m)}$$

Magnetic field at the point (X,Y,Z) using Biot-Savard Law:

$$\begin{aligned}
H(X,Y,Z) := \;& B_0 \leftarrow 0 \\
& B_1 \leftarrow 0 \\
& B_2 \leftarrow 0 \\
& \text{for } n \in 0..N-1 \\
& \quad \phi \leftarrow n \cdot \frac{2\cdot\pi}{N} \\
& \quad x \leftarrow X - R\cdot\cos(\phi) \\
& \quad y \leftarrow Y - R\cdot\sin(\phi) \\
& \quad z \leftarrow Z \\
& \quad D \leftarrow \left(x^2 + y^2 + z^2\right)^{\frac{3}{2}} \\
& \quad B_0 \leftarrow B_0 - \frac{\kappa}{D}\cdot z\cdot\cos(\phi) \\
& \quad B_1 \leftarrow B_1 - \frac{\kappa}{D}\cdot z\cdot\sin(\phi) \\
& \quad B_2 \leftarrow B_2 + \frac{\kappa}{D}\cdot(y\cdot\sin(\phi) + x\cdot\cos(\phi)) \\
& B
\end{aligned}$$

Calculation of the trajectory of an electron:

Initial conditions: Energy (eV) Polar and azimuthal angles

$$E := 3 \qquad \theta := 3\cdot\frac{\pi}{180} \qquad \alpha := 45\cdot\frac{\pi}{180}$$

Calculation of velocity components:

$$v := \sqrt{2\cdot E\cdot\chi}$$

$$vp := v\cdot\sin(\theta)$$
$$vz := v\cdot\cos(\theta)$$
$$vx := vp\cdot\cos(\alpha)$$
$$vy := vp\cdot\sin(\alpha)$$

$$C := \begin{bmatrix} 0 \\ 0 \\ -0.027 \\ vx \\ vy \\ vz \end{bmatrix}$$

$$D(t, C) := \begin{bmatrix} C_3 \\ C_4 \\ C_5 \\ \chi \cdot \left(C_4 \cdot H\left(C_0, C_1, C_2\right)_2 - C_5 \cdot H\left(C_0, C_1, C_2\right)_1 \right) \\ \chi \cdot \left(C_5 \cdot H\left(C_0, C_1, C_2\right)_0 - C_3 \cdot H\left(C_0, C_1, C_2\right)_2 \right) \\ \chi \cdot \left(C_3 \cdot H\left(C_0, C_1, C_2\right)_1 - C_4 \cdot H\left(C_0, C_1, C_2\right)_0 \right) \end{bmatrix}$$

Number of steps in the trajectory

$S := 60$

$\tau := \frac{.09}{v}$

(Solving differential equations using Runge-Kutta technique)

$NC := rkfixed(C, 0, \tau, S, D)$

$NX := NC^{\langle 1 \rangle}$ $NY := NC^{\langle 2 \rangle}$ $NZ := NC^{\langle 3 \rangle}$

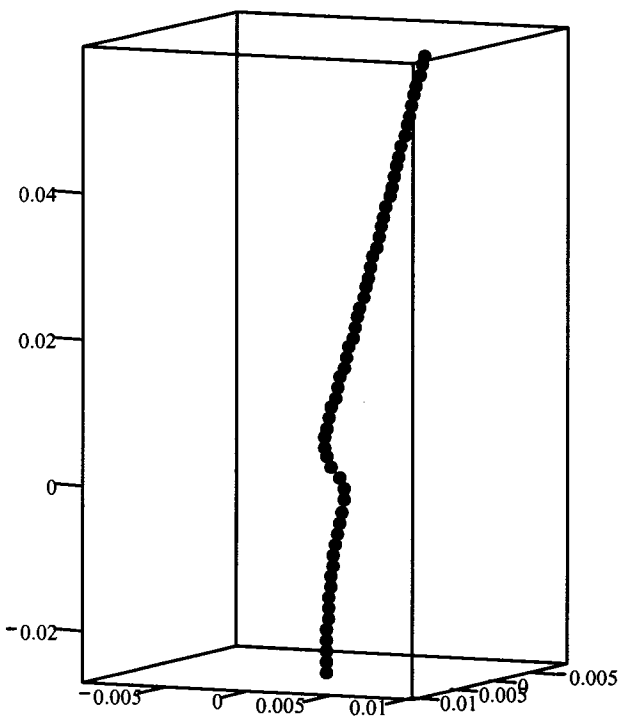

NX, NY, NZ

References

1. C. Von Sonntag, *The Chemical Basis of Radiation Biology* (Taylor and Francis, London, 1987).
2. J. F. Ward, Radiat. Res. **138**, S85 (1994).
3. H. Nikjoo, P. O'Neil, M. Terrissol, D.T. Goodhead, Radiat. Environ. Biophysics **38**, 31 (1999).
4. L. Sanche, IEEE Trans. Electrical Insulation, **28**, 789 (1993).
5. R.M. Marsolais, E.A. Cartier and P. Pluger, in *Excess Electrons in Dielectric Media*, edited by C. Ferradini and J.-P. Jay-Gerin, (CRC, Boca Raton, 1991), Chap. 2.
6. Z.-M. Liu, X.-L. Zhou, and J. M. White, Chem. Phys. Lett. **198**, 615 (1992).
7. X.-L. Zhou, S.R. Coon, and J .M. White, J. Chem. Phys. **92**, 1498 (1990).
8. P.M. Dehmer, in *Desorption Induced by Electronic Transitions*, DIET I, edited by N. H. Tolk, M. M. Traum, J. C. Tully and T. E. Madey (Springer, Berlin, 1983).
9. T. E. Madey, D. L. Doering, E. Bertel, and R. Stockbauer, Ultramicroscopy **11**, 187 (1983).
10. F. Weik and E. Illenberger, J. Chem. Phys. **103**, 1406 (1995).
11. L. Sanche, A. D. Bass, P. Ayotte, and I.I. Fabrikant, Phys. Rev. Lett. **75**, 3568 (1995).
12. P. Rowntree, P.-C. Dugal, D. Hunting and L. Sanche, J. Phys. Chem. **100**, 4546 (1996).
13. A.R. Burns, E.B. Stechel, D. R. Jennison and T. M. Orlando, Phys. Rev. B **45**, 1373 (1992).
14. C.O. Olsen and P.A. Rowntree, J. Chem. Phys. **108**, 3750 (1998).

15. R. Martel, A. Rochefort, and P. H. McBreen, J. Am. Chem. Soc. **116**, 5965 (1994).

16. D. V. Klyachko, P. Rowntree and L. Sanche, Surf. Sci. Lett. **346**, L49 (1996).

17. T. D. Harris, D. H. Lee, M. Q. Blumberg and C. R. Arumainayagam, J. Phys. Chem. **99**, 9530 (1995).

18. M. A. Huels, J. Khoury, B. Gueraud, B. Boudaiffa, P. C. Dugal, D. Hunting, L. Sanche, A. J. Waker, *Microdosimetry* (Royal Society of Chemistry, 1997), 89.

19. B. Boudaiffa, P. Cloutier, D. J. Hunting, M. A. Huels, L. Sanche, Science **287**, 1658 (2000).

20. B. Boudaiffa, D. J. Hunting, P. Cloutier, M. A. Huels, L. Sanche, Intern. J. Radiat. Biology **76**, 1209 (2000).

21. B. Boudaiffa, P. Cloutier, D. Hunting, M. A. Huels, L. Sanche, Radiat. Res. **157**, 227 (2002).

22. D. T. Goodhead, International J. of Radiation biology **65**, 7 (1994).

23. J. A. Laverne, S. M. Pimblott, Radiat. Res. **71**, 467 (1995).

24. G. Illiakis, Y. Wang, J. Guan, H. Wang, Oncogene **22**(37), 5834-5847, (2003)

25. V. V. Moissenko, R. N. Hamm, A. J. Waker, W. W. Prestwich, Radiat. Environ. Biophysics **37**, 167 (1998).

26. V. Cobut, Y. Frongillo, J. P. Patau, T. Goult, M.-J. Fraser, J.-P. Jay-Gerin, Radiat. Phys. Chem. **51**, 229 (1998).

27. E. J. Land, C. A. Ramsden, P. A. Riley, J. Photochem. & Photobiol. B: biology, **64**, 123-125 (2001).

28. W. C. Simpson, T. M. Orlando, L. Parenteau, K. Nagesha, L. Sanche, J. Chem. Phys. 108, 5027 (1998).

29. D. Antic, L. Parenteau, M. Lepage, L. Sanche, J. Phy. Chem. 103, 6611 (1999).

30. M. Hervé du Penhoat, M. A. Huels, P. Cloutier, J.-P. Jay-Gerin, L. Sanche, J. Chem. Phys. 114, 5755 (2001).

31. H. Abdoul-Carime, P. Cloutier, L. Sanche, Radiat. Res. 155, 625 (2001).

32. D. V. Klyachko, M. A. Huels, L. Sanche, Radiat. Res. 151, 177 (1999).

33. H. Abdoul-Carime, L. Sanche, Radiation Research 160(1), 86-94, (2003).

34. P. C. Dugal, H. Abdoul-Carime, L. Sanche, J. Phys. Chem. 104, 5610 (2000).

35. P. C. Dugal, M. A. Huels, L. Sanche, Radiat. Res. 151, 325 (1999).

36. H. Abdoul-Carime, P. C. Dugal, L. Sanche, Radiat. Res. 153, 23 (2000).

37. B. Boudaiffa, P. Cloutier, D. J. Hunting, M. A. Huels, L. Sanche, Science 287, 1658 (2000).

38. B. Boudaiffa, D. J. Hunting, P. Cloutier, M. A. Huels, L. Sanche, Intern. J. Radiat. Biology 76, 1209 (2000).

39. S. A. Krasnokutski, A. Yu. Ivanov, V. Izvekov, G. G. Sheina, Yu. P. Blagoi, J. Molecular Structure 482, 249 (1998).

40. Y. Zheng, P. Cloutier, D. Hunting, J. R. Wagner, L. Sanche, JACS **126**, 1002 (2004).

41 L. Sanche, Mass Spectrometry Rev. **21**, 349 (2002).

42. H. Abdoul-Carime, P. Cloutier, L. Sanche Radiation Research, **155,** 625-633 (2001).

43 M. A. Huels, B. Boudaiffa, P. Cloutier, D. Hunting, L. Sanche J. Am. Chem. Soc., 125, 4467 (2003).

Table 1. The area under thymidine peaks obtained by HPLC analysis of measurements performed at different stages of the sample treatment. A- the sample was analysed after spin coating, B- the sample was placed under vacuum but not irradiated, C- same as B except that the sample was irradiated at an incident electron energy of 30eV with an exposure of 7.2×10^{14} electron cm^{-2}.

Measurement condition	Area of thymidine at 260nm (a.u.)								Error* (%)
	1	2	3	4	5	6	7	Average	
A: After spin-coating	14.7	17.1	16.1	13.8	16.5	15.9	14.7	15.5	± 8
B: Not-irradiated	15.1	15.5	14.1	16.8	16.2	15.9	14.3	15.4	± 6
C: Irradiated	12.4	12.6	11.0	14.0	13.3	13.4	11.7	12.6	± 8

* Standard deviation divided by average ×100

Figure captions:

Figure 1. (Color online) Schematic diagram of the spin coating system: I- vacuum chamber, J- tube holder, K- sample substrate, L_1 and L_2- ball-bearing shafts, M- magnetic coupling, N- electric motor, O- Teflon spacer.

Figure 2. General view of UHV electron irradiator chamber, A- electron gun, B- linear drive, C- rotatable disk used as cylinder support, D- electron current detector, E- cylindrical sample substrate, F- quick access port, G- glove box sealed under an N_2 atmosphere, H- ion gauge.

Figure 3. Schematic diagram of the composite elements of the divergent beam low energy electron gun; a: the gradient of the non-uniform magnetic field (curved lines) and the simulated three dimensional electron trajectories for an emission at angle of 3° from the filament (shaded surface); b: cross section view of the gun in a position to bombard the inside of a tantalum cylinder used as sample substrate; c: multiple-electrode electron current detector.

Figure 4. Three-dimensional scan of an autoradiogram of the inside wall of a cylinder covered with sample molecules radiolabelled with ^{32}P. The vertical scale represents the radioactive intensity, which is proportional to the number of molecules covering the surface. The ^{32}P intensity is plotted as a function of its position along the length of the cylinder (horizontal coordinate) and angular position around the inner radius of the cylinder (B to N).

Figure 5. (Color online) HPLC/UV analysis of different thymidine samples. The separation of the products was performed using an ODS-AQ column with 10% methanol as the mobile phase and UV detection at 260 nm. In addition to the thymidine peak,

another main peak corresponding to thymine was detected near 8 min elution time. Its magnitude is considerably enhanced by irradiation with an exposure to 7.2×10^{14} electron cm^{-2} at 30 and 50 eV.

Figure 6. Measured quantum yields of thymine per incident electron impinging on thymidine films as a function of incident electron energy. The yields were determined from the initial slopes of the incident electron exposure-response curves at each incident energy recorded with the same incident current of 10.6 μA. The error bars correspond to the measurement uncertainty of each point. The curve is a guide to the eye.

Chapter III – Second article

Glycosidic bond cleavage of thymidine induced by low energy electrons

Yi Zheng, Pierre Cloutier, Darel J. Hunting, J. Richard Wagner, Léon Sanche

Journal of American Chemical Society, ***2004,*** 126, 1002.

Glycosidic bond cleavage of thymidine by low energy electrons

Yi Zheng, Pierre Cloutier, Darel J. Hunting, J. Richard Wagner*, Léon Sanche

Canadian Institutes of Health Research Group in the Radiation Sciences, Faculty of medicine, University of Sherbrooke, Sherbrooke, QC, Canada J1H 5N4

It is well known that high-energy ionizing particles induce DNA strand breaks, which can be toxic, mutagenic and recombinogenic. However, recent experiments and theoretical studies have demonstrated that at very low energies (5-20 eV), even below the ionization threshold, electrons induce single and double strand breaks in DNA via dissociative electron attachment.[1-3] Electrons of 0-20 eV are generated in large amounts as secondary particles in irradiated cells (~40,000 are produced by a 1 MeV electron) with a most probable energy lying below 10 eV.[4] Hence, because they carry a large portion of the energy of primary radiation, they are expected to induce a substantial amount of chemical damage. A detailed understanding of the mechanisms responsible for DNA damage via low-energy electron (LEE) attack requires knowledge of their interaction with individual basic compounds.[5] Damage to such compounds has been obtained by the analysis of species undergoing desorption from the condensed films during electron bombardment under high vacuum.[6-8] However, the majority of biological compounds, are non-volatile, and thus, do not desorb for detection using conventional systems. To solve this problem, we have developed a novel high vacuum system in which relatively large amounts of substrate can be bombarded (milligrams), and chemical modifications on the surface can be determined by HPLC and/or GC/MS analysis.[9] Here, we report our initial results with this apparatus, showing that LEE efficiently breaks the N-glycosidic bond of thymidine (dThd).

Thymidine was deposited on the inside surface of tantalum cylinders (3.2 cm × 2.5 cm diameter) by the addition of dThd in methanol to cylinders rotating at a speed of 1500 rpm under a vacuum of 400 m Torr. The resulting thin solid film of dThd consisted of 4 to 5 monolayers (2.5 nm). The distribution of molecules was homogenous as inferred by spin-coating using radioactive substrates and autoradiography. The sample was then irradiated with monoenergetic LEE in the range of 3-100 ±0.5 eV under high vacuum of 10^{-8} Torr and ambient temperature. After irradiation, the cylinders were transferred into a

glove box, which was constantly purged with an atmosphere of pure nitrogen or oxygen (humidity 20%). To recover dThd and its radiation products, the surface of the cylinder was washed repeatedly with methanol in the glove box, sonicated in the same solution, and evaporated to dryness under vacuum.

The mixture of dThd radiation products was examined by HPLC/UV and GC/MS (Figure 1). HPLC/UV analysis revealed the formation of several products. The appearance of products in non-irradiated samples can be attributed to physical contact of dThd with the cylinder surface as well as to sonication required for optimal recovery. The major product was identified as thymine by comparison of the HPLC retention time and UV spectrum to authentic standards (Figure 1a) and by comparison of GC/MS features (supplemental information). The yield of thymine was determined by GC/MS (Figure 1b, c). For these analyses, the initial solution of dThd was spiked with isotopically labeled thymine (α,α,α,H6-d_4-thymine) before spin-coating and LEE irradiation to correct for any losses of thymine during sample preparation. Thymine, including both labeled and natural isotopes, was then purified from the mixture of radiation products by HPLC. This step excludes the possible decomposition of dThd into thymine during the preparation of samples for GC/MS analysis. To estimate the percent decomposition of dThd into thymine, dThd was bombarded with LEE (15 eV) for relatively long exposure times (10 min) to overcome variability in the recovery of samples from the surface. Accordingly, the average decomposition of dThd was 30% on the basis of HPLC/UV analysis. From the same samples, the yield of thymine was 10% (2.7nmol) of the initially amount of dThd (26.5 nmol). Although the yield of thymine may have been affected by secondary processes at these exposures, one expected that the majority of thymine arose from single hits in view of its formation at low exposures (Figure 2). Thus, we estimated that thymine constituted approximately one-third (10% of 30%) of LEE-induced decomposition of dThd.

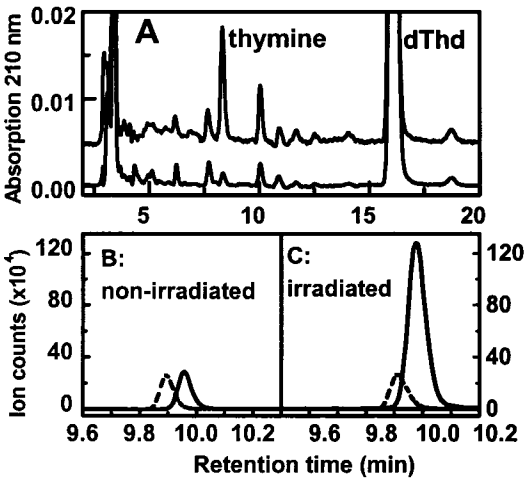

Figure 1. (A) Analysis of dThd radiation products by HPLC/UV. The upper and lower traces correspond to irradiated and non-irradiated samples of dThd respectively (irradiated samples were exposed to 1.9×10^{16} electrons of 15 eV). The separation of products was carried out using an analytical ODS-AQ column with 10% methanol in water as the mobile phase with detection at 210 nm. (B and C) Analysis of thymine by GC/MS with isotope dilution. The separation of thymine was achieved by derivatization with BSFTA and GC/MS analysis with selective monitoring at 270 m/z (solid curve) and 274 m/z (dashed curve), which corresponds to the molecular ions for non-labeled and d_4-labeled thymine, respectively (see supplemental information for details).

The formation of thymine as a function of electron energy (3-100 eV) exhibited a broad maximum around 15 eV indicating that, at this energy, thymine is produced essentially via the formation of a transient anion. At energies greater than 15 eV, the formation of thymine decreased and then increased gradually starting at 30 eV. From these preliminary results, the formation of thymine as a function of exposure time was studied in more detail near the resonance maximum of thymine formation at 15 eV (Figure 2). The linear part of this curve represents the pure interaction of LEE involving single collisions of incident electrons with dThd. At longer exposure times (>3 min), the yield of thymine reached a plateau because of changes in the film as a result of dThd decomposition and continuous trapping of electrons. Trapping of electrons by the film during exposure modified the surface potential and thus changed the energy of incident electrons. Both of these changes likely lowered the yield of thymine, explaining the deviation from linearity for long exposure times (>3 min). Nevertheless, for exposure times of less than 3 min, the formation of thymine from dThd could be attributed to the

interaction of electrons the dThd and not to other factors. A linear fit for data at the early times gives a quantum yield of 3.2 x 10^{-2} per incident electron or 32 thymine molecules per 1000 incident electrons.

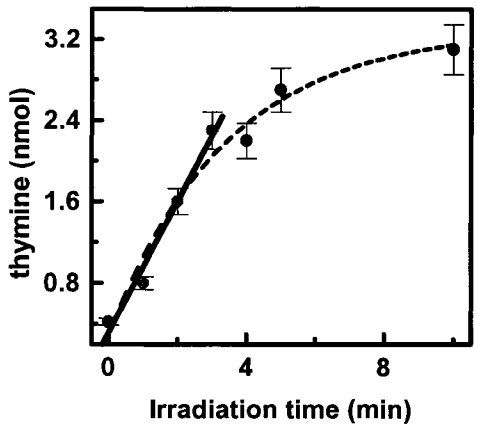

Figure 2. Time course of thymine formation by LEE. dThd was exposed to 15 eV electrons at a constant electron beam flux of 10.6 μA = 6.6 × 10^{13} electrons. The amount of thymine was determined by HPLC/UV and GC/MS analysis. The data was fit to a single exponential (dashed line) and to a line at initial times (solid line). Each data point corresponds to an average of three independent experiments.

For conversion of dThd to thymine, electrons with low kinetic energy probably localize in the anti-bonding orbitals of the N1-glycosidic bond of dThd. This can lead to either homolytic or hetereolytic cleavage. It is doubtful that thymine N1-centered radicals are involved because these species give diagnostic dimeric products that were not detected in our analysis.[11] In addition, no change in the yield of thymine was observed when oxygen, in place of nitrogen, was introduced into the irradiation chamber after irradiation. Thus, we propose that hetereolytic cleavage takes place with the formation of thymin-N1-yl anions and neutral 2-deoxy-D-ribose-C1(H)-yl radicals. The latter radicals may undergo reduction into 1,2-dideoxy-D-ribose or oxidation into 2-deoxy-D-ribose. Of these two products, 2-deoxy- D-ribose appears to be the main product as inferred by GC/MS analysis (see supporting information). Alternatively, 2-deoxy-D-ribose-C1(H)-yl radicals may give rise to other sugar radical species and final sugar decomposition products. It is important to note, however, that these radicals are not identical to those resulting from H-atom abstraction or deprotonation of pyrimidine nucleosides at C1' of the sugar moiety.

The release of thymine and other non-modified bases is an important pathway of damage upon exposure of DNA to ionizing radiation in the solid state.[12,13] This damage has been attributed to the oxidation of DNA involving either the deprotonation of base radical cations or fragmentation of initial sugar phosphate radical cations.[13-15] Alternatively, the ability of LEE to release thymine from dThd implies that LEE is involved in the release of this base from irradiated DNA. The higher electron affinity of pyrimidines compared to purines may explain the bias of base release at pyrimidine residues in irradiated DNA.[14,15] Moreover, the involvement of LEE is consistent with the independence of base release on the extent of hydration (<15 water molecules per DNA base).[13,14] If oxidative processes are involved in base release, then this process should increase with hydration due to transfer of water radical cations to the sugar moiety. Thus, novel reactions induced by LEE may explain the bias of base release at pyrimidines and the lack of an effect of hydration on base release during exposure of DNA to ionizing radiation.

In summary, our studies indicate that LEE efficiently breaks the N1-glycosidic bond of dThd. The mechanism of base release is likely different from other well-studied pathways of DNA damage, involving base ionization, OH radicals and solvated electrons. This work provides quantitative information of LEE-induced damage in complex biological systems that will be necessary to compare the chemical damage produced by LEE to that produced by other particles (e.g. α, β, UV, X rays).

Acknowledgment. This study was supported by the Canadian Institutes of Health Research (CIHR).

References

1. Boudaiffa, B.; Cloutier, P.; Hunting, D.; Huels, M. A.; Sanche, L. *Science* **2000**, *287*, 1658-1659.
2. Pan, X.; Cloutier, P.; Hunting, D.; Sanche, L. *Phys. Rev. Let.* **2003**, *90*, 208102(4).
3. Caron, L. G.; Sanche, L. *Phys. Rev. Let.* **2003**, *91 (11)*, 113201(4).
4. ICRC Report 31. International Commission on Radiation Units and Measurements, Washington DC. 1979.
5. Sanche, L. *Mass Spectrometry Rev.* **2002**, *21*, 349-369.

6. Abdoul-Carime, H.; Sanche, L. *Radiat. Res.* **2003**, *160*, 86-94, and references therein.
7. Huels, M. A.; Hahndorf, I.; Illenberger, E.; Sanche, L. *J. Chem. Phys.* **1998**, *108*, 1309-1312.
8. Abdoul-Carime, H.; Cloutier, P.; Sanche, L. *Radiat. Res.* **2001**, *155*, 625-633.
9. Zheng, Y.; Cloutier, P.; Hunting, D. J.; Wager, J. R.; Sanche, L. (unpublished results).
10. Huels, M. A.; Boudaiffa, B.; Cloutier, P.; Hunting, D.; Sanche, L. *J. Am. Chem. Soc.* **2003**, *125*, 4467-4477.
11. Wagner, J. R.; Cadet, J.; Fisher, G. J. *Photochem. & Photobiol.* **1984**, *40*, 589-597.
12. Swarts, S. G.; Sevilla, M. D.; Becker, D.; Tokar, C. J.; Wheeler, K. T. *Radiat. Res.* **1992**, *129*, 333-344.
13. Wagner, J. R.; Decarroz, C.; Berger, M.; Cadet, J. *J. Am. Chem. Soc.* **1999**, *121*, 4101-4110.
14. Razskazovskiy, Y.; Debije, M. G.; Bernhard, W. A. *Radiat. Res.* **2000**, *153*, 436-441.
15. Henle, E. S.;Roots, R.; Holley, W. R.; Chatterjee A. *Radiat. Res.* **1995**, *143*, 144-150.

Chapter IV – Third article

Chemical basis of DNA sugar-phosphate cleavage induced by low-energy electron

Yi Zheng, Pierre Cloutier, Darel J. Hunting, Léon Sanche, J. Richard Wagner

Journal of American Chemical Society: (2005) Accepted.

Chemical basis of DNA sugar-phosphate cleavage by low-energy electrons

*Yi Zheng, Pierre Cloutier, Darel J. Hunting, Léon Sanche, and J. Richard Wagner**

Group in the Radiation Sciences, Faculty of Medicine, Université de Sherbrooke, Sherbrooke, Québec, Canada J1H 5N4

AUTHOR EMAIL ADDRESS: Richard.Wagner@USherbrooke.ca

RECEIVED DATE: 05-2005

TITLE RUNNING HEAD: LEE-induced DNA sugar-phosphate cleavage

CORRESPONDING AUTHOR FOOTNOTE:

Group in the Radiation Sciences, Faculty of Medicine, Université de Sherbrooke, Sherbrooke, Québec, Canada J1H 5N4.

Telephone: 819-564-5421; 819-821-1170 ext.2286

Fax: 819-564-5442

ABSTRACT

DNA damage by low energy electrons (LEE) was examined using a novel system in which thin solid films of oligonucleotide tetramers (CGTA and GCAT) were irradiated with mono-energetic electrons (10 eV) under ultra high vacuum. The products of irradiation were examined by HPLC. These analyses permitted the quantitation of 16 non-modified nucleobase, nucleoside and nucleotide fragments resulting from the cleavage of phosphodiester and *N*-glycosidic bonds of each tetramer. The distribution of non-modified products suggests a mechanism of damage involving initial electron attachment to nucleobase moieties, followed by electron transfer to the sugar-phosphate backbone, and subsequent dissociation of the phosphodiester bond. Moreover, virtually all the non-modified fragments contained a terminal phosphate group at the site of cleavage. These results demonstrate that the phosphodiester bond breaks by a distinct pathway in which the negative charge localizes on the phosphodiester bond giving rise to non-modified fragments with an intact phosphate group. Conversely, the radical must localize on the sugar moiety to give as yet unidentified modifications. In summary, the reaction of LEE with simple tetramers involved dissociative electron attachment leading to phosphodiester bond cleavage and the formation of non-modified fragments.

KEYWORDS: Ionizing radiation, DNA damage, dissociative electron attachment.

INTODUCTION

DNA is the most important biological target of ionizing radiation.[1] DNA damage induced by ionizing radiation can primarily be attributed to water radiolysis products (hydroxyl radicals, solvated electrons, and H-atoms), radical ion pairs resulting from the ionization of DNA components, and finally, secondary low energy electrons (LEE). Previously, we demonstrated that direct bombardment of DNA with LEE gives single strand and double strand breaks in supercoiled plasmid DNA.[2,3] The ability of LEE to damage DNA is supported by extensive and detailed investigations of the basic interactions of LEE with nucleobases,[4-8] ribose derivatives,[9,10] oligonucleotides[11,12] and plasmid DNA.[13-15] Together, these studies suggest that LEE (0-20 eV) efficiently induces the formation of stable anions and radical fragments within DNA by a resonance process, i.e., dissociative electron attachment (DEA). Although this process likely leads to bond dissociation, the structure of stable products and their mechanism of formation remain to be established. Thus, a major goal of our research is to characterize LEE-induced products and link these products to deleterious effects in radiation biology.

The reaction of LEE with condensed-phase DNA components has been studied by the technique of electron stimulated desorption, which allows for the detection of small primary radicals and ions that undergo desorption from the surface of a solid target upon electron impact under ultra high vacuum (UHV), and in many cases, at cryogenic temperatures.[4-11,13] A major limitation of this technique is that it does not permit the detection of non-volatile products that remain on the target surface. In addition, this technique does not permit the detection of anions or cations without sufficient kinetic energy to escape the surface nor investigation of the chemical fate of initial radicals or ions, which depends on the phase (solid or liquid), as well as the presence of reactive solutes (oxygen, antioxidants). For these reasons, we have developed a novel irradiator in which relatively large quantities of

biological molecules (10-50 μg) can be bombarded with LEE at one time.[16] This system provides enough degraded material for preliminary chemical analysis of non-volatile products. Using this technique, we have demonstrated that LEE efficiently induced *N*-glycosidic bond cleavage of thymidine, liberating non-modified thymine and 2-deoxyribose as major stable products.[17a]

The structure of nearly 100 radiation-induced DNA lesions, including isomers, have been characterized from the oxidation of DNA components by hydroxyl radicals and single electron oxidation as well as from the reduction of DNA components by solvated electrons.[18] One can expect that LEE will produce novel modifications because these electrons have kinetic energy that can induce resonant processes, such as dissociative electron attachment. A good example of the difference between LEE and solvated electrons is that only LEE can induce strand breaks in DNA.[19] To continue our work with DNA, we have examined products arising from the irradiation of short oligonucleotides with LEE. The formation of DNA damage was detected by removal of the sample from the irradiated surface followed by HPLC analysis. In the present work, we focused on the analysis of non-modified fragments of CGTA and GCAT, which arise from cleavage at either the phosphodiester or *N*-glycosidic bonds (Chart 1; sites of cleavage are indicated by arrows). Each tetramer contains six sites for phosphodiester bond cleavage and four sites for *N*-glycosidic bond cleavage, leading to the potential formation of sixteen possible non-modified fragments.

Chart 1. Structure of oligonucleotide tetramer CGTA with sites of cleavage marked by arrows.

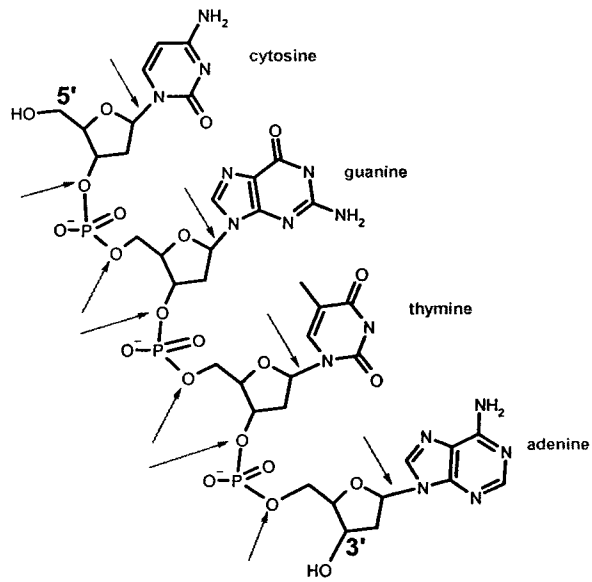

EXPERIMENTAL SECTION

Sample irradiation. Experimental details of the LEE irradiator and the procedure to irradiate samples were recently reported.[16] Briefly, 85 nmol of CGTA or GCAT (100 μg; MW=1174) was dissolved in 5 ml of 100 % HPLC grade methanol (Fisher Scientific, Montreal, QC) and the solution was deposited by spin-coating onto the inner surface of seven chemically clean tantalum cylinders (12 nmol/cylinder).[16] The average thickness of the film on the cylinder was 2.3 ± 0.1 nm (5 ± 0.2 monolayers (ML)), assuming both that the molecules are uniformly distributed on the surface of the cylinder and that the average density of DNA is 1.7 g cm^{-3}.[20] All manipulations of samples, before and immediately after irradiation, were carried out in a sealed glove box containing an atmosphere of dry nitrogen. The samples were transferred to the LEE irradiation chamber, which was subsequently evacuated for ~24 h to reach a pressure of about 10^{-9} torr at ambient temperature. The irradiator generated a uniform electron beam over the entire sample surface of the cylinder with an energy resolution of 0.5 eV full width at half-maximum. Each cylinder containing the sample was irradiated individually with possible adjustment of the time of irradiation, beam current, and incident electron energy. Under present conditions, the total electron density transmitted through the sample was approximately 7×10^{14} electrons/cm^2. From 4 to 15 eV, the current and irradiation time were adjusted to give an exposure well within the linear regime of the dose response curve and an equal number of electrons for each sample. The yield of products induced by 15 eV electrons at a constant electron beam flux of 10.6 μA = 6.6×10^{13} electron/s exhibited a linear relationship as a function of irradiation time up to 6 minutes. Within this linear regime, we can assume that the film does not accumulate any charge. The average thickness of the film (2.3 nm) was considerably smaller than the penetration depth (5-20 nm) of 4-15 eV electrons in liquid water or amorphous ice.[21a] Because the penetration depth is in fact smaller than the inelastic mean free path for

electronic excitation of biological solids (9-28 nm), electrons impinging on the film will be transmitted to the metal substrate and will, at most, lead to single inelastic scattering events with the molecules.[21b]

HPLC analysis. After irradiation with LEE, the samples were removed from UHV and placed into the dry nitrogen glove-box. The oligonucleotide tetramers and their radiation products were recovered from the surface with 12 ml of degassed 100 % HPLC grade methanol (Fisher Scientific), evaporated to dryness by rotary evaporation, and redissolved in 200 μl of nanopure grade H_2O. The recovery of material from the surface of the cylinder after deposition of tetramer on the cylinder (12 nmol/ cylinder) and insertion of the cylinder in UHV was approximately 70% (8.4 nmol /cylinder). The low recovery can be attributed to desorption during irradiation in UHV and to sticking of material that does not readily dissolve in methanol from the Ta surface. The material recovered from 2 cylinders was combined for subsequent single sample analysis (16.8 nmol/ sample). Half of the sample was treated with alkaline phosphatase (AP) (Roche Applied Science) for 1 h at 37°C to remove the terminal phosphate group of nucleotide containing fragments. The samples were then analyzed by HPLC. The HPLC system consisted of a Waters Alliance system equipped with a refrigerated autosampler, a 2690 solvent delivery module, and a 2487 dual wavelength absorbance detector. The mixture of products was separated on an ODS-AQ column (150 × 6 mm), maintained at 30 °C, using a linear gradient from 1% to 10% acetonitrile in buffer containing 25 mM ammonium acetate (pH 5.7) over an interval of 60 min and at a flow rate of 1.0 mL/min. The products were detected at 210 and 260 nm. The area of each product peak was normalized to the area of the parent compound to reduce variations due to recovery of the sample from the cylinder and subsequent reduction of the sample volume by rotary evaporation. The yield of LEE-induced products was determined by calibration with authentic reference compounds. The concentration of reference

compounds was estimated by the molar absorptivity of each mononucleotide component at 260 nm (pG=12010; pC=7050; pA=15200; pT=8400 $mol^{-1}cm^{-1}$; taken from http://www.basic.northwestern.edu /biotools/ oligocalc.html).

Standard compounds. Nucleobases (Cyt, Gua, Ade, Thy) and nucleosides (dCyd, dGuo, dAdo, dThd) were purchased from Sigma-Aldrich (St. Louis, MO). Oligonucleotide tetramers and the fragments without terminal phosphate group were purchased from Alpha DNA (Montreal, QC). They were purified by HPLC and their structure was confirmed by MSMS analysis (Q-Tof2; Waters/Micromass, Manchester, UK). Samples were dissolved in 50% acetonitrile in water containing 1 mM NaCl and electrosprayed at a rate of 0.6 µl/min in positive mode with 2.3 kV applied to the solvent. Calibration was performed using a solution of sodium/cesium iodide covering the m/z range from 200 to 1500. The cone voltage was set to 45 V and scan time was 4 sec/scan. The molecular ions ($M + Na^+$) of commercially available DNA fragments were: CGTA (m/z = 1172); GCAT (m/z = 1172); CGT (m/z = 882), GTA (m/z = 882), GT (m/z = 594), CG (m/z = 580), TA (m/z = 578) for CGTA (m/z = 1172), and GCA (m/z = 892), CAT (m/z = 866), GC (m/z = 579), CA (m/z = 563), AT (m/z = 578). In addition, several standard dinucleotide and trinucleotide fragments of CGTA and GCAT containing either a 3' or 5' terminal phosphate group were prepared by enzymatic digestion of the corresponding tetramer.[22] The preparation of fragments with a 3' terminal phosphate was carried out by partial digestion of the tetramers with micrococcal nuclease (Roche Applied Science). This treatment gave two fragments from CGTA (CGp and CGTp) as well as two fragments from GCAT (GCp, and GCAp). The standards for Cp and Gp were difficult to prepare using this procedure because of inefficient hydrolysis of the phosphodiester bond between CG or GC. Thus, Cp and Gp were prepared by complete digestion with an excess of enzyme. Conversely, the treatment of the tetramers with P1 nuclease (MP Biomedical) gave fragments containing a terminal

5'-phosphate, i.e., CGTA gave pA, pTA and pGTA and GCAT gave pCAT, pAT, and pT. The identity of dinucleotide and trinucleotide fragments containing a terminal phosphate group was subsequently confirmed by their transformation into fragments without a terminal phosphate (e.g., pTA $\rightarrow$ TA), using alkaline phosphatase, followed by co-chromatography of the resulting fragments with standard compounds.

RESULTS

The reaction of LEE with oligonucleotide tetramers resulted in the formation of a multitude of products as shown by HPLC analysis (**Figures 1 and 2, Table 1**). For electron energies between 4-15 eV, the yield of products increased as a function of energy from 4 eV to attain a maximum at 10-12 eV, and then the yield decreased to a minimum value at 14 eV. The profile of products appeared to be the same for electrons within this range of energies (4-15 eV). This work focuses on the formation of non-modified fragments of CGTA and GCAT, which included monomeric components (nucleobases, nucleosides and mononucleotides) and oligonucleotide fragments (dinucleotides and trinucleotides). The percentage of non-modified fragments to the total products (26%) was estimated from the total absorption of known and unknown LEE induced peaks at 260 nm divided by the total area of the tetramer. The non-modified fragments of CGTA and GCAT were identified in the product mixture by comparison of their chromatography properties with standard compounds. The majority of non-modified fragments were well separated using a gradient elution from 0 to 20% acetonitrile. For some analyses, the mobile phase or gradient was changed to identify and quantify products that were not well separated under routine conditions. A strong peak at 20 min was observed in both non-irradiated and irradiated samples and it can be attributed to an impurity in methanol. The size of this peak varied with the quality and batch of commercially available methanol. In addition, a number of oligonucleotide products were observed in non-irradiated samples, which together represented less than 10% of the absorption of LEE induced products (**Figures 1 and 2, bottom chromatogram**). These products can be attributed to physical contact of the tetramer to the Ta surface, as observed in previous studies with thymidine.[12,17b]

The reaction of LEE with tetramers led to the release of all four non-modified nucleobases with a bias for the release of nucleobases from terminal positions. The main

nucleobases released from CGTA included Cyt (peak 1, not shown) and Ade (peak 4) whereas those from GCAT included Gua (peak 2) and Thy (peak 3) (**Figure 1 for CGTA and Figure 2 for GCAT**). It should be noted that Thy release from the terminal position of GCAT was 3-fold higher than that from the internal position of CGTA (**Table 1**). Similarly, there was a bias for the release of Ade from the terminal compared to the internal position. In contrast, the release of Cyt was much more pronounced from the terminal position than from the internal position (10-fold). On the other hand, the release of Gua was not at all detected from the internal position of CGTA. The reaction of LEE with tetramers also led to the release of non-modified nucleosides and mononucleotides. In contrast to nucleobases, the release of nucleosides and nucleotides occurred exclusively from the terminal positions of each tetramer. The reaction of LEE with CGTA gave dCyd (peak 6) and dAdo (peak 8) as nucleoside fragments together with Cp (peak 5, not shown) and pA (peak 7) as mononucleotide fragments (**Figure 1; middle chromatogram**). It should be noted that dAdo appeared as a shoulder on a broad peak within this analysis. In addition, the peak containing Cp eluted near the solvent front, and thus, this product was detected using isocratic conditions with 100% buffer solution. On the other hand, the reaction of GCAT gave dThd (peak 20), traces of dGuo (peak 18), as well as the corresponding mononucleotides, pT (peak 19) and Gp (peak 17) (**Figure 2; middle chromatogram**). It should be noted that pT and Gp co-eluted under these conditions, and thus, they were separated using isocratic conditions with 100% buffer solution. From these results, we conclude that LEE induces the release of nucleoside or mononucleotide fragments from external positions but not from internal positions of the two tetramers. Because the release of monomeric fragments from internal positions requires the cleavage of two phosphodiester bonds, the lack of these fragments in the product mixture indicates that no more than one electron reacts with each target molecules under our conditions.

The reaction of LEE with CGTA and GCAT led to the liberation of several non-modified oligonucleotide fragments. For each tetramer, there were eight possible dinucleotide and trinucleotide fragments resulting from 3' or 5' cleavage of the four internal phosphodiester bonds. In the case of irradiated CGTA, the chromatogram showed the formation of CGp (peak 9), pTA (peak 11), CGTp (peak 13), and pGTA (peak 15) (**Figure 1; middle chromatogram**). In contrast, the corresponding fragments without a terminal phosphate group were minor or not detected in the initial product mixture (CG (peak 10), TA (peak 12, CGT (peak 14) and GTA (peak 16)). In the case of irradiated GCAT, the major dinucleotide and trinucleotide fragments were also found to contain a terminal phosphate group. The chromatogram showed the formation of fragments with a terminal phosphate group, including pAT (peak 23), GCAp (peak 25), and pCAT (peak 27), whereas the yield of fragments without a terminal phosphate was minor (GCA (peak 26)) or not detected (GC (peak 22), AT (peak 24), CAT (peak 28)); **Figure 2; lower chromatogram**). Finally, the same pattern of cleavage was observed for the loss of mononucleotides from terminal positions of tetramers. Although this cleavage gave fragments with and without a terminal phosphate, the yield of fragments with a phosphate was much greater than that without a phosphate. For example, the yield of Cp was 0.29 ±0.02 whereas that of dCyd was only 0.06 ±0.01 in irradiated CGTA (**Table 1**). The same differences were also observed for pA and dAdo in irradiated CGTA as well as Gp and dGuo, and pT and dThd in irradiated GCAT. Thus, the formation of six major non-modified fragments out of a total of twelve possible fragments for each tetramer indicates that LEE induces the cleavage of phosphodiester bonds to give non-modified fragments with a terminal phosphate rather than a terminal hydroxyl group.

The presence of fragments containing a terminal phosphate was supported by treatment of the samples with alkaline phosphatase and comparison of the two chromatograms before

and after treatment (**Figures 1 and 2**). Alkaline phosphatase removes the terminal 3' or 5' phosphate groups, and thus, converts fragments with a terminal phosphate to those without a terminal phosphate. In the case of CGTA, alkaline phosphate treatment led to the conversion of CGp to CG (peak 9 → peak 10), and so on, for the conversion of pTA to TA (peak 11 → peak 12), CGTp to CGT (peak 13 → peak 14), and pGTA to GTA (peak 15 → peak 16) (see connecting peaks between middle and top chromatograms, **Figure 1**). The cleavage of mononucleotide fragments with a terminal phosphate was supported by the conversion of pA to dAdo (peak 7 → peak 8) and an increase in the yield of dCyd after treatment with alkaline phosphatase (peak 6). It should be noted that the peak area of fragments containing a terminal phosphate was smaller than the corresponding fragments without the phosphate. This effect may be attributed to peak tailing as a result of interactions between acidic silanol groups of the solid phase and charged terminal phosphate groups of nucleotide products. Similarly, treatment of irradiated GCAT with alkaline phosphatase revealed the conversion of fragments with a terminal phosphate to those without the phosphate. For example, pAT converted to AT (peak 23 → peak 24), GCAp to GCA (peak 25 → peak 26) and pCAT to CAT (peak 27 → peak 28) (see connecting peaks between middle and top chromatograms; **Figure 2**). Although GCp (peak 21) co-eluted with an impurity under these conditions, the corresponding fragment without the terminal phosphate, GC (peak 22), greatly increased upon treatment with alkaline phosphatase. The separation of Gp (peak 17) and pT (peak 19) was poor under these conditions, and thus, the effect of alkaline phosphatase can be seen by an increase of the yield of dGuo (peak 19) and dThd (peak 20), respectively (**Figure 2**). The analysis of non-modified fragments of CGTA and GCAT confirms the nature of phosphodiester bond cleavage induced by LEE which gives non-modified fragments containing a terminal phosphate group.

Figure 1 (Zheng et al.)

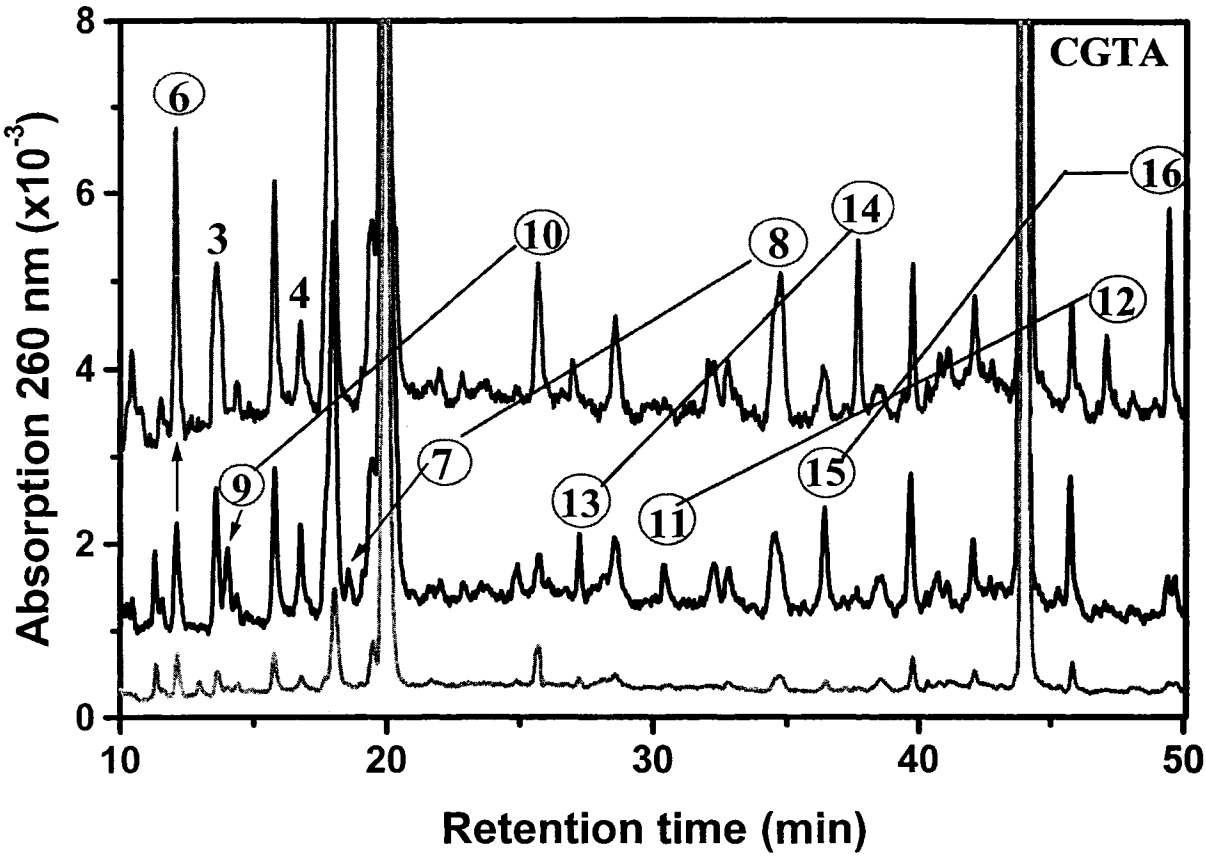

Figure 1. HPLC analysis of LEE-induced damage to CGTA. CGTA was exposed to 1.9 × 10^{16} electrons with an energy of 10 eV. The lower chromatogram (green) depicts the analysis non-irradiated samples. The middle and upper chromatograms correspond to irradiated samples, which were treated without (black) and with alkaline phosphatase (red), respectively. Blue lines illustrate the conversion of products with a terminal phosphate to those without. The identity of peaks is given in Table 1.

Figure 2 (Zheng et al.)

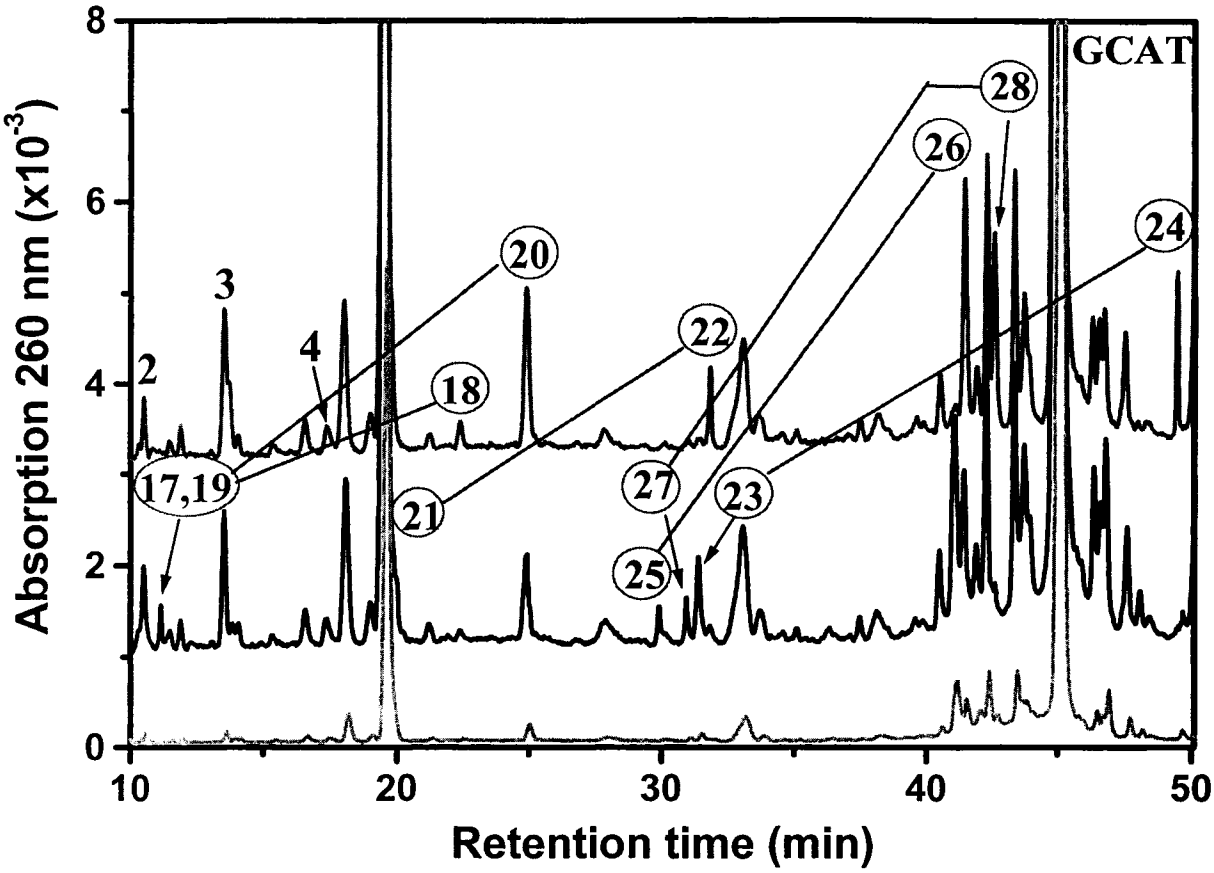

Figure 2. HPLC analysis of LEE-induced damage to GCAT. GCAT was exposed to 1.9 × 10^{16} electrons with an energy of 10 eV. The lower chromatogram (green) depicts the analysis non-irradiated samples. The middle and upper chromatograms correspond to irradiated samples, which were treated without (black) and with alkaline phosphatase (red), respectively. Blue lines illustrate the conversion of products with a terminal phosphate to those without. The identity of peaks is given in Table 1.

Table 1. Yield of LEE-induced products of irradiated tetramers.[a]

CGTA (16.8 nmol)			GCAT (16.8 nmol)		
Product	Peak #	Yield (nmol)	Product	Peak #	Yield (nmol)
Nucleobases					
Cyt	1	0.27 ± 0.05	Gua	2	0.22 ± 0.03
Gua	2	n.d.[b]	Cyt	1	0.03 ± 0.05
Thy	3	0.12 ± 0.02	Ade	4	0.11 ± 0.01
Ade	4	0.35 ± 0.07	Thy	3	0.35 ± 0.02
Nucleosides and mononucleotides					
Cp	5	0.29 ± 0.06	Gp	17	0.11 ± 0.01
dCyd	6	0.06 ± 0.01	dGuo	18	0.00 ± 0.01
pA	7	0.19 ± 0.04	pT	19	0.23 ± 0.01
dAdo	8	0.05 ± 0.01	dThd	20	0.10 ± 0.01
Dinucleotides and trinucleotides					
CGp	9	0.19 ± 0.04	GCp	21	0.16 ± 0.01
CG	10	n.d.	GC	22	n.d.
pTA	11	0.11 ± 0.02	pAT	23	0.22 ± 0.01
TA	12	n.d.	AT	24	n.d.
CGTp	13	0.20 ± 0.04	GCAp	25	0.31 ± 0.02
CGT	14	n.d.	GCA	26	0.04 ± 0.01
pGTA	15	0.23 ± 0.05	pCAT	27	0.27 ± 0.01
GTA	16	n.d.	CAT	28	n.d.
Total		2.06 ± 0.07			2.15 ± 0.08

[a]Tetramer sequence is given starting from the 5' position. Tetramers were exposed to 10 eV electrons with an incident exposure of 1.9×10^{16}. Yields were obtained from HPLC analysis (**Figures 1 and 2**). They represent the average of 3 and 7 independent experiments for CGTA and GCAT, respectively, with the error given in standard deviation. The sequence is written from 5' (left) to 3' (right) positions with p indicating the presence of a terminal phosphate group.

[b]not detected.

DISCUSSION

A major question in the mechanism of LEE-induced strand breaks in DNA is whether the electron initially localizes on the nucleobase, and then transfers to the phosphodiester bond, or whether direct electron localization occurs. According to density functional theory calculations and experimental evidence, at very low energies (< 3 eV), there are two possibilities for the localization of LEE on DNA. One possibility involves direct attachment of the incident electron to a π^* orbital of the phosphate group forming a local transient negative ion (TNI).[15,23] The other possibility involves resonance capture of the electron by the lowest π^* orbital of one of the DNA bases, followed by electron transfer to the π^* orbital of the phosphate group.[24] The net result of both possibilities is the formation of a transition state with an extra electron in the usually unfilled P=O π^* orbital that can lead, via curve crossing to a σ^* anion state, to cleavage of the phosphodiester bond.[23,24] It is reasonable to assume that the same processes operate for electrons of 10 eV as well as for electrons of lower energy (0-3 eV). For example, Grandi et. al.[26] have reported the formation of a shape resonance for uracil near 9 eV. This transient anionic state, which should also exist for DNA bases, could transfer its excess electron to unfilled orbitals of the phosphate group, lying at higher energy in a manner similar to that described for electrons of lower energy (< 3 eV).[23] Furthermore, Martin et al.[15] compared their experimental results on single strand breaks in plasmid DNA induced by 0-4 eV electrons with those on the damage imparted to the isolated DNA bases by electrons of the same energies. The yield functions for strand breaks could be reproduced in magnitude and line shape by a model that simulates the electron capture cross section as it might appear in DNA owing to the π^* anion states of the bases. The attachment energies and the magnitude of the cross section were taken from electron transmission measurements in the gaseous bases.[27] The peak magnitudes were scaled to reflect the

inverse energy dependence of the electron capture cross sections. Under the assumption that equal numbers of each base are resident in DNA, the contributions from each base were simply added. Although such a comparison suggest that electrons are initially captured by nucleobases, we need to examine the formation of products by direct chemical analysis to test this hypothesis.[15]

The amount of cleavage at each phosphodiester bond may be estimated from the yield of each non-modified fragment (**Scheme 1**). From these analyses, the yield of cleavage varied about 3-fold depending on the site of cleavage. If the electron was solely captured directly into the usually unfilled P=O π^* orbital, then according to the structure of oligonucleotide tetramers, there should be an equal probability of breaking the phosphodiester bond at all sites. As seen from **Scheme 1**, however, this is not the case; phosphodiester bond cleavage significantly varies from one site to the other. Therefore, we must conclude that electron transfer contributes to phosphodiester bond cleavage. Interestingly, the yield of phosphodiester cleavage was enhanced at the terminal positions of one of the tetramers (GCAT). The effect of the end was even more pronounced for base release although it is not known at this point whether base release arises from DEA of the *N*-glycosidic bond or from DEA of the phosphodiester bond followed by subsequent reactions of carbon centered sugar radicals (see below; discussion on base release). This effect may be explained by the number of available sites for electron transfer such that electrons at internal nucleobases can transfer to two phosphodiester bonds whereas those at external nucleobases can only transfer to one bond. In agreement with this hypothesis, the difference in yield between cleavage sites becomes smaller when the distribution of cleavage is calculated for individual nucleobases (**Scheme 1**). Alternatively, the greater cleavage at terminal positions may be due to greater accessibility of terminal compared to internal positions toward initial electron attachment. Indeed, LEE-induced desorption of CN and OCN fragments from a

series of oligonucleotides was previously found to be inversely proportional to chain length ($n<9$).[28] In summary, the present work shows that phosphodiester bond cleavage depends on nucleobase and sequence but more studies will be necessary to clarify the nature of this phenomenon.

Once the electron has localized on the phosphodiester bond, there are two possible pathways leading to cleavage of this bond (**Scheme 2**). Pathway A involves scission of the C-O bond and gives carbon-centered radicals (C5'or C3' radicals) and phosphate anions as termini, whereas pathway B results in cleavage of the P-O bond giving alkoxyl anions together with phosphoryl radicals. On the basis of our analysis of fragments from oligonucleotide tetramers, we demonstrate that cleavage of the phosphodiester bond primarily takes place via the formation of a sugar radical and a phosphate anion (path A). The cleavage of C-O and P-O bonds of the phosphodiester group, leading to the formation of phosphoryl radicals and dephosphorylated C3' radicals of the sugar moiety was previously reported in ESR studies of argon-ion irradiated and -irradiated hydrated DNA.[29,30] Recently, the ESR spectra of both C3' and C5' radicals were extracted from the neutral radical spectrum of irradiated DNA containing electron and hole scavengers.[31] In view of the greater bond dissociation energy of C-O (334 kJ/mol) compared to P-O (92 kJ/mol), it is remarkable that C-O bond cleavage was the dominating process on the basis of ESR studies (95%).[29] A possible interpretation of the latter result, as well as our results, is that the bond breaking process takes place by electron attachment into an unfilled orbital lying at a much higher energy (i.e., 10 eV = 960 kJ/mol) than the thermodynamic threshold of C-O bond dissociation. In this case, phosphodiester bond cleavage would not depend on bond energy considerations but rather on the availability of dissociating anionic states at the energy of the captured electron.

The release of unaltered nucleobases from tetramers can be explained by two different mechanisms of *N*-glycosidic bond cleavage. Previously, we showed that LEE (0-15 eV) efficiently induced the cleavage of thymidine to thymine.[17a] Similar results have also been reported for thymidine in the gas phase.[17b] Thus, it is reasonable to propose a similar pathway not only for the release thymine (Thy), but also to the release of other nucleobases (Ade, Cyt, and Gua) from oligonucleotide tetramers. Involvement of this pathway in base release suggests that there may be a competition between the transfer of initially captured electrons of the nucleobase to either the *N*-glycosidic bond or the phosphodiester bond. Assuming that all base release is due to this reaction, the initial capture of electrons by nucleobases becomes independent of the nucleobase (Scheme 1), and thus, the variation in the yield of base release and phosphodiester cleavage must arise from sequence dependent differences in the probability of transferring electrons from the base to the *N*-glycosidic and phosphodiester bonds.

The release of nucleobases from oligonucleotide tetramers can also be explained by the initial formation of carbon-centered radicals at the sugar moiety. In particular, the release of non-modified nucleobases is a major pathway of OH radical induced damage to DNA, which involves initial H-atom abstraction from sugar carbon positions.[32,33] The deprotonation of sugar radical cations can also lead to the same sugar radicals. From the latter studies, the yield of sugar radicals is comparable to the yield of unaltered base release, indicating that the majority of sugar radicals lead to base release.[33] Therefore, in the present work, one expects that the yield of base release will be equal to that of phosphodiester bond cleavage at a specific site. For example, initial *N*-glycosidic bond cleavage will result in a sugar radical that in turn can lead to phosophodiester bond cleavage, and as well, initial phosphodiester bond cleavage will lead to a sugar radical that in turn can give base release. In this way, the products of both reactions will be equal irregardless of the partition

between the two possible pathways of formation. This scenario is consistent with the yield of base release and phosphodiester cleavage for terminal bases (e.g. C of CGTA; Scheme 1). However, the yield of base release is smaller than expected for internal bases; e.g. the release of Gua (~0) and Thy (0.12) was small compared to phosphodiester bond cleavage at G (0.29 + 0.11) and T (0.19 + 0.19). Thus, the nature or fate of initial radicals (1', 3' or 5' sugar radicals) must be remarkably different than that at terminal sites. In particular, the low yield of base release for internal bases points to the formation of products derived from 5', 3' or 1' carbon-centered sugar radicals that retain the nucleobase moiety. Interestingly, the order of DEA mediated base release at internal positions of oligonucleotides (Thy ~ Ade > Cyt > Gua) differs from that observed for hydroxyl radical reactions (Cyt > Thy > Ade > Gua).[33] The low release of Gua has been related to the ability of Gua to undergo electron transfer with intermediate sugar radicals. Additional studies will be necessary to probe the unique chemistry of sugar radicals derived from DEA of phosphodiester and *N*-glycosidic bonds.

The formation of strand breaks and base release was studied in the irradiation of short oligonucleotides in crystalline form with 70 keV X-rays.[34-36] The formation of oligonucleotide fragments was attributed to direct ionization of the sugar moiety, leading to initial sugar radical cations. The latter radicals are believed to deprotonate, and through a number of intermediate steps, induce base release and phosphodiester cleavage. Interestingly, the results of X-ray and LEE irradiation were similar. Both irradiation systems resulted in the predominant formation of 3' and 5'-end phosphorylated strand fragments. Similar to LEE irradiation, there was also a preference for cleavage at termini positions in X-ray irradiation although this effect was dependent on the DNA sequence.[35] Whereas the distribution of phosphodiester cleavage was clearly affected by the nature of the nucleobase in LEE irradiation, there was little or no variation of base specific cleavage

reported for X-rays.[36] Nevertheless, the similarities of the two systems underline the importance of DEA in the direct effect of damage by ionizing radiation.

Scheme 1. Distribution of damage by sites of cleavage

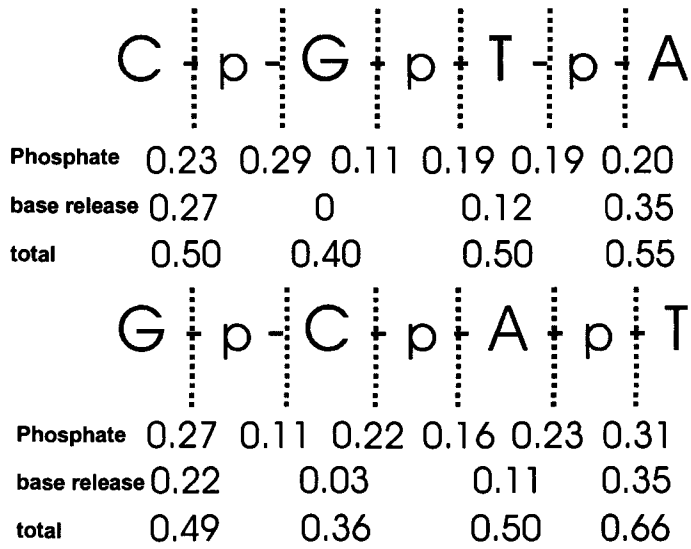

Scheme 2. Proposed pathways for phosphate ester bond cleavage of DNA. Pathway A is the major process, whereas pathway B is the minor that could be hardly detected.

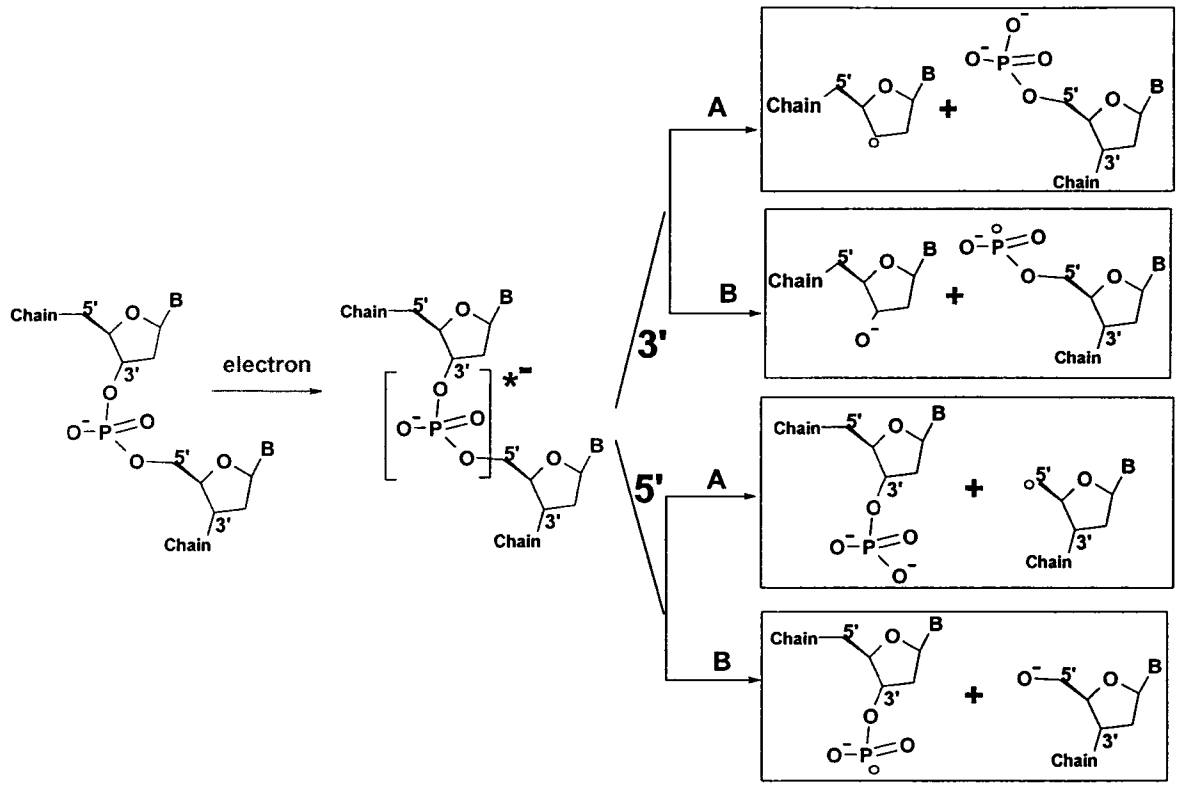

SUMMARY

The present work demonstrates that LEE induce phosphodiester bond cleavage and nucleobase release in oligonucleotide tetramers. LEE may directly localize on the phosphate group, but electron capture by other components followed by electron transfer to the sugar-phosphate backbone must also contribute to the rupture of phosphodiester bonds. The mechanism of phosphodiester bond cleavage is proposed to involve dissociative electron attachment. This mechanism entails two possible modes of phosphodiester bond cleavage: one reaction involves the formation of transient alkoxyl anions of the sugar moiety together with phosphoryl radicals, whereas the other reaction involves the formation of carbon-centered sugar radicals with intact phosphate anions. On the basis of product analysis, LEE irradiation of tetramers gave non-modified fragments containing a terminal phosphate group while those without a phosphate group were minor. Thus, the mechanism of phosphodiester bond cleavage involves cleavage of the C-O bond rather than P-O bond. In addition, we also report the release of non-modified nucleobases from irradiated tetramers; however, these products may arise from direct *N*-glycosidic bond cleavage or by an indirect pathway involving carbon-centered sugar radicals. The present study provides a chemical basis for the formation of strand breaks by the reaction of LEE with DNA.

ACKNOWLEDGMENT: The authors thank Dr. Klaus Klarskov for ESI/MSMS analysis. Financial support for this work was provided by the Canadian Institutes of Health Research (CIHR).

SUPPORTING INFORMATION: Mass spectra of commercial standards of oligonucleotides, trinucleotides and dinucleotides.

REFERENCES

(1) Connell, P.; Kron, S.; Weichselbaum, R. *DNA Repair* **2004**, *3*, 1245-1251.

(2) Boudaiffa, B.; Cloutier, P.; Hunting, D.; Huels, M. A.; Sanche, L. *Science* **2000**, *287*, 1658-1662.

(3) Boudaiffa, B.; Cloutier, P.; Hunting, D.; Huels, M. A.; Sanche, L. *Radiat. Res.* **2001**, *157*, 227-234.

(4) Huels, M. A.; Hahndorf, I.; Illenberger, E.; Sanche, L. *J. Chem. Phys.* **1998**, *108*, 1309.

(5) Aboul-Carime, H.; Cloutier, P.; Sanche, L. *Radiat. Res.* **2001**, *155*, 625.

(6) Denifl, S.; Ptasinska, S.; Hrusak, J.; Scheier, P.; Mark, T. D. *J. Phys. Chem. A* **2004**, *108*, 6562-6569.

(7) Abdoul-Carime, H.; Gohlke, S.; Illenberger, E. *Phys. Rev. Let.* **2004**, *92*, 168103.

(8) Klyachko, D. V.; Huels, M. A.; Sanche, L. *Radiat. Res.* **1999**, *151*, 177.

(9) Antic, D.; Parenteau, L.; Sanche, L. *J. Phys. Chem. B* **2002**, *104*, 4711.

(10) Ptasinska, S.; Denifl, S.; Scheier, P.; Mark, T. D. *J. Chem. Phys.* **2004**, *120*, 8505.

(11) Dugal, P.-C.; Abdoul-Carime, H.; Sanche, L. *J. Phys. Chem. B* **2000**, *104*, 5610.

(12) Abdoul-Carime, H.; Dugal. P.-C.; Sanche, L. *Radiat. Res.* **2002**, *153*, 23.

(13) Huels, M. A.; Boudaiffa, B.; Cloutier, P.; Hunting, D.; Sanche, L.; *J. Am. Chem. Soc.* **2003**, *125(15)*, 4467-4477.

(14) Pan X.; Cloutier P.; Hunting D.; Sanche L. *Physical Review Letters.*, **2003**, *23, 90(20),* 208102

(15) Martin, F.; Burrow, P. D.; Cai, Z.; Cloutier, P.; Hunting, D.; Sanche, L. *Phys. Rev. Let.* **2004**, *93*, 068101.

(16) Zheng, Y.; Cloutier, P.; Wagner, J. R.; Sanche L. *Review of Scientific Instruments*, **2004**, *75*, 4534.

(17) (a) Zheng, Y.; Cloutier, P.; Hunting, D. J.; Wagner, J. R.; Sanche, L. *J. Am. Chem. Soc.* **2004**, *126*, 1002. (b) Abdoul-Carime, H.; Gohlke, S.; Fischbach E.; Scheike, J.; Illenberger E. *Chem. Phys. Let.* **2004**, *387*, 267.

(18) Cadet, J.; Bellon, S.; Douki, T.; Frelon, S.; Gasparutto, D.; Muller, E.; Pouget, JP.; Ravanat, JL.; Romieu, A.; Sauvaigo, S. *Journal of Environmental Pathology, Toxicology & Oncology,* **2004**, *23(1)*,33-43.

(19) Beach, C.; Fuciarelli, AF.; Zimbrick, JD. *Radiat. Res.* **1994**, *137(3)*, 385.

(20) Fasman, G. D. *Handbook of Biochemistry and Molecular Biology*, 3rd ed.; CRC Press: Boca Raton, FL, 1995.

(21) (a) Meesungnoen, J.; Jay-Gerin, J.-P.; Filali-Mouhim, A.; Mankhetkorn, S. *Radiat. Res.* **2002**, *158*, 657. (b) Leclerc, G.; Goulet, T.; Cloutier, P.; Jay-Gerin, J.-P.; Sanche, L. *J. Phys. Chem.* **1987**, *91*, 4999.

(22) White, J. S. *Source Book of Enzymes*, CRC Press: Boca Raton, FL, 1997.

(23) Li, X.; Sevilla, M. D.; Sanche, L. *J. Am. Chem. Soc.* **2003**, *125*, 13668.

(24) Berdys, J.; Anusiewicz, I.; Skurski, P.; Simons, J. *J. Am. Chem. Soc.* **2004, *126*,** 6441, and the reference therein.

(25) (a) Berdys, J.; Anusiewicz, I.; Skurski, P.; Simons, J. *J. Phys. Chem. A.* **2004**, *108*, 2999. (b) Berdys, J.; Skurski, P.; Simons, J. *J. Phys. Chem. B.* **2004**, *108*, 5800.

(26) Grandi, A.; Gianturco, F. A.; Sanna, N. *Phys. Rev. Lett.* **2004**, *93*, 048103.

(27) Aflatooni, K.; Gallup, G.A.; Burrow, P.D. *J. Phys. Chem. A* **1998**, *102*, 6205.

(28) Abdoul-Carime, H.; Sanche, L. *Radiat. Res.* **2001**, *156*, 151-157.

(29) Becker, D.; Bryant-Friedrich, A.; Trzasko, C.; Sivilla, M. D. *Radiat. Res.* **2003**, *160*, 174.

(30) Becker, D.; Razskazovskii, Y.; Callaghan, M.; Sevilla, M. D. *Radiat. Res.* **1996**, *146*, 361-368.

(31) Shukla, L.; Pazdro, R.; Becker, D.; Sevilla, M. D. *Radiat. Res.* **2005**, *163*, 591-602.

(32) Von Sonntag, C. *The Chemical Basis of Radiation Biology*, Taylor & Francis, New York, 1987.

(33) Henle, E. S.; Roots, R.; Holley, W. R.; Chatterjee, A. *Radiat. Res.* **1995**, *143*, 144.

(34) Debije, M. G.; Razakazovskiy, Y.; Bernhard, W. A. *J. Am. Chem. Soc.* **2001**, *123*, 2917-2918.

(35) Razakazovskiy, Y.; Debiji, M. G., Howerton, S. B.; Williams, L. D.; Bernhard, W. A. *Radiat. Res.* **2003**, *160*, 334-339.

(36) Razakazovskiy, Y.; Debiji, M. G.; Bernhard, W. A. *Radiat. Res.* **2003**, *159*, 663-669.

Chapter V – Fourth article

Phosphodiester and N-glycosidic bond cleavage in DNA induced by 4-15 eV electrons

Yi Zheng, Pierre Cloutier, Darel J. Hunting, J. Richard Wagner, Léon Sanche

Journal of Chemical Physics: in preparation.

PHOSPHODIESTER AND N-GLYCOSIDIC BOND CLEAVAGE IN DNA INDUCED BY 4-15 EV ELECTRONS

*Yi Zheng, Pierre Cloutier, Darel J. Hunting, J. Richard Wagner and Léon Sanche**

Group in the Radiation Sciences, Faculty of Medicine, Université de Sherbrooke, Sherbrooke, Québec, Canada J1H 5N4

Abstract

Thin molecular films of the short single strand of DNA (GCAT) were bombarded under vacuum by electrons of energies between 4 and 15 eV. Ex vacuo analysis by high pressure liquid chromatography of the samples exposed to the electron beam revealed the formation of a multitude of products. Among these, 12 fragments of GCAT were identified by comparison with reference compounds and their yields were measured as a function of electron energy. For all energies, scission of the backbone gave non modified fragments containing a terminal phosphate, with negligible amounts of fragments without the phosphate group. This indicates that phosphodiester bond cleavage by 4-15 eV electrons involves cleavage of the C-O bond rather than the P-O bond. The yield functions exhibit maxima at 6 and 10-12 eV, which were interpreted as due to the formation of transient anions leading to fragmentation. Below 15 eV, these resonances dominate bond dissociation processes. All four non-modified bases are released from the tetramer, by cleavage of the N-glycosidic bond, which occurs principally via the formation of core-excited resonances located around 6 and 10 eV. The formation of the other non-modified products leading to cleavage of the phosphodiester bond is suggested to occur principally via two different mechanisms: (1) the formation of a core-excited resonance on the phosphate unit followed by dissociation of the transient anion and (2) dissociation of the CO bond of the phosphate group formed by resonance electron transfer from the bases. In each case, phosphodiester bond cleavage leads chiefly to the formation of stable phosphate anions and sugar radicals with minimal amounts of alkoxyl anions and phosphoryl radicals.

RECEIVED DATE:
TITLE RUNNING HEAD: LEE-induced DNA cleavage
*CORRESPONDING AUTHOR:

Group in the Radiation Sciences, Faculty of Medicine, Université de Sherbrooke, Sherbrooke, Québec, Canada J1H 5N4.
Telephone: (819) 346-1110, ext. 14678
Fax: (819) 564-5442
email address: Leon.Sanche@USherbrooke.ca

I. Introduction

In recent years, processes induced by low energy electrons (LEE) in biomolecules have attracted considerable attention. The major impetus to investigate these processes has arisen from the important role of LEE in radiobiology [1]. Since the detrimental biological effects of ionizing radiation are usually caused by damage to the genome, most of the work related to LEE damage to biomolecules has been focused on DNA and its basic constituents (i.e. the bases and the deoxyribose and phosphate groups).

The first LEE scattering experiments on RNA and DNA basic constituents were performed on uracil and the DNA bases by Aflatooni et al. [2], who measured electron transmission through a gas cell of these molecules. Later, systematic gas-phase investigations of stable anion production by LEE impact on uracil [3,4,5] and the DNA bases [6,7,8,9,10,11,12] provided considerable insight into the mechanisms of damage to DNA induced by the secondary electrons of low energies produced by ionizing radiation. Dissociative electron attachment (DEA) to these biomolecules was found to contribute significantly to fragmentation. High hydrogen loss was observed without any measurable amount of stable parent anions. Furthermore, experiments carried out on partly deuterated thymine at the carbon positions indicated that the high hydrogen loss induced by LEE impact on the DNA bases was site-specific: below 2 eV, DEA generated the N-dehydrogenated transient anion $(T_D\text{-}H)_N^-$ which decayed by hydrogen cleavage from the N sites, but not from the C positions [13,14]. The four DNA bases were also investigated in the form of thin multilayer films, but fewer anions of different masses were measured than in the gas phase. The difference is principally due to the inability of the heavier anions to overcome the polarization potential that they induce in the film [15] causing them to remain trapped in the target.

The formation of anions and cations by LEE impact on the gaseous 2-deoxyribose sugar ($C_5H_{10}O_4$) [16] as well as on solid films of the sugar-like analogs, tetrahydrofuran (THF), 3-hydroxytetrahydrofuran, and α-tetrahydrofuryl alcohol [17,18] were investigated by mass spectrometry. The majority of the anion yield for these molecules arose from the dissociation of transient anions associated with electron attachment to the furan ring forming core-excited resonances above about 5 eV and shape resonances below that energy. High resolution electron energy loss spectroscopy was also used to measure the damage induced within thin solid films of THF. The production of aldehydes within such films condensed on a solid Kr substrate was reported by Breton et al. [19]. So far, the phosphate unit of DNA has only been investigated from condensed phase Na $PO_2(OH)_2$ [20], in the OH^- anion DEA channel.

The most complex DNA unit investigated by LEE impact in the gas phase has been Thymidine (dT) [21]. The results indicate that electrons with energies below 3 eV dissociate dT forming $(dT\text{-}H)^-$ and $(2\text{-deoxyribose-}OH)^-$ and $(T\text{-}H)^-$ with a break at the N1 position. The dT results were corroborated by measurements of the products formed in LEE bombardment of the solid in UHV [22], which established thymine arising from N1-glycosidic bond cleavage of dT, as being the most abundant fragment (i.e. about one third of dT decomposition at 15 eV).

Although gas-phase investigations have so far been limited to molecules of the size of Td, in condensed phase experiments, it has been possible to investigate LEE induced damage on the entire DNA molecule. These studies have included the measurement of single and double strand breaks as a function of electron energy in the range 0-100 eV [23,24,25,26,27], as well as stable anion formation via DEA and dipolar dissociation (DD) within the range 0-20 eV [28]. The DEA process was also investigated in oligonucleotides,

ranging from four to 40 bases long, by analyzing the anions [20] and neutral products [29,30,31,32,33] induced by LEE impact on self assembled monolayer films.

Even though in vacuo mass spectrometric analysis of the fragments desorbing from DNA provides information on elementary processes, most of the products remain on the substrate and cannot be analyzed. Hence, it becomes difficult to obtain a complete picture of DNA damage induced by LEE and understand the details of the mechanisms involved. In principle, an analysis of all major products formed by LEE impact on DNA should allow one to provide the complete fragmentation pathways. This may be achieved by recuperating the products from vacuum and analysing them outside vacuum by chemical methods such as electrophoresis and chromatography with or without mass analysis. In practice, however, only SSB, DSB and multiple DSB from plasmid DNA (3197 base pairs) could be analyzed outside vacuum by electrophoresis [23-25]. In this case, the large amplification factor in detection sensitivity that results from the change in the topology of plasmid (e.g. from the supercoiled to the circular and linear configuration, respectively), when one or two strand are broken, allowed us to detect damage at low levels by electrophoresis. However, such a huge amplification factor does not exist for other DNA damages, which could not be analyzed due to insufficient production of degraded material by conventional LEE bombardment procedures [23-25].

To solve this problem, we developed a new type of LEE irradiator capable of processing large amounts of nonvolatile organic and biomolecules spread out on a large surface area [34,35]. In initial experiments, we examined the total mixture of products resulting from LEE bombardment of thymidine by HPLC/UV and GC/MS analysis [22]. Subsequently, we irradiated with 10 eV electrons the short oligonucleotides CGTA and GCAT containing the four DNA nucleobases thymine (T), cytosine (C), guanine (G) and

adenine (A) and the sugar-phosphate backbone [34]. The fragments were detected by removal of the sample from the irradiated surface followed by HPLC/UV analysis. The analysis of LEE-induced damage in the short oligonucleotides showed a multitude of products, including as a major class of fragments non-modified nucleobases, nucleosides and nucleotides that arose from cleavage of the phosphodiester and *N*-glycosidic bonds. As shown in Fig. 1 for GCAT, each tetramer contained 12 potential sites of cleavage (labelled 5 to 16) for phosphodiester bonds and four potential sites (labelled 1 to 4) of cleavage for *N*-glycosidic bonds, giving a total of 32 possible fragments.

In the present work, we identified the non-modified DNA units, which result from cleavage of GCAT at positions 1 to 16 in Fig. 1. For those which gave a measurable signal upon HPLC/UV analysis, we measured their yields as a function of electron energy in the range 4-15 eV. The magnitude of fragmentation at specific sites was found to depend on the base sequence context and electron energy. The information gained from this dependence provides considerable insight into the mechanisms of LEE-induced cleavage of the N-glycosidic and phosphodiester bonds in DNA.

2. Experiments

The tetramer GCAT was bombarded in the LEE irradiator [35] shown systematically in Fig. 2. The biomolecules were spin coated onto the inner surface of tantalum cylinders which were placed on a rotary platform housed in an UHV system, where their inner walls were bombarded by a diverging LEE beam having an absolute energy spread of 0.5 eV FWHM. Figure 2 shows the principle of operation of this irradiator. Electrons are emitted from a tantalum disk cathode and pass through the apertures at the center of four molybdenum disks electrodes (Fig. 2a). The latter serve as a defocusing electron lens to expel electrons away from the gun axis and thereby produce a

divergent electron beam. Subsequently, the electrons enter an electric field free region, where a small coil produces a non-uniform magnetic field. The purpose of this coil is to modify the trajectories of the electrons; first by collimating them on the axis and then, in the diminishing magnetic field region, by releasing them toward a molybdenum cylindrical mesh grid. After reaching the grid, the electrons are accelerated to the desired energy by an electric field between the grid and the metal substrate. The uniformity of the electron current over the inner wall of the cylinders can be adjusted by inserting the grid into the detector, shown in figure 2b, which is composed of 12 identical cylindrical electron collectors. After irradiation, the tantalum cylinders are removed from UHV and the samples are dissolved in an appropriate solvent.

In the present experiments, 100 μg of GCAT was dissolved in 5 ml methanol and the solution was deposited by spin-coating onto the inner surface of seven chemically clean tantalum cylinders (~14 μg /cylinder) [35]. The average thickness of the film on the cylinder was 2.3 ± 0.1 nm (5 ± 0.2 monolayers (ML)), assuming both that the molecules were uniformly distributed on the surface of the cylinder and that the average density of DNA is 1.7 g cm^{-3} [36]. All manipulations of samples, before and immediately after irradiation, were carried out in a sealed glove box containing an atmosphere of pure dry nitrogen. The samples were transferred to the LEE irradiation chamber, which was subsequently evacuated for ~24 h to reach a pressure of about 10^{-9} torr at ambient temperature. The irradiator generated a uniform electron beam over the entire sample surface of the cylinder. Each cylinder containing the sample was irradiated individually with possible adjustment of the time of irradiation, beam current, and incident electron energy. Under present conditions, the total electron density transmitted through the sample was approximately 7×10^{14} electrons/cm^2. Samples were irradiated at 4, 6, 8, 10, 12, 14

and 15 eV. Due to the large number of data points required to produce yield functions for all products analyzed smaller energy intervals were not considered practical. Nevertheless, the present results allow us to describe the general behavior of the yields vs. energy and determine the position of broad maxima and minima within ± 1 eV. From 4 to 15 eV, the current and irradiation time were adjusted to give an exposure well within the linear regime of the dose response curve and an equal number of electrons to each sample. Since we expect surface charging to cause deviation of this linear regime, we consider that the films did not accumulate a significant amount of electrons or holes during our experiments. Furthermore, the average thickness of the film (2.3 nm) was considerably smaller than the penetration depth (5-20 nm) of 4-15 eV electrons in liquid water or amorphous ice [37]. Because the penetration depth is in fact smaller than the inelastic mean free path for electronic excitation of biological solids (9-28 nm) [38], almost every electron impinging on the film should, at the most, lead to single inelastic scattering event and hence be transmitted to the metal substrate and not charge by the film.

After irradiation with LEE, the samples were removed from UHV and placed into the dry nitrogen glove-box. Then, the tetramer and radiation products were recovered from the surface using 12 ml of degassed methanol. The sample was evaporated to dryness and finally redissolved in 200 μl of nanopure grade H_2O. Half of the sample was treated with alkaline phosphatase (AP) (Roche Applied Science) for 1 h at 37°C to remove the terminal phosphate group of the nucleotide fragments. The samples were then analyzed by HPLC-UV. The HPLC system consisted of a Waters Alliance system equipped with a refrigerated autosampler, a 2690 solvent delivery module, and a 2487 dual wavelength absorbance detector. The mixture of products was separated on an ODS-AQ column (150 × 6 mm), maintained at 30 °C, using a linear gradient from 1% to 10% acetonitrile in buffer

containing 25 mM ammonium acetate (pH 5.7) over an interval of 60 min and at a flow rate of 1.0 mL/min. The products were detected at 210 and 260 nm. The yield of LEE-induced products was determined by calibration with authentic reference compounds, as described previously [34]. The concentration of reference compounds was estimated by the molar absorptivity of each mononucleotide component at 260 nm (G=12010; C=7050; A=15200; T=8400 mol^{-1} cm^{-1}; values taken from http://www.basic.nwu.edu/biotools/ oligocalc.html). The area under each product peak was normalized to the area of the parent compound in order to reduce variations in the yield due to recuperation and concentration of the sample from the irradiated surface.

3. Results

As previously observed from bombardment of CGTA and GCAT with 10 eV electrons [35], the interaction of 4-15 eV electrons with GCAT gave a multitude of products. This is seen in the HPLC analysis of the products at all bombardment energies. An example of an HPLC analysis of GCAT exposed to 15 eV electrons is shown in Fig. 3. The numbers over each of the peaks correspond to the cleavage positions shown in figure 1. The large peak near 20 min was due to an impurity in commercial methanol. In addition, a number of oligonucleotide derived products appeared in non-irradiated samples (<10% of the total absorption) that can be attributed to the physical contact of the tetramer to the Ta surface [22]. Cleavage of the four glycosidic bonds of GCAT (1-4) led to the release of G, C, A and T (Figure 3). The release of C was observed under alternative chromatography conditions, i.e., using buffer at pH 4, which permitted the separation of C from other early eluting peaks. As previously observed with 10 eV electrons and verified by changing the base sequence [34], base release was stronger from the terminal positions. The majority of nucleotide fragments were well separated under the present conditions. The major

fragments included Gp (site 8), GCp (12), and GCAp (16) in going from 5' to 3', and similarly, Tp (13), TAp (9), and TACp (5) in going from 3' to 5'. As expected, the release of chain fragments from internal positions, which would have required the break of two strands with one electron, was not observed. The yield of each fragment was quantitated by treatment with alkaline phosphatase, which removes the terminal phosphate group and greatly improves the chromatography properties. For example, upon treatment with alkaline phosphatase, GCAp (cleavage at 16, lower chromatogram) converts to GCA (upper chromatogram) (Figure 3). For each bombardment energy, the magnitude of the peaks of the compounds identified from HPLC analysis was tabulated as a percentage of the original amount of GCAT. Accordingly, the yield of each fragment is given in Table 1. In agreement with our previous and more detailed analysis of the fragments produced by 10 eV electrons[35], the results indicate that LEE mainly induce cleavage at C-O of the phosphodiester bond giving fragments with a terminal phosphate group. In contrast, cleavage at the P-O bond of the phosphodiester bond, which gives fragments with a terminal OH group, was minor or negligible.

The linearity of the yields of products vs. electron exposure was established by measuring the area under each peak of the products seen in HPLC analysis and plotting the sum of these areas as a function of time of bombardment. Figure 4 shows such yields expressed as a percentage of the original amount of GCAT processed by 15 eV electrons during 0 to 5 min. The error bars in the figure correspond to twice the standard deviation of a Gaussian fit to eight independent measurements. Within this error margin the total yield of fragments is found to be a linear function of exposure. Above a 5 min exposure this linearity is broken. The upper limit of the linear regime was therefore considered to be 5 min for a beam flux of 6.6×10^{13} electrons/s. Within this regime, the yields of products are

considered to result from a single electron hit, since damage resulting from multiple successive collisions is necessarily non linear with exposure. The results reported in this article were obtained at the 5 min limit to maximize the signal and reduce statistical errors.

The incident electron energy dependence of the yield of the bases is shown in Fig. 5. With the exception of cytosine whose maximum occurs at 12 eV, the other curves exhibit maxima at 10±1 eV, with a rise beyond 14 eV. According to experimental errors the small rise at 6 eV may not necessarily be significant, but a shoulder definitively exists near this energy. This maximum also appears in the yield functions of some of the monomers dG and dGp and oligomers pCAT and pAT shown in Figs 6 and 7, respectively. The strongest monomer signal (Fig. 6) is found in the yield function thymidine phosphate (pT) which exhibits a maximum at 10± 1 eV. For the other monomers, a broad peak appears around 12 ± 1 eV. Similarly, for oligomer formation, a broad maximum occurs within 10-12 eV region. Interestingly, with the exception of the very small dG yield, a strong dip in the monomer and oligomer yield function is always present at 14 eV, partly due to a sharp rise in the yield beyond that energy. As shown by the comparison in Fig. 8, this strong minimum has been observed in the yield function for SSB in dry plasmid films of DNA bombarded with LEE under UHV [23]. Also shown in Fig. 8 are the yield function for DSB and H^- desorption induced by LEE on similar films [28] and the results of the present experiments, which gave the strongest signal for nucleobase release and monomer and oligomer formation (i.e., T, pT and pCAT); it may be noted that the latter compounds all contain thymine. There exists a striking resemblance between the yield functions obtained in the present experiments and that for SSB from plasmid DNA; i.e., a dip near 14 eV, a shoulder near 6 eV and a broad peak around 10 eV. The H^- yield shown at the bottom of Fig. 8 is the strongest anion desorption signal observed from plasmid DNA films, but

similar functions have been observed for O^- and OH^- with yields at least two orders of magnitude smaller [28]. Besides the results shown in Fig. 8, a maximum in the yield function of OCN and CN desorption from LEE bombardment of 6 to 12 base-pairs oligonucleotide films has also been observed within the 10-12 eV region [39,40]. *It is clear from all these results that any type of experiment*, whether it measures very small fragments like CN, OCN, H^-, O^- and OH^-, or SSB and DSB in a long double strand of DNA, or various damages on a very short single strand of DNA, *produce yield functions with a strong maximum in the 10-12 eV region.* So far, the only exception to this general behavior occurs with self assembled monolayer films of DNA chemisorbed on gold. In this case, where a chemical bond exists between the substrate and the target molecule, maxima in desorbed anion yields are observed within the 6-8 eV region [20].

4. Discussion

In previous work, it has been shown that the maxima observed in the yield functions for DNA damage induced by electrons of energy below 15 eV are caused by the formation of transient negative ions located at the bases or sugar and phosphate groups [1,41]. We therefore interpret the strong maximum seen in the curves of Figs 5-7 as an enhancement of damage due to the formation of such anions in the 10-12 eV range. As seen from Fig. 8 and previous results on oligonucleotides [39,40], these transitory anions seem to control most of fragmentation processes observed so far by LEE impact on dry DNA below 15 eV. Temporary anions can either dissociate into a negatively charged fragment and a neutral moiety or the electron can leave the trapping molecular site unaltered or in an electronically excited state. In the latter case, bond dissociation can also occur if the excited state is dissociative. When the electron leaves a molecular trapping site, it can be recaptured at

another site where again the same scenario can be available for the decay of the newly formed local anion.

Owing to the possibility of intramolecular electron transfer at non-thermal energies within DNA [26,42] it is not always easy to precisely describe the mechanism responsible for a particular damage. In the case of GCAT (Fig. 1), the observed bond cleavage at positions 1 and 5, for example, could be the results of electron capture and temporary localization on guanine or the nearby sugar or phosphate group of the nucleotide. The same process could occur at the other nucleotides.

Electron transfer in a single nucleotide was investigated theoretically by the group of Simon, using ab initio methods combined with the polarized continuum model in a self-consistent reaction field, to describe the effect of surrounding solvent or other DNA units [42,43,44]. They considered electrons that attach either to the lowest π^*-orbital of cytosine and thymine or to a P=O π^*-orbital of a phosphate unit. They examined a range of electron kinetic energies representative of the energy width of the lowest π^*-resonance states involved and determined how the rates of cleavage of the sugar-phosphate C-O σ-bond depend on energy and on the solvation environment. In the P=O attachment study, they showed that electrons of ca. 1.0 eV could attach to form a π^*-anion, which then could break either a 3' or 5' O-C σ-bond connecting the phosphate to either of two attached sugar groups. For both cytosine and thymine, the group of Simons [42-45] evaluated the adiabatic through-bond electron transfer rate with which the attached electron moves from the base, through the deoxyribose, and onto the phosphate unit and then causes cleavage of the sugar-phosphate σ-bond. Their findings show that the single strand break (SSB) rate depends significantly on the electron energy and upon the solvation environment near the

DNA base. Li et al. [46] studied theoretically cleavage of this bond by direct electron attachment to a sugar-phosphate model. They found that beyond ~ 0.5 eV electron direct attachment into the P=O π^* orbital followed by curve crossing to the σ^* orbital could lead to 3' and 5' O-C bond cleavage without electron transfer, if the transient anion lived a sufficient time. Similarly, according to the work of Berdys et al. [43,44], near 0 eV electrons may not easily attach directly (i.e., vertically) to the phosphate units, but can produce the metastable P=O π^* anion above 2 eV. The hypothesis of electron transfer from a base to the phosphate group was later corroborated by the measurements of SSB in DNA below 5 eV [26], but mass spectrometry studies of gaseous thymidine indicate that electron transfer from the base to the sugar does not occur [47]. Furthermore, it has been found from recent calculations on electron scattering from A and B form DNA, that owing to internal electron diffraction within the strands, the capture probability is much larger on the phosphate group than in on any of the other fundamental units [48].

Even though electron transfer calculations were made with electrons of energies lower than 5 eV, occupying the lowest unfilled molecular π^* and σ^* orbitals, numerous other unfilled orbitals exist at higher energies, in all of the basic units of DNA, that could have considerable overlap with each other. This overlap would cause the transfer integrals between these wavefunctions to be large and favorize electron transfer between the basic units of a nucleotide. Thus, in our results, the 10 eV resonance can either be formed by a single electron attaching to a previously unfilled orbital (i.e. a shape resonance) or be captured by the positive electron affinity of an excited electronic state. In the latter case of a core-excited resonance, electron transfer is unlikely because it requires a three-electron jump [49]; however, the lifetime of such resonances is usually sufficiently long to promote dissociation of the anion. *Core-excited resonances should therefore be associated with*

direct DEA to a basic unit without previous electron transfer. For shape resonances the lifetime is usually too short above ~ 5 eV for dissociation [50,51] and electron detachment or transfer is highly probable. Grandi et al. [52] have reported the formation of a shape resonance for uracil near 9 eV. This transient anionic state, which should also exist for the DNA bases, could transfer its excess electron to higher-lying unfilled orbitals of the phosphate group in a manner similar to the mechanism described below 3 eV [44-45]. However, in this case electron transfer would cause the transformation of a shape resonance into a core-excited resonance on the phosphate group, if we accept the general notion that shape resonances are too short-lived below ~ 5 eV to cause fragmentation [50,51].

To gain further insight into the different possibilities, we display in Fig. 9, the percentage probability of strand break and base release at different sites along the backbone of GCAT based on the magnitude of the yields measured at 6, 10 and 15 eV. As seen, this probability is strongly dependent on site and electron energy, *indicating that the nature and position of the base and the electron scattering mechanism play a role in DNA damage.* Experiments with CGTA at a fixed energy of 10 eV also revealed that the position of the base within the chain has a considerable effect on both phosphodiester and N-glycosidic bond cleavage. In general more damage is sustained by the terminal nucleotides. These offer a larger volume for interaction of the incoming electron wavefunction and we thus expect a higher probability for electron capture at the terminal nucleotides, which should translate into more damage at these positions. The interaction volume at internal positions is the same, so there we expect the same probability and mechanism of dissociation by electron capture by a sugar and phosphate group. The 10 eV result in Fig. 9 shows variations up to a factor of three in internal strand breaks. The latter exhibit a preponderance for bond rupture at the 3' position, but variations up to a factor of two are

found for yields at the 5' positions. At 6 eV, there exists a factor of 2.3 between the yields of 3' internal SSB. Such large variations *for breaking the same internal bond* strongly suggest that the bases C and A are involved in the bond breaking process. *This implies that electron transfer from these bases to the phosphate group occurs and leads to dissociation of the phosphodiester bond.* Electron transfer would also cause a higher rupture rate at the terminal phosphates, since electrons captured by G and T can only flow to position 5 and 16 in Fig. 1, respectively, whereas electrons captured by C and A have to be shared by localization at positions 8, 9 and 12, 13, respectively.

Once the electron has formed a transient anion of the phosphate group either directly or via electron transfer, there are two possible pathways leading to cleavage of the phosphodiester bond. Scission of the C-O bond can occur at positions 5, 9, 13 (Fig. 1) and 8, 12, 16 to give a 3' or 5' carbon-centered radical and a phosphate anion termini, respectively. The other possibility leads to P-O bond cleavage at positions 6, 7, 10, 11, 13 and 15 and provides an alkoxyl anion together with a phosphoryl radical. Thus, these reactions can take place at either the 3'-side or the 5'-side of the phosphodiester bond. On the basis of product analysis, nearly all non-modified fragments of the tetramer irradiated by 4-15 eV electrons, contained a terminal phosphate group, whereas fragments without this phosphate group, i.e., a terminal hydroxyl group, were negligible. Thus, these results demonstrate that cleavage of the phosphodiester bond by 4-15 eV electrons takes place via the formation of a sugar radical and a phosphate anion, as previously demonstrated in the analysis of the products obtained from bombardment with 10 eV electrons.

At resonance energies, the comparison of our results with the dissociative electron attachment (DEA) yields obtained from experiments performed both in the gas phase and on thin molecular films of the bases, suggests that the release of unaltered nucleobases from

GCAT can be explained by dissociation of a transient base anion leading to cleavage of the *N*-glycosidic bond. H^- desorption yields, when induced by electron impact on such films produce yield functions with a maximum at 10 eV with an intensity similar to that seen in Fig. 5. This strong resonance, probably of the core-excited type would therefore be responsible for the previously observed breakage of thymidine to thymine and 2-deoxyribose upon bombardment of a solid film [22] and the 10-eV feature present in the yield functions of the non-modified nucleobases in G, A and T shown in Fig. 5. Here, if electron transfer from another group were involved as the main mechanism of scission of the N-glycosidic bond, one would expect more similarity between the yield functions of Fig. 5 and between the yields displayed in Fig. 9.

The representation of Fig. 9 further demonstrates that the magnitude of bond scission at some positions varies appreciably with electron energy whereas at others this magnitude remains practically constant. For instance, bond scission at position 9 accounts for 21% of the breaks at 6 eV, a value that reduces to 8% and 11% at 10 and 15 eV. Bond breakage at position 12 doubles from 6 to 10 eV and almost triples from 6 to 15 eV. On the other hand, phosphodiester bond cleavage at position 13 remains constant at all energies. Interestingly, the amount of total damage in the terminal nucleotides is inverted in going from 6 to 15 eV: 35% of the damage at 6 eV occurs on the guanine nucleotide compared to 23% on thymidine nucleoside at the other end, whereas at 15 eV, 34% of the damage occurs on dGp and 24% on dTp. Thus, the mechanism of bond scission changes with electron energy.

Since above 14 eV, electron resonances are not expected to dominate the electron scattering process, we expect the yields at 15 eV to represent mostly dissociation via direct excitation of dissociative electronically excited states, whereas at lower energy, the yields

of products induced by direct inelastic scattering would be strongly modulated by the formation of different transient anions at 6 and 10 eV having different dissociation pathways. The direct scattering contribution to the yields necessarily involves no electron transfer and direct electronic excitation on the basic unit is responsible for bond cleavage. However, considering the strong common dip in the yield functions of Figs 5 and 6, we do not expect such direct contributions to be very significant in the yields of monomer and oligomer below 14 eV.

With the additional information of Fig. 9, we interpret the small hump or shoulder in the yield functions of T, G, pT, dGp, pAT and pCAT as due to the formation of one or more transient anions around 6 eV. This resonance always involves the bases thymine and guanine and, with the exception of dGp, occurs at a terminal nucleotide. No distinct features were observed below 9 eV in the anion yield functions obtained from electron scattering from solid films of these bases, but in gaseous thymine the yield function for the formation of $(C_4H_5N_2O)^-$, $(C_3H_2NO)^-$, $(C_3H_4N)^-$, $(OCN)^-$ and $(CN)^-$ exhibits a maximum near 6 eV [6-12]. Furthermore, as seen from Fig. 8, a shoulder exists around 6 eV in the yield of SSB from plasmid DNA, but not in the yield for DSB and H^- desorption. If the 6 eV transient anion leading to base release arose from electron transfer to bases from a sugar or phosphate group, a resonance signal in the adenine and cytosine yield function should also be seen. Hence, as in the case of the 10 eV resonance, electron transfer does not seem to be involved in the 6 eV resonant N-glycosidic bond scission process.

5. Conclusions

On the basis of product analysis, LEE irradiation of GCAT gave non-modified fragments containing a terminal phosphate group, while those without a phosphate group were negligible. Thus, the mechanism of phosphodiester bond cleavage by 4-15 eV

electrons involves cleavage of the C-O bond rather than the P-O bond. The phosphodiester bond cleavage essentially involves the formation of either a C3' or C5' sugar radical and a phosphate anion. We also reported the release of the four non-modified nucleobases from GCAT irradiated with 4-15 eV electrons. These analyses corroborate the results previously obtained at a single energy of 10 eV [34].

As previously found in experiments with plasmid DNA, *below 14 eV, the yield of LEE-induced damage products in GCAT is dominated by the formation of transient anions located around 6 and 10 eV*. Beyond 14 eV, direct LEE impact is believed to contribute substantially to the damage. The effect of the different mechanism of fragmentation is seen in the modification of the repartition of the strand breaks and base release to different positions along the chain with electron energy. According to the present results, electrons can transfer from the bases to the backbone but the inverse does not occur to a substantial extent. Since base release is observed, we conclude that both shape and core-excited resonances are formed by electron attachment to the bases. The latter resonance can retain the electron for a sufficiently long period to allow dissociation of the N-glycosidic bond. Shape resonances, which are known to be much shorter-lived beyond ~5 eV, are not expected to contribute to dissociation, but would be responsible for electron transfer to the phosphate group, leading to the formation of a local shape or core-excited resonance on that group. The latter transient anionic state could dissociate or decay by electron emission, leaving the phosphate group in a dissociative electronic excited state; both processes would break the phosphodiester bond. The formation of such a core-excited resonance on the phosphate group requires the transformation of a single extra electron anion state (a shape resonance) into a two electron one-hole state (a core excited resonance) by electron transfer.

Figure 1. Structure of oligonucleotide GCAT with numbered sites of cleavage

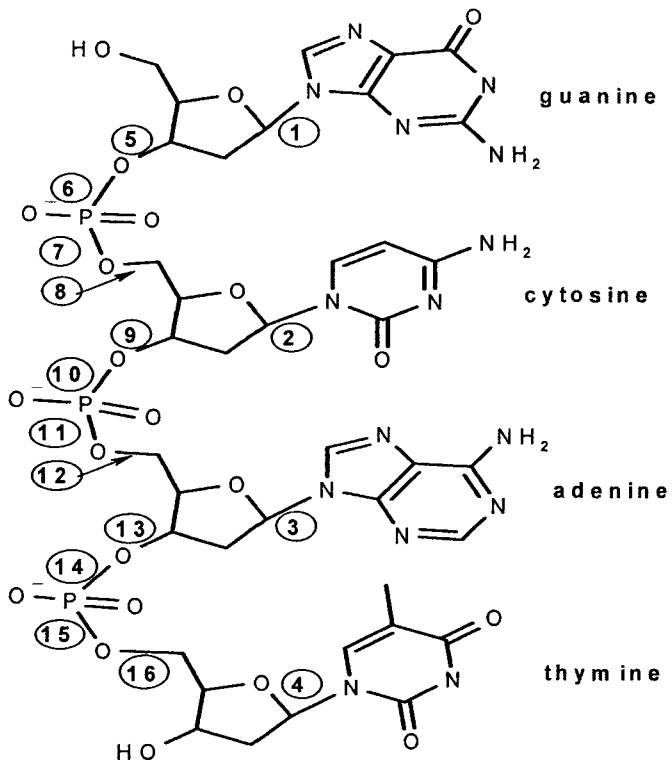

Figure 2. Schematic diagram of the elements of the divergent beam low energy electron (LEE) irradiator; a: cross section view of the gun in a position to bombard the inside wall of a tantalum cylinder used as sample substrate, b: multiple-electrode electron current detector. From ref. 35.

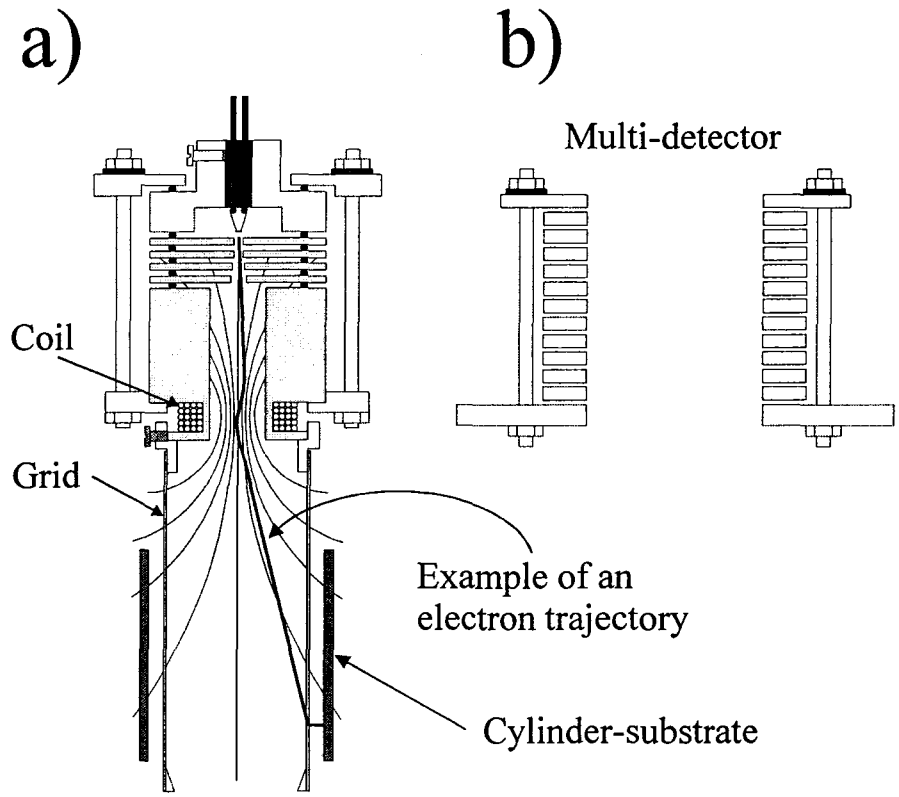

Figure 3. HPLC-UV analysis of DNA exposed to LEE. GCAT was exposed to 1.9 x 10^{16} electrons with an energy of 15 eV. The lower and upper chromatograms correspond to samples treated without and with alkaline phosphatase, respectively. The identity of the peaks in the chromatograms is given in Table 1. The numbers correspond to break positions identified in Fig. 1.

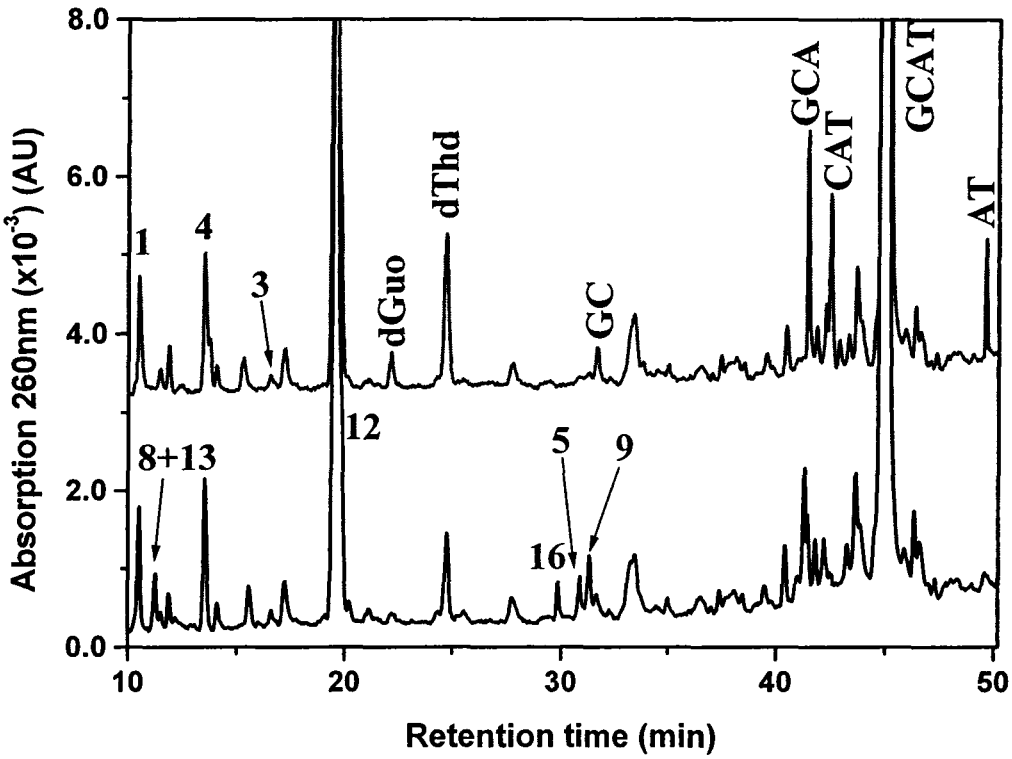

Figure 4. Exposure response for the total damage produced to GCAT by 15 eV electrons at a constant beam flux of 6.6 x 10^{13} electron/s. The error bar (20%) corresponds to the twice standard deviation from 8 exposures.

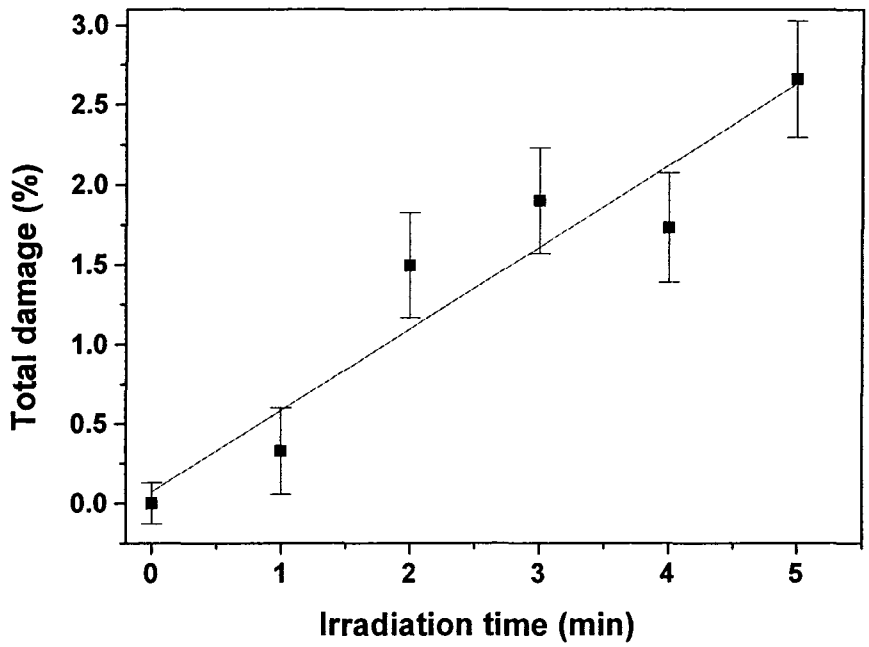

Figure 5. Dependence of the yield of nucleobases on the energy of 4-15 eV electrons. The error bars represent the standard deviation (9%) of eight individual measurements fitted to a Gaussian function. Similar errors were found for all other curves in this figure and in figures 6 and 7.

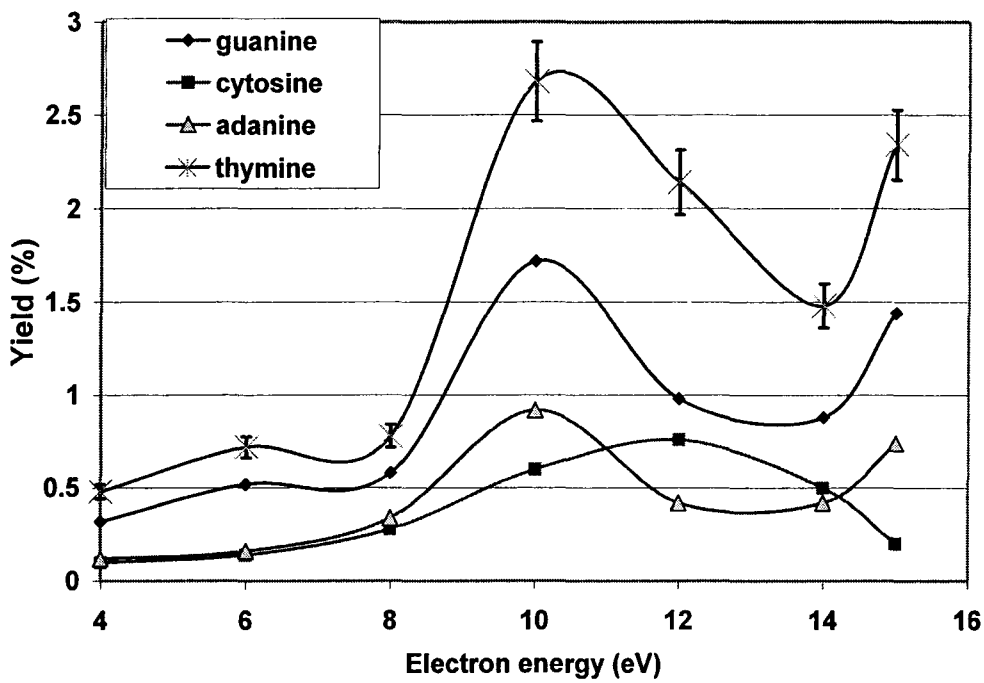

Figure 6 Dependence of the yield of mononucleotides on the energy of 4-15 eV electrons.

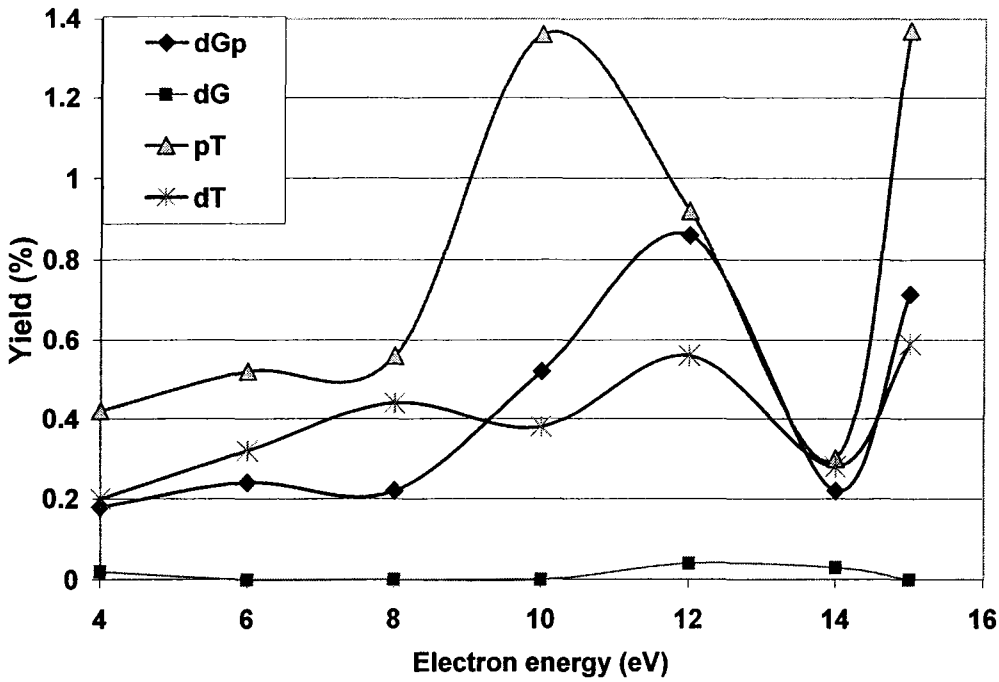

Figure 7. Dependence of the yield of oligonucleotide fragments on the energy of 4-15 eV electrons.

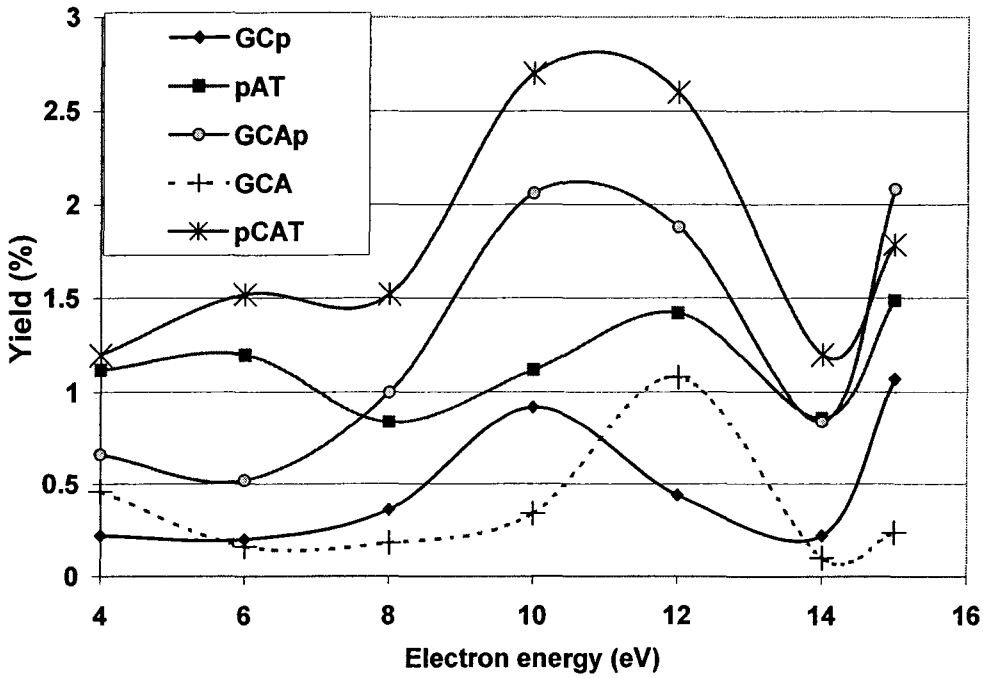

Figure 8 Comparison of fragmentation yields induced by 3-20 eV electrons. The irradiated compounds are: GCAT (top) with products identified in the legend; plasmid DNA, a-DSB, b-SSB (Reprinted from ref. 23); c-linear DNA, d-plasmid DNA (bottom curve) (Reprinted from ref. 28).

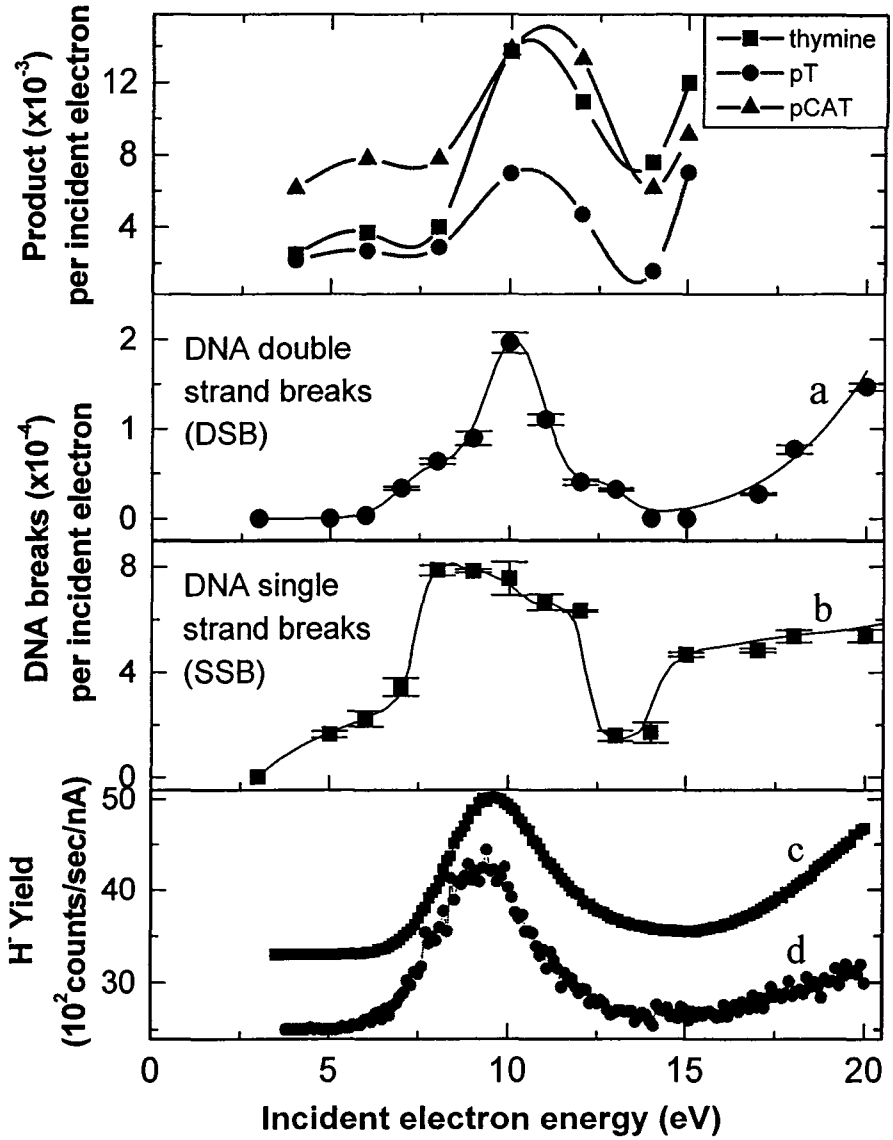

Figure 9 Comparison of percentage distribution of damage by sites of cleavage at three different electron energies, considering that the total damage of phosphate and base release equals to 100%.

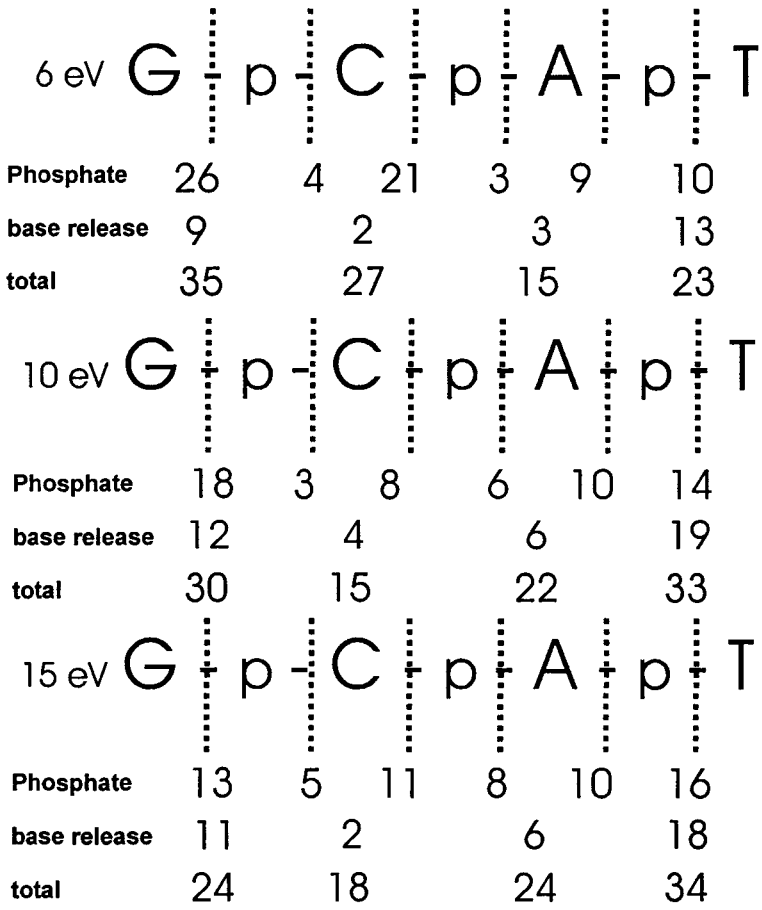

Table 1. Yield of products induced by LEE irradiation of the tetramer GCAT.[a]

5`GCAT (16.8 nmol)		
Break position in Scheme 1	Product	Yield (nmol)
1	G	0.24 ± 0.03
2	C	0.03 ± 0.05
3	A	0.12 ± 0.01
4	T	0.39 ± 0.02
5	pCAT	0.30 ± 0.01
6	dGuo	0 ± 0.05
7	CAT	0 ± 0.05
8	Gp	0.12 ± 0.01
9	pAT	0.25 ± 0.01
10	GC	0 ± 0.05
11	AT	0 ± 0.05
12	GCp	0.18 ± 0.01
13	pT	0.23 ± 0.01
14	GCA	0.04 ± 0.01
15	dThd	0.13 ± 0.01
16	GCAp	0.35 ± 0.02
Total		2.38 ± 0.12

[a]GCAT was exposed to 1.9×10^{16} electrons of 15 eV

REFERENCES

1. L. Sanche, Mass Spectrom. Rev. **21**, 349 (2002).

2. K. Aflatooni, G.A. Gallup, P.D. Burrow, J. Phys. Chem. A **102**, 6205 (1998).

3. S. Feil, K. Gluch, S. Matt-Leubner, P. Scheier, J. Limtrakul, M. Probst, H. Deutsch, K. Becker, A. Stamatovic, T.D. Märk, J. Phys. B: At. Mol. Opt. Phys. **37**, 3013 (2004).

4. S. Denifl, S. Ptasińska, G. Hanel, B. Gstir, M. Probst, P. Scheier, T.D. Märk, J. Chem. Phys. **120**, 6557 (2004).

5. G. Hanel, B. Gstir, S. Denifl, P. Scheier, M. Probst, B. Farizon, M. Farizon, E. Illenberger, T.D. Märk, Phys. Rev. Lett, **9018**, 8104 (2003).

6. See for example, S. Denifl, S. Ptasińska, M. Probst, J. Hrušák, P. Scheier, T.D. Märk, J. Phys. Chem. A **108**, 6562 (2004).

7. M.I. Sukhoviya, I.A. Petruschko, M.I. Shafranyosh, Book of Abstr. IX ECSBM, Prague, Czech Republic, 2001.

8. R. Abouaf, J. Pommier, H. Dunet, Int. J. Mass Spectrom. **226**, 397 (2003).

9. S. Denifl, S. Ptasińska, M. Cingel, S. Matejcik, P. Scheier, T.D. Märk, Chem. Phys. Lett. **377**, 74 (2003).

10. S. Gohlke, H. Abdoul-Carime, E. Illenberger, Chem. Phys. Lett. **380**, 595 (2003).

11. H. Abdoul-Carime, S. Gohlke, E. Illenberger, Phys. Rev. Lett. **92**, 168103-1 (2004).

12. S. Ptasińska, S. Denifl, V. Grill, T.D. Märk, P. Scheier, S. Gohlke, M.A. Huels, E. Illenberger, Angew. Chem. Int. Ed. **44**, 1657 (2005).

13. H. Abdoul-Carime, S. Gohlke, E. Illenberger, Phys. Rev. Lett. **92**, 168103-1 (2004).

14. S. Ptasińska, S. Denifl, V. Grill, T.D. Märk, P. Scheier, S. Gohlke, M.A. Huels, E. Illenberger, Angew. Chem. Int. Ed. **44**, 1657 (2005).

15. M.A. Huels, L. Parenteau, M. Michaud, L. Sanche, Phys. Rev. A **51**, 337 (1995).

16. S. Ptasińska, S. Denifl, P. Scheier, T.D. Märk, J. Chem. Phys. **120**, 8505 (2004).

17. D. Antic, L. Parenteau, M. Lepage, L. Sanche, J. Phys. Chem. **103**, 6611 (1999).

18. D. Antic, L. Parenteau, L. Sanche, J. Phys. Chem. B **104**, 4711 (2000).

19. S.-P. Breton, M. Michaud, C. Jäggle, P. Swiderek, L. Sanche, J. Chem. Phys. **121**, 11240 (2004).

20. X. Pan, L. Sanche, Phys. Rev. Lett. **94**, 198104 (2005) and submitted article.

21. H. Abdoul-Carime, S. Gohlke, E. Fischbach, J. Scheike, E. Illenberger, Chem. Phys. Lett. **387**, 267 (2004).

22. Y. Zheng, P. Cloutier, D.J. Hunting, J.R. Wagner, L. Sanche, JACS **126**, 1002 (2004).

23. B. Boudaiffa, P. Cloutier, D. Hunting, M.A. Huels and L. Sanche, Science **287**, 1658 (2000).

24. B. Boudaïffa, P. Cloutier, D. Hunting, M.A. Huels and L. Sanche, Rad. Res. **157**, 227 (2002).

25. M.A. Huels, B. Boudaïffa, P. Cloutier, D. Hunting and L. Sanche, JACS **125**, 4467 (2003).

26. F. Martin, P.D. Burrow, Z. Cai, P. Cloutier, D.J. Hunting and L. Sanche, Phys. Rev. Lett. **93**, 068101-1 (2004).

27. Z. Cai, P. Cloutier, D. Hunting and L. Sanche, J. Phys. Chem. B **109**, 4796 (2005).

28. X. Pan, P. Cloutier, D. Hunting and L. Sanche, Phys. Rev. Lett. **90**, 208102-1 (2003).

29. P.-C. Dugal, M.A. Huels and L. Sanche, Rad. Res. **151**, 325 (1999).

30. H. Abdoul-Carime, P.-C. Dugal and L. Sanche, Rad. Res. **158**, 23 (2000).

31. P.-C. Dugal, H. Abdoul-Carime and L. Sanche, J. Phys. Chem. B **104**, 5610 (2000).

32. H. Abdoul-Carime and L. Sanche, Rad. Res. **156**, 151 (2001).

33. H. Abdoul-Carime and L. Sanche, Int. J. Rad. Biol. **78**, 89 (2002).

34. Y. Zheng, P. Cloutier, D.J. Hunting, L. Sanche and J.R. Wagner, submitted.

35. Y. Zheng, P. Cloutier, J.R. Wagner, L. Sanche, Rev. Sci. Instrum. **75**, 4534 (2004).

36. G.D. Fasman, *Handbook of Biochemistry and Molecular Biology*, 3rd ed.; CRC Press, Boca Raton, FL, 1995.

37. J. Meesungnoen, J.-P. Jay-Gerin, A. Filali-Mouhim, S. Mankhetkorn, Radiat. Res. **158**, 657 (2002).

38. G. Leclerc, T. Goulet, P. Cloutier, J.-P. Jay-Gerin, L. Sanche, J. Phys. Chem. **91**, 4999 (1987).

39. H. Abdoul-Carime, P.-C. Dugal, L. Sanche, Radiat. Res. **153**, 23 (2002).

40. H. Abdoul-Carime, S. Gohlke, E. Fischbach J. Scheike, E. Illenberger, Chem. Phys. Let., **387**, 267 (2004).

41. A.D. Bass and L. Sanche, in *Charged particle and photon interactions with matter: Chemical, physicochemical and biological consequences with applications*, edited by Y. Hatano, A. Mozumder (Marcel Dekker Inc. New York, 2004).

42. R. Barrios, P. Skurski, J. Simons, J. Phys. Chem. B **106**, 7991 (2002).

43. J. Berdys, I. Anusiewicz, P. Skurki, J. Simons, JACS **126**, 6441 (2004).

44. J. Berdys, P. Skurski, J. Simons, J. Phys. Chem. B **108**, 5800 (2004).

45. J. Berdys, I. Anusiewicz, P. Skurki, J. Simons, J. Phys. Chem. A **108**, 2999 (2004).

46. X. Li, M.D. Sevilla, L. Sanche, J. Am. Chem. Soc. **125**, 13668 (2003).

47. S. Ptasińska, S. Denifl, P. Scheier, E. Illenberger and T.D. Märk, submitted.

48. L.G. Caron and L. Sanche, submitted.

49. P. Rowntree, H. Sambe, L. Parenteau and L. Sanche, Phys. Rev. B **47**, 4537 (1993).

50. M. Allan, J. Electr. Spectr. Rel. Phenom. **48**, 219 (1989).

51. H. Hotop, M.-W. Ruf, M. Llan, I.I. Fabrikant, Adv. At. Mol. Opt. Phys. **49**, 85 (2003).

52. A. Grandi, F.A. Gianturco, N. Sanna, Phys. Rev. Lett. **93**, 048103 (2004.).

Chapter VI - Discussion

Thymidine

Using the apparatus described in Chapter II, we were able to produce sufficient quantities of degraded compound for analysis by HPLC and GC/MS. Thymidine is the primary compound investigated in our system. Since DNA nucleosides are non-volatile biomolecules, they may easily degrade if using the apparatus mentioned in section I.5.2. This was the first study of LEE bombardment of dThd in condensed phase followed by chemical analysis.

The result of chemical analysis revealed the formation of several products. The major product was identified as thymine by comparison of the retention time and UV spectrum to authentic standards in HPLC analysis. In GC/MS analysis, sugar derivatives 2-deoxyribonolactone, 2,3-dideoxyribose and 2-deoxyribose have been identified.

The other perspective of this study is the product quantification, which is determined by GC/MS with isotopic internal standards. For thymine, the initial solution of dThd was spiked with isotopically labeled thymine (d_4-thymine) in order to correct for any losses of thymine during sample preparation. The labeled and natural isotopes of thymine were then purified from the mixture of products by HPLC to exclude the possible decomposition of dThd into thymine during the preparation of samples for GC/MS analysis. The yield of thymine increased from 0.42 nmol in non-irradiated samples to 3.21 nmol in irradiated samples (15 eV for 10 min) for samples initially containing 26.5 nmol dThd. Thus, 10% of dThd was transformed into thymine upon exposure to LEE of 15 eV. The average total decomposition of dThd was approximately 30% and thymine represents approximately 1/3 of the total decomposition products of dThd.

These analyses revealed the formation of thymine being the most abundant product. It suggests that LEEs irradiation of thymidine efficiently cleaves the N-glycosidic bond, leading to the formation of thymine and sugar derivatives. In comparison, base release is 20 times lower in γ-irradiation for the same dose of 61 KGy, it is inefficient in UV-irradiation (Angelov et al., 1997), and it is not induced with solvated electrons and only 15-20% of OH radicals attack the sugar moiety leading to base release OH radicals (von Sonntag, 1987). It shows that LEEs induce damage very efficiently and that the mechanism of damage is different than the well-studied pathways of DNA damage, involving base ionization, OH radicals and solvated electrons.

Along the same line of work, the fragmentation of gaseous Thymidine (dT) by LEE impact was investigated (Abdoul-Carime et al., 2004a). Their results indicated that electrons with energies below 3 eV dissociate dT forming $(dT\text{-}H)^-$ and $(2\text{-deoxyribose-}OH)^-$ and $(T-H)^-_{N1}$ with a break at the N1 position. These results were consistent with our measurements of the products formed in LEE bombardment of solid dT in UHV.

The importance of this research is that it tests the performance of a novel experimental apparatus, i.e. a reliable system for further study the complex DNA damages induced by LEE. This work also provides *quantitative* information of LEE induced damage in complex biological systems.

3'- and 5'-monophosphate thymidine (dTp)

As the second molecule in this study, both 3'and 5'-monophosphate thymidine were investigated individually to compare the effect of 3'and 5'position under the same LEE irradiation condition.

The HPLC analyses show that exposure of dTp to LEE (3-100eV) induces the formation of thymine and thymidine. Similarly, α,α,α,H6-d_4-thymine (0.53 nmol) was added as internal standard to the original solution of dTp (26.5 nmol). Thus the formation of thymine was quantified. It showed that thymine induced by LEE irradiation of 3'-dTp or 5'-dTp at 15 eV was almost identical, approximately 1.3 and 1.4%, respectively (Table 1).

Table 1. Quantitative analysis of products obtained from LEE irradiation of dTp using HPLC/UV and GC/MS. Sample was exposed to 1.9×10^{16} electrons of 15 eV.

Sample		Thymine / dTp[b] (%)	Thymine / total damage (%)	dThd / total damage (%)
dT-5'MP	Non-irradiated[c]	3.5		
	Irradiated	**4.9**	**11**	**3.8**
dT-3'MP	Non-irradiated	3.7		
	Irradiated	**5.0**	**14**	**4.5**

The results indicate two major pathways of damage for the reaction of LEE with dTp: *cleavage of the glycosidic bond and the phosphodiester bond.* One involving cleavage of the glycosidic bond separating the base moiety and sugar phosphate group, which leads to the release of non-modified thymine; and the other, implicating cleavage of the phosphodiester bond, which leads to the release of non-modified thymidine. The latter pathway of cleavage involves localization of LEE within the phosphodiester bond (3'CO-P or P-O5'C) followed by rupture of the phosphodiester bond, which leads to the release of non-modified thymidine. This is supported by theoretical studies suggesting that cleavage of the phophosdiester bond (3'CO-P or P-5'OC) is highly favored via the formation of 3'C-O or 5'C-O radical anions by non-ionizing resonant processes, such as dissociative electron attachment (<15 eV) (Li et al., 2003).

The base release reaction was also observed in the previous study of dThd which was proposed by the pathway of N-glycosidic bond cleavage. However, there is another possibility. For example, the release of non-modified nucleobases is a major product of hydroxyl radical induced damage to DNA, which involves initial H-atom abstraction from C4' and C1' as well as other positions, followed by decomposition of the sugar moiety (von Sonntag, 1987; Henle et al., 1995). In the phosphodiester bond cleavage pathway dissociative electron attachment can produce carbon-centered radicals at the sugar moiety, which are expected to lead to the release of non-modified nucleobases by analogous reactions. In fact, the yield of thymine is three times larger than that of dThd (table 1). It indicates that both pathways of N-glycosidic bond and phosphodiester bond cleavages must exist in DNA and lead to base release. Which pathway is the main source of base release by LEE? In addition, although the effect of 3'and 5' position seems similar in the monophosphate nucleotide at electron energy of 15 eV, in DNA may it be different? Both questions need to be verified in the study of oligonucleotides.

Oligo GCAT and CGTA

The results of GCAT and CGTA are mainly discussed in the third article (chapter IV). In this study, 16 non-modified nucleobase, nucleoside and nucleotide fragments resulting from the cleavage of phosphodiester and *N*-glycosidic bonds of each tetramer were identified.

Mechanism of phosphate ester bond cleavage

On the basis of our analysis of fragments from oligonucleotide tetramers, we demonstrated that *cleavage of the phosphodiester bond primarily takes place via the formation of a sugar radical and a phosphate anion* (Scheme 4). In general, once the

electron has localized on the phosphodiester bond, there are two possible pathways leading to cleavage of this bond. The one shown in Scheme 4 involves scission of the C-O bond and gives carbon-centered radicals and phosphate anions as termini. The other results in cleavage of the P-O bond and gives alkoxyl anions together with phosphoryl radicals (not shown). From the radical chemistry, the final products of both pathways are expected to be different, leading to oligomers with and without a terminal phosphate group, respectively. However, nearly exclusively fragments containing a terminal phosphate were detected from chemical analysis. Moreover, virtually all the non-modified fragments contained a terminal phosphate group at the site of cleavage. These results demonstrate that the phosphodiester bond breaks by a distinct pathway in which the negative charge localizes on the phosphodiester bond giving rise to non-modified fragments with an intact phosphate group. Conversely, the radical must localize on the sugar moiety to give as yet unidentified modifications. It indicates that the phosphodiester bond breaks induced by LEE dominantly lead to the C-O bond rupture rather than P-O bond.

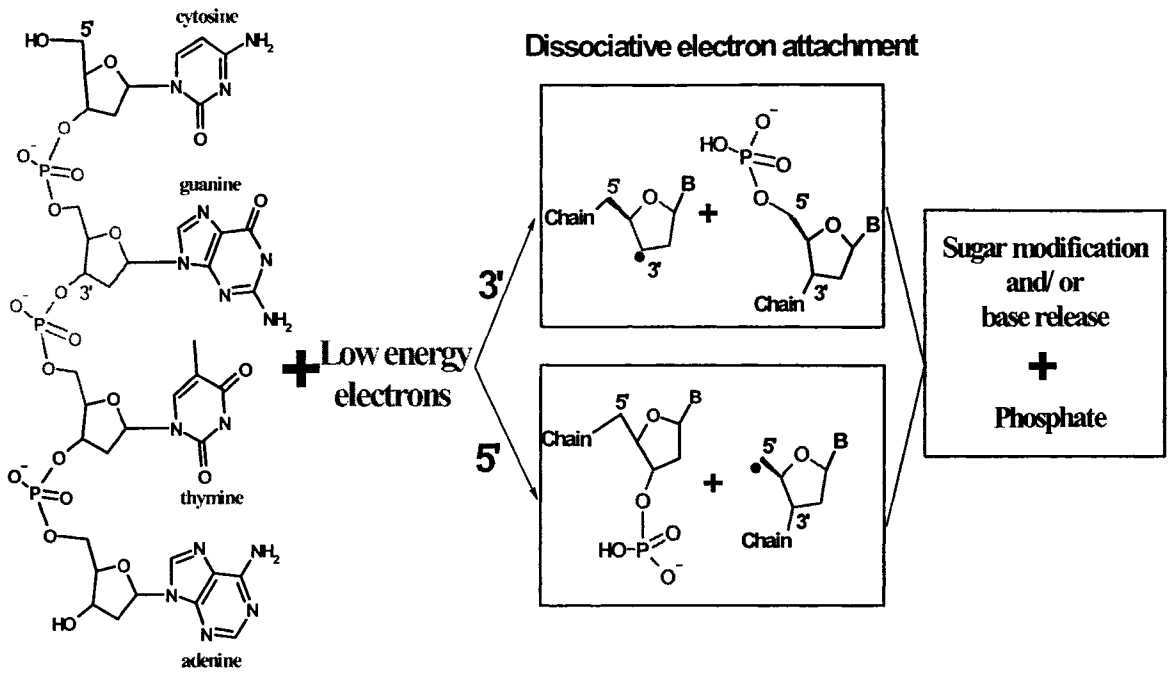

Scheme 4. Proposed pathways for phosphate ester bond cleavage of DNA.

The formation of both carbon-centered and phosphoryl radicals was previously reported by electron spin resonance (ESR) studies of DNA exposed to ionizing radiation (Becker et al., 2003). Recently, the C5' carbon centered radical of the sugar moiety was also proposed to exist in irradiated DNA (Shukla et al., 2005). It was reported that carbon-centered radicals contribute about 95% of total radicals from phosphodiester bond dissociation attacked by LEE. It also suggested that C-O bond cleavage was the dominating process on the basis of ESR studies.

A possible interpretation of the latter result, as well as our results, is that the bond breaking process takes place by electron attachment into an unfilled orbital lying at a much higher energy (i.e., 10 eV = 960 kJ/mol) than the thermodynamic threshold of C-O bond dissociation. In this case, phosphodiester bond cleavage would not depend on bond energy

considerations but rather on the availability of dissociating anionic states at the energy of the captured electron.

Electron transfer

Theoretical calculation of electron attachment to several biomolecules including excised DNA fragments (Barrios et al., 2002; Berdys et al., 2004a, 2004b, 2004c), using *ab initio* methods combined with the polarized continuum model in a self-consistent reaction field, suggests a model of damage in DNA systems caused by LEE. It was suggested that electrons can attach either to the lowest π^{*-}orbital of cytosine and thymine or to a P=O π^{*-} orbital of a phosphate unit. Electrons of ca. 1.0 eV could attach to form a π^{*-} anion, which then could break either a 3' or 5' O-C σ-bond connecting the phosphate to either of the two attached sugar groups. For both cytosine and thymine, the adiabatic through-bond electron transfer rate was evaluated with which the attached electron moves from the base, through the deoxyribose, and onto the phosphate unit and then causes cleavage of the sugar-phosphate σ-bond. Their findings show that the single strand break (SSB) rate depends significantly on the electron energy and upon the solvation environment near the DNA base. Direct attachment can produce a metastable P=O π^* anion, but this process would require electrons with energy >2 eV.

In our results of oligo product analysis, the variation between terminal and internal cleavage is more consistent with a mechanism involving initial capture of the electron by the nucleobase followed by electron transfer to the phosphodiester bond. This hypothesis is consistent with the approximately two-fold greater cleavage at the terminal compared to internal positions because the transfer of electrons can only take place to a single phosphodiester bond for terminal nucleobases, while the transfer will be shared between

two sites for internal nucleobases. In contrast, initial capture of LEE by the phosphodiester bonds would be expected to give an equal distribution of cleavage products. Although the indirect pathways of electron transfer leading to phosphodiester bond cleavage have been described for electrons of energies below 4 eV (Barrios et al., 2002; Berdys et al., 2004a, 2004b, 2004c), we propose that similar pathways may also be operative for 10 eV electrons used in the present experiments. Quantum dynamics calculations for the scattering of LEE from uracil (Grandi, et al., 2004; Gianturco & Lucchese, 2004a) and glycine (Gianturco & Lucchese, 2004b) were performed and obtained several open-channel shape resonances. For uracil, a feature at 9 eV in the excess electron resonant wave functions could be related to experimental findings on dissociative electron attachment (DEA) yields that follow the initial formation of the calculated transient anion states. This transient anionic state, which should also exist for pyrimidine bases, could transfer its excess electron to unfilled orbitals of the phosphate group lying at higher energy in a manner similar to that described below 3 eV (Grandi, et al., 2004).

The distribution of non-modified products suggests a mechanism of damage involving initial electron attachment to nucleobase moieties, followed by electron transfer to the sugar-phosphate backbone, and subsequent dissociation of the phosphodiester bond. In summary, the reaction of LEE with simple tetramers involved dissociative electron attachment leading to phosphodiester bond cleavage and the formation of non-modified fragments.

3'-side or the 5'-side cleavage

The backbone reactions leading to strand break can take place at either the 3'-side or the 5'-side of the phosphodiester bond. Comparison of phosphate and base release yields

at cleavage sites with three electron energies is shown in scheme 5. Three incident electron energies of 6, 10 and 15 eV are corresponding to maxima in the yield curves as a function of electron energy, which representing the typical energy where DEA occur in DNA. That is, the distribution reflects the product yield mainly due to DEA. This scheme displays a significant yield difference in the 3'- and 5'-side cleavage positions. There is at least 2 times greater yield of oligomer products with 5'-phosphorylated ends than with 3'-ends, especially in the internal sites of 6 and 10 eV. This suggests that phosphodiester bond cleavage induced by LEE may have more tendencies to occur at the 3'-side of DNA than 5'-side. In contrast, there was no strong pattern of cleavage with respect to either the nature of the neighboring nucleobase, comparing the tetramer GCAT with CGTA.

According to the mechanism of electron transfer, electrons first attach to the nucleobase and then transfer to the sugar phosphodiester backbone. From a perspective of the chemical structure, the transfer pathways from the N-glycosidic bond to the 3' or 5' positions of 2-deoxyribose are different. A possible explanation for preferring 3' cleavage is that the dissociating anionic states at the 3'-side may have a lower energy level to capture electrons than those at the 5'-side. On the other hand, when the incident electron energy is increased from 10 eV to 15 eV the difference of 3'-side and 5'-cleavage is less significant. It indicates that electron transfer in DNA is likely occurring only at low energy. Because at higher energy direct attachment can be the prominent process leading to phosphodiester bond cleavage, there is an equal probability of electron attachment to 3'-side or 5'-side of deoxyribose. In addition, core-excited resonance will replace shape resonance at higher energy, in which electron transfer can hardly take place once electron capture has occurred to form a transient negative ion (Martin et al., 2004).

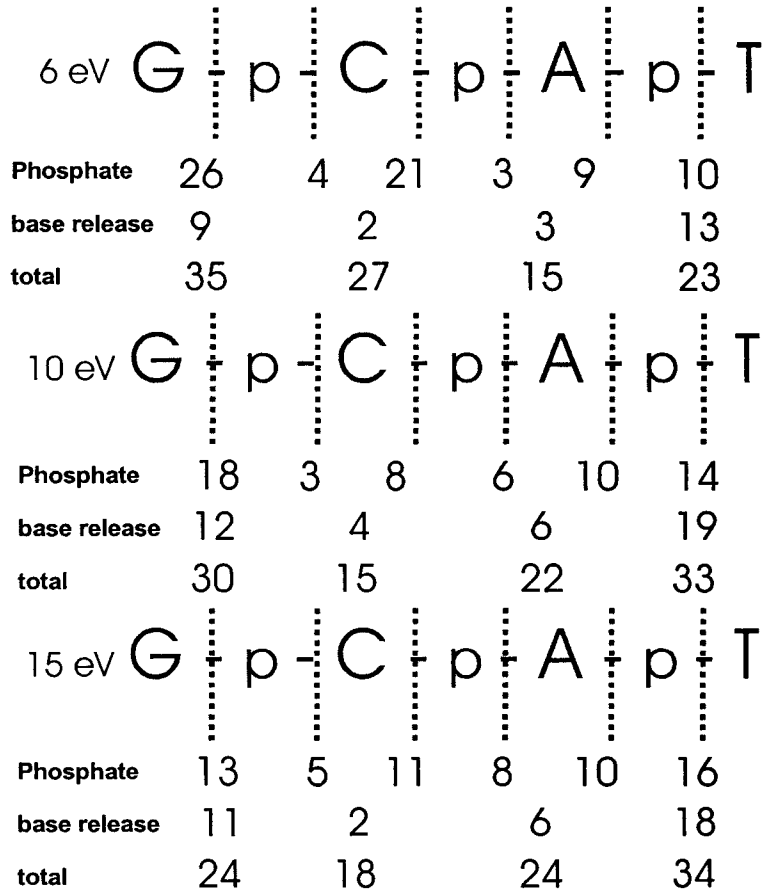

Scheme 5. Comparison of the distribution of damage by sites of cleavage at three different electron energies, assuming that the total damage of phosphate and base release equals 100. The oligomer sequences are given using standard notation, reading from left-to-right 5'-to-3'.

This observation is consistent with previous studies indicating 1.8 greater yield of oligomer products with 5'-phosphorylated ends than with 3'-ends within X-irradiated crystalline DNA (Debije et al., 2001). Our results suggest that *LEE leads to a higher yield of phosphodiester bond cleavage at the 3'-side than the 5'-side.*

Oligo with stable abasic site

From analysis of DNA damage, however, it is difficult to distinguish between the initial attachment of LEE to phosphate groups and the initial attachment to bases followed by transfer to phosphate groups. Modified oligomer with stable abasic site were designed to study the effect of nucleobase on electron transfer. In such oligos, containing a stable abasic site, therefore, electron transfer from a specific base to the phosphodiester bond was inhibited.

Four modified oligomers with different stable abasic sites: XCAT, GXAT, GCXT and GCAX, where X denotes a stable abasic site, were irradiated by LEE. Similarly, HPLC and specific enzymes such as alkaline phosphatase, were involved to identify the main products of damage. Compared to the non-modified tetramer, GCAT, it is shown that the presence of an abasic site greatly decreases the yield of strand break in the oligo. For the phosphodiester bond cleavage and base release of abasic oligos at incident electron energy of 15 eV, the total yields are approximately 7 and 4 times less than that of GCAT, respectively.

The sites of cleavage in GCXT by mono-energetic LEE were examined from 4 to 15 eV electron energy ranges. Interestingly, LEE induced cleavage reactions were greatly impeded next to the abasic site (Scheme 6), especially at low energy range. For example, the phosphodiester bond cleavages at 4 and 5 sites are about 50% decreased at 10 eV compared to that of at 15 eV. According to the mechanism of electron transfer, DNA bases initially capture LEE, and then, the electrons are transferred to the sugar-phosphate group, which induces sugar-phosphate C-O bond rupture. Our results demonstrate that such electron transfer in DNA occurs more likely with low energy electron (< 10 eV). With

electrons of higher energy, the electrons may attach directly to the sugar phosphate backbone leading to a strand break even in the modified oligomer with an abasic site, such as 4 and 5 (Scheme 6).

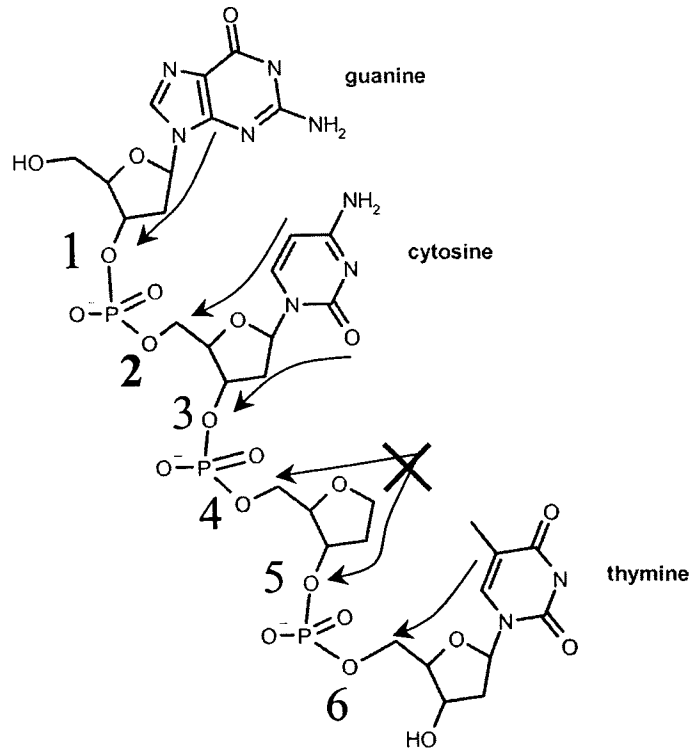

Scheme 6. Structure of GCXT (X denotes an abasic site) with arrow and number pointing to the possible direction of electron transfer and sites of phosphodiester bond cleavage.

Because the work of abasic oligo was not yet finished at the low electron energy range, a complete comparison of data can not be shown here. Nevertheless, since at the very low energy, the mechanism of electron transfer appears to be the dominant process rather than direct attachment, phosphodiester bond cleavage next to the abasic site is expected to be impeded. By comparing the yields of cleavage as a function of electron energy, we can determine the ratio of LEE-mediated electron transfer to attachment and display a shift of these two mechanisms from low to high energy. Thus, the study will give us a more precise interpretation of electron transfer in DNA damage.

In summary, our studies support electron transfer of LEE from the base moiety to the sugar-phosphate backbone in DNA as suggested by theoretical studies. Such a mechanism of damage suggests that the capture of non-thermalized electrons with 4-10 eV of energy by DNA bases may be an important factor in DNA damage in living cells.

Chapter VII - Conclusions

Chemical analysis of DNA damage induced by LEE was systematically investigated using a new low-energy electron irradiation system in which relatively large amounts of target compounds can be irradiated. Starting with small DNA components, nucleosides, nucleotides, oligonucleotides, etc. the reaction of low energy electrons was investigated by direct analysis of the products by HPLC, GCMS and LCMS.

The preliminary results indicate two major pathways of damage for the reaction of LEE with dTp: *cleavage of the N-glycosidic bond and the phosphodiester bond.* Cleavage of the glycosidic bond separating the base moiety and sugar phosphate group leads to the release of non-modified thymine (as well as detected in the dThd). Cleavage of the phosphodiester bond leads to the release of non-modified thymidine.

The above mechanisms of cleavage are supported in the further studies of oligonucleotide tetramers. On the basis of our analysis of fragments from GCAT, CGTA, and tetramer with an abasic site, we demonstrate that cleavage of the phosphodiester bond primarily takes place via the formation of a sugar radical and a phosphate anion. The phosphodiester bond breaks by a distinct pathway in which the negative charge localizes on the phosphodiester bond giving rise to non-modified fragments with an intact phosphate group. Conversely, the radical must localize on the sugar moiety to give as yet unidentified modifications. *It indicates that the phosphodiester bond breaks induced by LEE dominantly lead to C-O bond rather than P-O bond rupture.*

Another interesting observation in our study addresses electron transfer in DNA. From results of oligonucleotide product analysis, the variation between terminal and internal cleavage was more consistent with a mechanism involving initial capture of the

electron by the nucleobase followed by electron transfer to the phosphodiester bond. This hypothesis is consistent with the approximately two-fold greater cleavage at the terminal compared to internal positions because the transfer of electrons can only take place to a single phosphodiester bond for terminal nucleobases, while the transfer should be shared between two sites for internal nucleobases. *We therefore conclude that electron transfer from these bases to the phosphate group occurs prior to dissociation of the phosphodiester bond.* Since base release was observed, both shape and core-excited resonances can be formed by electron attachment to the bases. The latter resonance can retain the electron for a sufficiently long period to allow dissociation of the N-glycosidic bond. Shape resonances, which are known to be much shorter-lived beyond ~5 eV, are not expected to contribute to dissociation, but may be responsible for electron transfer to the phosphate group, leading to the formation of a local shape or core-excited resonance on that group. The latter transient anionic state could dissociate or decay by electron emission, leaving the phosphate group in a dissociative electronic excited state; both processes would break the phosphodiester bond. The formation of such a core-excited resonance on the phosphate group requires the transformation of a single extra electron anion state (a shape resonance) into a two electron one-hole state (a core excited resonance) by electron transfer.

The study of oligonucleotides with stable abasic sites strongly suggest that electron transfer is important in LEE-induced DNA damage. Firstly, compared to the non-modified tetramer GCAT, it was shown that the presence of an abasic site significantly decreases the yield of strand break in a series of oligonucleotide tetramers. Secondly, LEE induced cleavage reactions were greatly impeded next to the abasic site, especially in the low energy range. These results indicate that electron transfer in DNA is more likely to occur

with low energy electron (< 6 eV) rather than with electrons with higher energy, which are more likely to attach directly to the sugar phosphate backbone.

Based on the results of product identification, we suggest potential reaction pathways for secondary electron attack on DNA. These studies will increase our understanding of the mechanisms of DNA damage induced by ionizing radiation that are in turn responsible for the deleterious biological effects.

Acknowledgements

I would like to thank Prof. Léon Sanche for the opportunity to pursue my Ph. D. study at his research group, for his advice and encouragement, and overall for kind relationship.

I would like to thank Prof. J. Richard Wagner for the opportunity to study at his laboratory, for his guidance and encouragement, and informative discussions.

I would like to thank Prof. Darel J. Hunting for his friendly encouragement and help, for being the co-director of this project.

I am very grateful for Mr. Pierre Cloutier, Mr. Luc Parenteau and Mr. Daniel Robillard for their technical support from the beginning to the end.

I would like to thank my colleagues in the lab: Sébastien Tremblay, Francois Bergeron and Johann Riviere for helps in the new techniques and interesting discussions in experiments.

I appreciate the help and encouragement from Prof. Jean-Paul Jay-Gerin for French course.

I thank the professors of the Department of Nuclear Medicine & Radiobiology for excellent courses and students of this Department for friendship.

I thank Prof. Peter Dedon, Prof. Patrick Ayotte and Prof. Michael Huels for the very helpful critical reviews of this manuscript.

I am very grateful to my family: my parents, my daughter, sister and brother, for their unconditional support of my studies.

References

Abdoul-Carime, H., Cloutier, P., Sanche L. (2001) Low energy (5-40 eV) electron stimulated desorption of anions from physisorbed DNA bases. *Radiation Res.,* 155, 625-633.

Abdoul-Carime, H., Dugal, P.-C., Sanche, L. (2000) Damage induced by 1-30 eV electrons on thymine and bromouracil substituted oligonucleotides. *Radiat. Res.* 153, 23.

Abdoul-Carime, H., Gohlke, S., Fischbach, E., Scheike, J., Illenberger, E. (2004)a Thymine excision from DNA by subexcitation electrons. *Chem. Phys. Lett.* 387, 267.

Abdoul-Carime, H., Gohlke, S., Illenberger, E. (2004)b Site-Specific Dissociation of DNA Bases by Slow Electrons at Early Stages of Irradiation. *Phys. Rev. Lett.* 92, 168103-1.

Abdoul-Carime, H., Sanche, L. (2001) Sequence specific damage to oligonucleotides induced by 3-30 eV electrons. *Radiat. Res.* 156, 151-157.

Abdoul-Carime, H., Sanche, L. (2002) Fragmentation of short single DNA strands by 1-30 eV electrons : Dependence on base identity and sequence. *Int. J. Rad. Biol.* 78, 89.

Abouaf, R., Pommier, J., Dunet, H. (2003) Negative ions in thymine and 5-bromouracil produced by low energy electrons. *Int. J. Mass Spectrom.* 226, 397.

Adams, R.L.P., Knowler, J.T. and Leader, D.P. (1981) in *The biochemistry of the Nucleic Acids*, 10th ed., Chapman and Hall, New York.

Aflatooni, K., Gallup, G.A., Burrow, P.D. (1998) Electron attachment energies of the DNA bases. *J. Phys. Chem. A* 102, 6205.

Angelov, D., Spassky, A., Berger, M., Cadet, J. **(1997)** High-Intensity UV Laser Photolysis of DNA and Purine 2'-Deoxyribonucleosides: Formation of 8-Oxopurine Damage and Oligonucleotide Strand Cleavage as Revealed by HPLC and Gel Electrophoresis Studies. *J. Am. Chem. Soc. 119*, 11373-11380.

Antic, D., Parenteau, L., Lepage, M., Sanche, L. (1999) Low energy electron damage to condensed phase deoxyribose analogs investigated by electron stimulated desorption of H^- and electron energy loss spectroscopy. *J. Phys. Chem. B* 103, 6611.

Antic, D., Parenteau, L., Sanche, L. (2000) Electron stimulated desorption of H^- from condensed phase deoxyribose analogs : dissociative electron attachment vs. resonance decay into dipolar dissociation. *J. Phys. Chem. B* 104, 4711.

Barrios, R., Skurski, P., Simons, J. (2002) Mechanism for damage to DNA by low-energy electrons. *J. Phys. Chem. B* 106, 7991.

Bass, A. D. & Sanche, L. (2004) in *Charged particle and photon interactions with matter: chemical, physicochemical and biological consequences with applications*, edited by Hatano, Y. & Mozumder, A., Marcle Decker Inc., New York.

Becker, D., Bryant-Friedrich, A., Trzasko, C., Sivilla, M. D. **(2003)** Electron spin resonance study of DNA irradiated with an Argon-ion beam: evidence for formation of Sugar phosphate backbone radicals. *Radiat. Res. 160*, 174.

Berdys, J., Anusiewicz, I., Skurki, P., Simons, J. (2004)a Damage to model DNA fragments from very low-energy (<1 eV) electrons. *JACS* **126**, 6441.

Berdys, J., Anusiewicz, I., Skurki, P., Simons, J. (2004)b Theoretical Study of Damage to DNA by 0.2-1.5 eV Electrons Attached to Cytosine. *J. Phys. Chem. A* **108**, 2999.

Berdys, J., Skurski, P., Simons, J. (2004)c Damage to model DNA fragments by 0.25-1.0 eV electrons attached to a thymine π^* orbital. *J. Phys. Chem. B* **108**, 5800.

Boudaiffa, B., Cloutier, P., Hunting, D., Huels, M.A., Sanche, L. (2000)a Resonant formation of DNA strand breaks by low-energy (3 to 20 eV) electrons. *Science* 287, 1658-1660.

Boudaïffa, B., Cloutier, P., Hunting, D., Huels, M.A., Sanche, L. (2000)c Les électrons de trés faible énergie produisent des lésions de l'ADN. *Méd. Sci.* 16, 1281.

Boudaïffa, B., Cloutier, P., Hunting, D., Huels, M.A., Sanche, L. (2002) Cross sections for low-energy (10-50 eV) electron damage to DNA. *Radiat. Res.* 157, 227.

Boudaiffa, B., Hunting, D. J., Cloutier, P., Huels, M. A., Sanche, L. (2000)b Induction of single and double strand breaks in plasmid DNA by 100 to 1500 eV electrons. *Int. J. Radiat. Biol.* 76, 1209.

Box, H. C., Potter, W. R. and Budzinski, E. E. (1975) The reduction of nucleotides by ionizing radiation: Uridine 5'phosphate and cytidine 3'phosphate. *J. Chem. Phys.*, 62, 3476-3478.

Breton, S.-P., Michaud, M., Jäggle, C., Swiderek, P., Sanche, L. (2004) Damage induced by low-energy electrons in solid films of tetrahydrofuran. *J. Chem. Phys.* 121, 11240.

Cadet J., Berger M., Douki T., Ravanat, J. L. (1997) Oxidative damage to DNA: formation, measurement and biological significance. *Rev. Physiol. Biochem. Pharmacol.* 131, 1-87.

Cadet J., Douki T., Gasparutto D., Ravanat, J. L. (2003) Oxidative damage to DNA: formation, measurement and biochemical features. *Mutat. Res.* 532, 5-23.

Cai, Z., Cloutier, P., Hunting, D., Sanche, L. (2005) Comparison between X-ray Photon and Secondary Electron Damage to DNA in Vacuum. *J. Phys. Chem. B* 109, 4796.

Cobut, V.; Frongillo, Y.; Patau, J. P.; Goulet, T.; Fraser, M.-J.; Jay-Gerin, J.-P. (1998) Monte carlo simulation of fast electron and proton tracks in liquid water-I : physical and physicochemical aspects. *Rad. Phys. Chem.* 51, 229.

Davies M.J., Gilbert B. C., Hazlewood C., Polack N. P. (1995) EPR spin-trapping of radical damage to DNA. *J. Chem. Soc. Perkin Trans.* 2, 13-21.

Debije, M., Razskazovsliy, Y., Bernhard, W. A. (2001) The yield of strand breaks resulting from direct-type effects in crystalline DNA X-irradiated at 4 K and room temperature. *J. Am. Chem. Soc.* 123, 2917-2918.

Denifl, S., Ptasinska, S., Cingel, M., Matejcik, S., Scheier, P., Märk, T.D. (2003) Electron attachment to the DNA bases thymine and cytosine. *Chem. Phys. Lett.* 377, 74.

Denifl, S., Ptasinska, S., Hanel, G., Gstir, B., Probst, M., Scheier, P., Märk, T.D. (2004)a Electron attachment to gas-phase uracil. *J. Chem. Phys.* 120, 6557.

Denifl, S., Ptasinska, S., Probst, M., Hrušák, J., Scheier, P., Märk, T.D. (2004)b Electron attachment to the gas-phase DNA bases cytosine and thymine. *J. Phys. Chem. A* 108, 6562.

Devlin, T. M. (1997) in Textbook of Biochemistry with clinical correlations, 4th ed., Wiley-Liss, New York.

Dizdaroglu, M., Jaruga, P., Ririncioglu, M., Rodriguez, H. (2002) Free radical-induced damage to DNA : mechanisms and measurement. *Free Radi. Bio. & Med.* 32, 1102-1115.

Dugal, P.-C., Abdoul-Carime, H., Sanche, L. (2000) Mechanisms of low energy (0.5-30 eV) electron-induced pyrimidine ring fragmentation within thymine and halogen-substituted single strands of DNA. *J. Phys. Chem. B* 104, 5610.

Dugal, P.-C., Huels, M.A., Sanche, L. (1999) Low-energy (5025 eV) electron damage to homo-oligonucleotides. *Radiat. Res.* 151, 325.

Feil, S., Gluch, K., Matt-Leubner, S., Scheier, P., Limtrakul, J., Probst, M., Deutsch, H., Becker, K., Stamatovic, A., Märk, T.D. (2004) Partial cross sections for positive and negative ion formation following electron impact on uracil. *J. Phys. B*: At. Mol. Opt. Phys. 37, 3013.

Folkard, M., Prise, K.M., Vojnovic, B., Davies, S., Roper, M.J., Michael, B.D. (1993) Measurement of DNA damage by electrons with energies between 25 and 4000 eV. *Int. J. Radiat. Biol.* 64, 651.

Gohlke, S., Abdoul-Carime, H., Illenberger, E. (2003) Dehydrogenation of adenine induced by slow (<3 eV) electrons. *Chem. Phys. Lett.* 380, 595.

Gianturco, F.A., Lucchese, R.R. (2004)a Radiation damage of biosystems mediated by Secondary electrons: Resonant precursors for uracil molecules. *J. Chem. Phys.* 120, 7446.

Gianturco, F.A., Lucchese, R.R. (2004)b Resonant Capture of Low-Energy Electrons by Gas-Phase Glycine: A Quantum Dynamics Calculation. *J. Phys. Chem. A* **108**, 7056.

Grandi, A., Gianturco, F.A., Sanna, N. (2004) H^- desorption from uracil via metastable electron capture. *Phys. Rev. Lett.* **93**, 048103-1.

Hanel, G., Gstir, B., Denifl, S., Scheier, P., Probst, M., Farizon, B., Farizon, M., Illenberger, E., Märk, T.D. (2003) Electron Attachment to Uracil: Effective Destruction at Subexcitation Energies. *Phys. Rev. Lett.* 90, 188104.

Henke, B.L., Knauer, J.P., Premaratne, K., (1981) The characterization of x-ray photocathodes in the 0.1–10-keV photon energy region. *J. Appl. Phys.* 52, 1509.

Henke, B.L., Smith, J. A., Attwood, D.T. (1977) 0.1–10-keV x-ray-induced electron emissions from solids—Models and secondary electron measurements. *J. Appl. Phys.* 48, 1852.

Henle, E. S., Roots, R., Holley, W. R., Chatterjee, A. **(1995)** DNA strand breakage is corrected with unaltered base release after gamma irradiation. *Radiat. Res. 143*, 144.

Hervé du Penhoat, M.A., Huels, M.A., Cloutier, P., Jay-Gerin, J.P., Sanche, L. (2001) Electron stimulated desorption of H^- from thin films of thymine and uracil. *J. Chem. Phys.* 114, 5755.

Huels, M. A., Parenteau, L., Sanche, L. (2004) Reactive scattering of 1-5 eV O^- in films of tetrahydrofuran. *J. Phys. Chem. B* 108, 16303.

Huels, M.A., Boudaïffa, B., Cloutier, P., Hunting, D., Sanche, L. (2003) Single, double and multiple double strand breaks induced in DNA by 3-100 eV electrons. *JACS* 125, 4467.

Huels, M.A., Parenteau, L., Michaud, M., Sanche, L. (1995) Kinetic-energy distributions of O^- produced by dissociative electron attachment to physisorbed O_2. *Phys. Rev.* A 51, 337.

Hutchinson F. (1985) Chemical changes induced in DNA by ionizing radiation. *Progress in Nucleic Acid Research & Molecular Biology*, 32, 115-154.

Ibach, H., Mills, D.L. (1982) in Electron Energy Loss Spectroscopy and Surface Vibration, Academic, New York.

Kimmel, G.A., Orlando, T.M., (1995) Low-Energy (5–120 eV) Electron-Stimulated Dissociation of Amorphous D_2O Ice: $D(^2S)$, $O(^3P_{2,1,0})$, and $O(^1D_2)$ Yields and Velocity Distributions. *Phys. Rev. Lett.* 75, 2606.

Klyachko, D.V., Huels, M.A., Sanche, L. (1999) Halogen anion formation in 5-halo-uracil films : X rays vs. subionization electrons. *Radiat. Res.* 151, 177.

Lepage, M., Letarte, S., Michaud, M., Motte-Tollet, F., Hubin-Franskin, M.-J., Roy, D., Sanche, L. (1998) Electron spectroscopy of resonance-enhanced vibrational excitations of gaseous and solid tetrahydrofuran. *J. Chem. Phys.* 109, 5980.

Li, X., Sanche, L., Sevilla, M.D. (2002) Dehalogenation of 5-Halouracils after Low Energy Electron Attachment: A Density Functional Theory Investigation. *J. Phys. Chem. A* **106**, 11248.

Li, X., Sevilla, M. D., Sanche, L. (2003) Density functional theory studies of electron interaciton with DNA : can zero eV electrons induce strand breaks? *JACS* 125, 13668.

Li, X., Sevilla, M.D., Sanche, L. (2004) Hydrogen Atom Loss in Pyrimidine DNA Bases Induced by Low-Energy Electrons: Energetics Predicted by Theory. *J. Phys. Chem. B* **108**, 19013.

Martin, F., Burrow, P.D., Cai, Z., Cloutier, P., Hunting, D.J., Sanche, L. (2004) DNA strand breaks induced by 0-4 eV electrons : the role of shape resonances. *Phys. Rev. Lett.* 93, 068101-1.

McGowan, C. H. (2003) Running into problems: how cells cope with replicating damaged DNA. *Mutat. Res.* 532, 75-84.

Naaman, R., Haran, A., Nitzan, A., Evans, D., Galperin, M. J. (1998) Electron Transmission through Molecular Layers. *J. Phys. Chem. B* 102, 3658.

Nogues, C., Cohen, S.R., Daube, S.S., Naaman, R. (2004) Electrical properties of short DNA oligomers characterized by conducting atomic force microscopy. *Phy. Chem. Chem. Phy.* 6, 4459.

Palmer, RE., Rous, P. (1992) Resonances in electron-scattering by molecules on surface. *Rev. Mod. Phys.* 64, 383-440.

Pan X. and Sanche, L. (2005) Mechanism and site of attack for direct damage to DNA by Low-energy electrons. *Phy. Rev. Lett.* 94, 198104.

Pan, X., Abdoul-Carime, H., Cloutier, P., Bass, A.D., Sanche, L. (2005) D^-, O^- and OD^- desorption induced by low-energy (0–20 eV) electron impact on amorphous D2O films. *Radiat. Phys. Chem.* 72, 193.

Pan, X., Cloutier, P., Hunting, D., Sanche, L. (2003) Dissociative Electron Attachment to DNA. *Phys. Rev. Lett.* 90, 208102-1.

Pendry, J.B. (1974) in Low Energy Electron Diffraction, Academic, London.

Ptasinska, S., Denifl, S., Grill, V., Märk, T.D., Scheier, P., Gohlke, S., Huels, M.A., Illenberger, E., (2005) Bond-selective H^- ion abstraction from thymine. *Angew. Chem. Int. Ed.* 44, 1657.

Ptasinska, S., Denifl, S., Scheier, P., Märk, T.D. (2004) Inelastic electron interaction (attachment/ionization) with deoxyribose. *J. Chem. Phys.* 120, 8505.

Rakhovskaia, O., Wiethoff, P., Feulner, P. (1995) Thresholds for electron stimulated desorption of neutral molecules from solid N_2, CO, O_2 and NO. *Nucl. Instrum. Methods B* 101, 169.

Ray, S.G., Daube, S.S., Naaman, R. (2005) On the capturing of low-energy electrons by DNA. *Proc. Natl. Acad. Sci.* 102, 15.

Regulus, P., Spessotto, S., Gateau, M., Cadet, J., Favier, A., Ravanat, J. (2004) Detection of new radiation-induced DNA lesions by liquid chromatography coupled to tandem mass spectrometry. *Rapid Commun. Mass Spectrom.* 18, 2223-2228.

Sanche, L. (1991) Primary interactions of low-energy electrons in condensed matter. In: Jay-Gerin J-P, Ferradini C, editors. Excess electrons in dielectric media. Boca Raton: CRC Press., p 1-42.

Sanche, L. (1995) Interaction of low-energy electrons with atomic and molecular solids. *Scanning Microsc.* 9, 619-656.

Sanche, L. (2000) Electron resonances in desorption induced by electronic transitions. *Surf. Sci.* 451, 82-90.

Sanche, L. (2002) Nanoscopic aspects of radiobiological damage: fragmentation induced by secondary low-energy electrons. *Mass. Spectrom.* 21, 349.

Sanche, L., Michaud, M. (1984) Interaction of low-energy electrons (1—30 eV) with condensed molecules: II. Vibrational-librational excitation and shape resonances in thin N_2 and CO films. *Phys. Rev. B* 30, 6078.

Scheer, A. M., Aflatooni, K., Gallup, G.A., Burrow, P.D. (2004) Bond breaking and temporary anion states in uracil and halouracils : implications for DNA bases. *Phys. Rev. Lett.* 9206, 8102.

Sevilla, M. D., Becker, D., Yan, M., Summerfield, S. R. (1991) Relative abundance of primary radical ions in γ-irradiated DNA: Cytosine vs thymine anions and guanine vs adenine cations. *J. Phys. Chem.* 95, 3409-3415.

Shukla L.I., Pazdro R., Becker, D., Sevilla, M. D. (2005) Sugar radicals in DNA : isolation of neutral radicals in gamma-irradiated DNA by hole and electron scavenging. *Radiat. Res.* 163, 591-602.

Sukhoviya, M. I., Petruschko, I. A., Shafranyosh, M. I. (2001) Book of Abstr. IX ECSBM, Prague, Czech Republic.

Swarts, S.; Sevilla, M.; Becker, D.; Tokar, C. and Wheeler, K. (1992) Radiation-induced DNA damage as a function of hydration. I. Release of unaltered bases. *Radiat. Res.* 129, 333.

Tanabe, T., Noda, K., Saito, M., Starikov, E.B., Tateno, M. (2004) Regular Threshold-Energy Increase with Charge for Neutral-Particle Emission in Collisions of Electrons with Oligonucleotide Anions. *Phys. Rev. Lett.* 93, 043201-1.

von Sonntag, C. (1987) in *Chemical basis if radiation biology,* von Sonntag C. Taylors & Francis London, London.

Wagner, J. R., Decarroz, C., Berger, M., Cadet, J. (1999) hydroxyl-radiacal-induced decomposition of 2'-deoxycitidine in aerated aqueous solutions. *J. Am. Chem. Soc.* 121, 4101-4110.

Zheng, Y., Cloutier, P., Hunting, D.J., Wagner, J.R., Sanche, L. (2004) Glycosidic bond cleavage of thymidine by low-energy electrons. *JACS* 126, 1002.